Three Dispersed Magnetorheological Fluids in Dampers for Manufacturing Applications

Department of Mechanics, Mathematics and Management
MECHANICAL AND MANAGEMENT ENGINEERING
Ph.D. Program SSD: ING-IND/16–
MECHANICAL TECHNOLOGY AND SYSTEMS

Final Dissertation

Three Dispersed Magnetorheological Fluids in Dampers for Manufacturing Applications

By
Giovanna BRUNETTI

Referees:

Prof. Antonio Alessandro LICCIULLI

Dr. Ahmad BAROUTAJI

Supervisors:

Prof. Ing. Michele DASSISTI

Prof. Ing. Abdul Ghani OLABI

Coordinator of Ph.D. Program:
Prof. Ing. Giuseppe Pompeo DEMELIO

Course XXXI MECHANICAL AND MANAGEMENT ENGINEERING Ph.D. Program

Three Dispersed Magnetorheological Fluids in Dampers for Manufacturing Applications

Summary

Sinossi

All’interno di questa tesi sono descritte le attività di ricerca condotte durante l’intero dottorato, che hanno riguardato lo sviluppo di un modello che mettesse in relazione il funcional requirement richiesto a un device basato su fluidi magnetoreologici con le caratteristiche del fluido e della progettazione del device stesso; inoltre è stato formulato e testato un fluido magnetoreologico innovativo tridisperso.
I fluidi magnetoreologici (MRF) sono inclusi nella classe degli "smart materials” poiché alcune delle loro proprietà fisiche possono essere modificate su applicazione di uno stimolo esterno.
In particolare, la viscosità è la caratteristica controllabile più importante, che infatti può essere modificata con l'applicazione di un campo magnetico esterno. La modifica è rapida (nell'ordine dei millisecondi) e reversibile. L’entità della variazione della viscosità può essere controllata anche variando l'intensità del campo magnetico applicato esternamente. La viscosità può essere vista come la dissipazione di energia interna fino a raggiungere il limite dello yield stress. Operare sulla viscosità permette di controllare, in tempi brevissimi, la trasmissione di coppia/forza ogni coppia di superfici in reciproco movimento. La tecnologia dei fluidi magnetoreologici consente ai progettisti di progettare un'ampia gamma di dispositivi e sistemi con flessibilità e affidabilità rilevanti.
I fattori che fluidi magnetoreologici sono molti: la dimensione delle particelle che costituiscono la frazione solida, la distribuzione della diamtero medio, la loro forma e la loro concentrazione. Diversi additivi vengono utilizzati per prevenire la sedimentazione e per ridurre l'attrito tra le particelle, al fine di stabilizzare la sospensione delle particelle nel fluido.
In generale, l'applicazione dei fluidi magnetoreologici ai dispositivi è ora limitata dall'inconveniente della loro stabilità in termini di sedimentazione: quando il campo magnetico esterno viene rimosso, le particelle tendono ad agglomerarsi a causa della magnetizzazione residua e quindi il fluido sedimenta.
I fluidi magnetoreologici sono ampiamente utilizzati oggigiorno in molti per applicazioni di ingegneria civile e nei campi dell’automotive e del biomedicale. A parte l'uso di MRF nel processo di finitura superficiale ottica dell’azienda QEDTechnology^{tm}, al momento non sono presenti sul mercato applicazioni per l’ambito manifatturiero. Ciò è dovuto al fatto che i device sperimentali che sono stati progettati erano e sono pensati unicamente per specifiche applicazione e quindi non vi è uno standard unico. Oltretutto i tempi di setup sono molto lunghi. Chiaramente, i difetti che caratterizzano la della tecnologia dei fluidi magnetoreologici (il primo fra tutti è la sedimentazione, come già è stato detto) hanno ulteriormente allontanato l’idea di creare un device per applicazioni manifatturiere.

Gli obiettivi di questa tesi sono stati:
1. porre le basi per lo sviluppo di un dispositivo innovativo basato su MRF utilizzabile per applicazioni manifatturiere, con particolare riferimento alla sua capacità di smorzare forze esterne caratterizzate da frequenze ed intensità differenti;
2. progettare un fluido magnetoreologico innovativo con una migliore risposta alla sedimentazione da impiegare nel dispositivo di smorzamento per applicazioni manifatturiere.

Questo studio parte da un'accurata indagine bibliografica su:
1. Dispositivi basati su MRF, al fine di comprendere a fondo i diversi dispositivi e le loro caratteristiche di progettazione;
2. le caratteristiche chimiche degli MRF e della formulazione di MRF;
3. la combinazione di una specifica formulazione MRF con un dispositivo basato su MRF, per capire come le prestazioni richieste a un dispositivo basato su MRF siano influenzate dal design del dispositivo e dall'MRF contenuto all'interno del dispositivo stesso.

Il processo di progettazione di un nuovo dispositivo basato sulla tecnologia dei fluidi magnetoreologici parte dai requisiti funzionali del dispositivo stesso e investe entrambi gli ambiti:
- le caratteristiche fisiche di un fluido magnetoreologico in termini di viscosità nello stato attivato e nello stato non attivato (on- e off-state), yield stress e sedimentazione;
- le caratteristiche operative del dispositivo stesso in termini di modalità operativa e progettazione dei circuiti magnetici.

I due obiettivi sono stati pienamente raggiunti nei seguenti termini.
Per quanto riguarda la base di conoscenza per lo sviluppo di un dispositivo innovativo basato su fluidi magnetoreologici utilizzabile per applicazioni manifatturiere, con particolare riferimento alla capacità di smorzare forze esterne caratterizzate da frequenze diverse, questo scopo è stato raggiunto tramite una profonda classificazione di tutta la letteratura scientifica disponibile sull'argomento. Lo studio è stato condotto partendo dall'analisi dell'approccio progettuale dei dispositivi esistenti e sperimentali basati su fluidi magnetoreologici, per poi passare all'indagine del corpus di conoscenze esistente sulla corretta combinazione del design del dispositivo e della formulazione del fluido magnetoreologico per soddisfare requisiti progettuali specifici. Infine, si è giunti a una classificazione di tutti i device esistenti basate su fluidi magnetoreologici includendo anche tutte le possibili applicazioni manifatturiere.
Per quanto riguarda, invece, la progettazione di un fluido magnetoreologico innovativo con una risposta migliore al fenomeno della sedimentazione da impiegare nel dispositivo di smorzamento per applicazioni manifatturiere, sono state formulate diverse soluzioni per creare un nuovo fluido magnetoreologico tridisperso. Il fluido è tridisperso perché la frazione solida prevede due distribuzioni dei diametri medi di particelle dell'ordine del micron con l'aggiunta di una distribuzione di nanoparticelle, creando coì un inverse ferrofluid. Le varie alternative sono state create variando la percentuale di combinazione dei due differenti diametri medi delle particelle di dimensioni micron e la forma delle nanoparticelle (sferiche o esaginali). Queste combinazioni e quindi nuove formulazioni sono state testate dal punto di vista della sedimentazione e dal punto di vista del comportamento magnetico. I risultati sul processo di sedimentazione sono stati interessanti, poiché è stato osservato che la presenza di nanoparticelle sferiche mitiga il processo di sedimentazione, espresso in termini di velocità di sedimentazione e di rapporto di sedimentazione, cioè il rapporto tra altezza dello strato sedimentato e l'altezza della colonna di fluido magnetoreologico sotto esame. Nessuna differenza significativa nel comportamento magnetico è stata, invece, rilevata anche utilizzando una modellazione basata sul modello di Ising. Ulteriori indagini future possono portare a fluidi più performanti utili per ambito manifatturiero, in considerazione del fatto che appunto la sedimentazione è un fattore critico per tale ambito di applicazione applicazione.

Il modello estratto dal corpus di conoscenze studiato ha riconosciuto i seguenti ellementi chiave per un corretto processo di progettazione:

- soluzioni di progettazione strutturale,
- modelli utilizzati per descrivere il comportamento di smorzamento,
- caratteristiche di smorzamento in valve mode,
- prestazioni di smorzamento,
- fattori che influenzano le prestazioni di smorzamento,
- requisiti di progettazione del circuito magnetico.

La classificazione dei modelli comportamentali per smorzatori basati su fluidi magnetoreologici estrapolata da questo accurato studio dello stato dell'arte permette di spiegare le condizioni per realizzare un efficace meccanismo di smorzamento. Questo corpus di conoscenze può essere utilizzato per spiegare e prevedere come viene esercitato l'effetto di smorzamento di questi dispositivi. I sistemi di smorzamento basati su fluidi magnetoreologici esercitano una forza di smorzamento in

reazione alla frequenza di eccitazione data da una data sollecitazione forzante (in termini di frequenza e intensità), che differisce solo per i valori di range di vibrazione dipendenti dal dominio di applicazione.
Una volta acquisita questa conoscenza sul funzionamento dello smorzamento basato su fluidi magnetoreologici, essa può essere estesa anche ad altre applicazioni, come quelle appunto legate all'ambito manifatturiero. Uno smorzatore basato su fluidi magnetoreologici potrebbe essere facilmente utilizzato per la testa porta-mandrino, portautensile, bracci di cambio utensile, utensili come frese e così via semplicemente modificando le dimensioni geometriche dell'attuatore, mantenendo inalterato il meccanismo di scarico del nucleo. Infatti, la scalabilità è una caratteristica peculiare dei device basati su fluidi magnetoreologici.
La progettazione, quindi, di un nuovo ammortizzatore basato su MRF per applicazioni di produzione è quindi quasi una conseguenza naturale del corpus di conoscenze qui riassunto.

Abstract

Magnetorheological fluids (MRFs) are included in the class of "smart materials" since their viscosity can be quickly and reversibly changed upon the application of an external magnetic field.
Even if MRF technology is exploited nowadays in many different fields (civil engineering, automotive, biomedical), very few manufacturing applications are on the market at the moment because of MRFs main drawback: sedimentation.
This thesis aims to put the basis for the development of an innovative MRF damping device for manufacturing applications and to design an innovative MRF with improved response to the sedimentation to be employed in the damping device for manufacturing applications.
The study starts from an accurate bibliographic investigation on MRF based devices, chemical features of MRFs and MRF formulations. This corpus of knowledge was organized into a model which can be used to explain the relationship between the functional requirements an MRF based device has to meet and the corresponding combination of chemical and physical properties of the fluids and the device itself (and so the MR operational mode selected); so, a rationale is provided to select the best fluid for the specific application, with particular focus on damping devices. Once the knowledge on the MRF damping functioning is gained, it can be extended to manufacturing applications. So, the designing process of a novel MRF-based damper for manufacturing applications is thus a consequence of the corpus of knowledge collected in this thesis.
The experimental section of this work focuses, then, on the formulation of a novel three-dispersed MRF for damping devices with enhanced resistance to sedimentation. The experimental fluids were tested from the point of view of sedimentation and magnetization behavior. With regards to sedimentation, interesting results were reached.

Keywords

MRFs, smart materials, magnetic fields, magnetorheological fluids, three dispersed, inverse ferrofluids

Nomenclature

Vectors are stated in **bold**; constants are stated in *italics*.

α [no unit]	Fluid efficiency ratio.
A [J]	Hamaker constant.
a [m]	Magnetic particle diameter.
A [m^2]	Area of actuation surface.
β [no unit]	Coupling parameter for the relative permeabilities of the continuous phase and the particles.
B [T]	Magnetic flux density.
c [no unit]	Empirical factor depending on the flow velocity profile in valve mode.
c [kg/s]	Viscous coefficient.
D [m]	Displacement.
ΔP [Pa]	Pressure drop in valve mode.
ΔP_η [Pa]	Pure rheological component of pressure drop in valve mode.
ΔP_{mr} [Pa]	Magnetorheological component of pressure drop in valve mode.

η [Pa*s]	Dynamic viscosity.
η_{po} [Pa*s]	Post-yield dynamic viscosity in the Bi-viscous Model in presence of magnetic field.
η_{pr} [Pa*s]	Pre-yield dynamic viscosity in the Bi-viscous Model in presence of magnetic field.
η_{eq} [Pa*s]	Equivalent dynamic viscosity in Herschel-Bulkley model.
$\mathbf{e_r}$	Versor for the separation vector **r.**
$\mathbf{e_\vartheta}$	Versor perpendicular to versor $\mathbf{e_r}$.
φ	Volume fraction of particles in a MRF.
E	Total magnetic energy in Ising model.
F_1 [Pa/s]	First figure of merit.
F_2 [m^2/s^3]	Second figure of merit.
F_3 [no unit]	Third figure of merit.
$\mathbf{F^B}$ [N]	Brownian random force.
$\mathbf{F^{ext}}$ [N]	Hydrodynamic friction force due to linear deformation velocity.
$\mathbf{F^H}$ [N]	Hydrodynamic force due to friction among particles.
$\mathbf{F^I}$ [N]	Inter-particles force due to dipole-dipole interaction.
$\mathbf{F_{mr}}$ [N]	Magnetic field dependent component.
$\mathbf{F_\eta}$ [N]	Pure rheological viscous component.
F_0 [N]	Magnetostatic force.
f [N]	Damping force
f_c [kg/s]	Hysteresis magnitude.
f_0 [N]	Damper force offset.
$\gamma_{c,1}$ [%]	First critical strain amplitude.
$\gamma_{c,2}$ [%]	Second critical strain amplitude.
$\dot{\Upsilon}$ [1/s]	Shear rate.
g [m]	Gap size of the MRF orifice in operational modes.
G' [Pa]	Storage modulus.
G'' [Pa]	Loss modulus.
h [m]	Height (distance betwee the two actuation interfaces)
h*[m]	Steric barrier length.
H [A/m]	External magnetic field.
I [Amp]	Current intensity.
h_{ij} [m]	Distance between two particles surfaces.
$\varkappa$ [no unit]	Control ratio.
k_B [J/K]	Boltzmann constant.
K_H [no unit]	Consistency index.
k_{om} [no unit]	Operational mode constant.
λ [no unit]	λ parameter, ratio between thermal energy and magnetic moments interaction.
LDE [J/cm^3]	Lifetime Dissipated Energy.
μ [N/A^2]	Scalar Magnetic permeability.
μ_0 [N/A^2]	Magnetic permeability of vacuum.

μ_f [N/A^2]	Carrier fluid relative magnetic permeability.
μ_p [N/A^2]	Particles relative magnetic permeability.
$\mathbf{m}$ [A/m^2]	Magnetic moment.
m [kg]	Mass of a single particle.
Mn [no unit]	Mason number.
M_s [A/m]	Saturation magnetization for particles.
P [W]	Dissipated mechanical power.
Pe [no unit]	Peclet number.
Q [m^3 s]	Volumetric flow rate of the MRF.
θ [rad]	Angle between the external magnetic field $\mathbf{H_0}$ and the versor $\mathbf{e_r}$.
ρ [kg/m^3]	MRF density.
r [mm]	Separation vector between two particles i and j.
S [m/s]	Relative speed of one surface in respect on the other in shear mode.
τ [Pa]	Shear stress.
τ_{mr}[Pa]	Yield stress depending from an externally applied magnetic field.
τ_y [Pa]	Maximum yield stress.
T [K]	Absolute temperature.
t_c [s]	Characteristic time for particles chains formation.
τ_{yd}[Pa]	Dynamic yield stress in the Bi-viscous model.
τ_{ys}[Pa]	Static yield stress in the Bi-viscous model.
v [m/s]	Actual fluid velocity field of the MRF when flowing.
V [m^3]	Minimum active fluid volume.
$\mathbf{v^0}$ [m/s]	Imposed fluid velocity field when flowing.
w [m]	Width of orifice in operational modes.
$\hat{W}_e$ [Pa/s]	Electrical power density.
W_e [W]	Electrical power.
$\hat{W}_m$ [Pa/s]	Mechanical power density.
W_m [W]	Mechanical power.
$\dot{x}$ [m/s]	Damper velocity.
z [m]	Hysteretic variable.

1. Introduction

Magnetorheological fluids (MRFs) are included in the class of "smart materials" since some of their physical properties can be changed upon the application of an external stimulus.
In particular, the main controllable property of MRFs is the viscosity, which can be modified with the application of an external magnetic field. The change is quick (in the order of milliseconds) and reversible [1]. Furthermore, the amount of change in viscosity can also be controlled by varying the intensity of the externally applied magnetic field [2]. The viscosity can be seen as the internal energy dissipation or the corresponding yield stress [3] [4]. Operating on viscosity permits to control, in a very short time-gap, the torque/force transmission between any couple of surfaces. Magnetorheological fluids technology makes it possible for designer-engineers to design a wide range of devices and systems with unique flexibility and reliability.
The history of smart fluids dates back to the late 1940s, with the initial discovery and development of MRFs credited to J. Rabinow [5] and contemporary of Electrorheological fluids (ERFs) to W. M. Winslow [6]. Rabinow's research moved from the idea of a fluid with magnetic particles activated by an external magnetic field. Different formulations were developed and tested using an innovative clutch based on these fluids (Figure.1). In fact, it was designed in such a way that the fluid operated in small shear gaps. These gaps were contained between the case connected to the input-shaft and some disks connected to the output shaft. Inner and outer shafts were both made of magnetic material in order to be easily magnetized and so to become part of the magnetic circuit, along with the coils used to generate the external magnetic field. When torque control was needed, a magnetic field was applied through the passing of electric current in the coils, connecting or disconnecting the input shaft with the output one. Nowadays MRF-based clutches are still based on Rabinow's design, even if since then on, a lot of innovation and research has been performed both on materials and devices design. At present, MRFs are very attractive for a huge number of different applications, such as dampers, clutches, brakes.

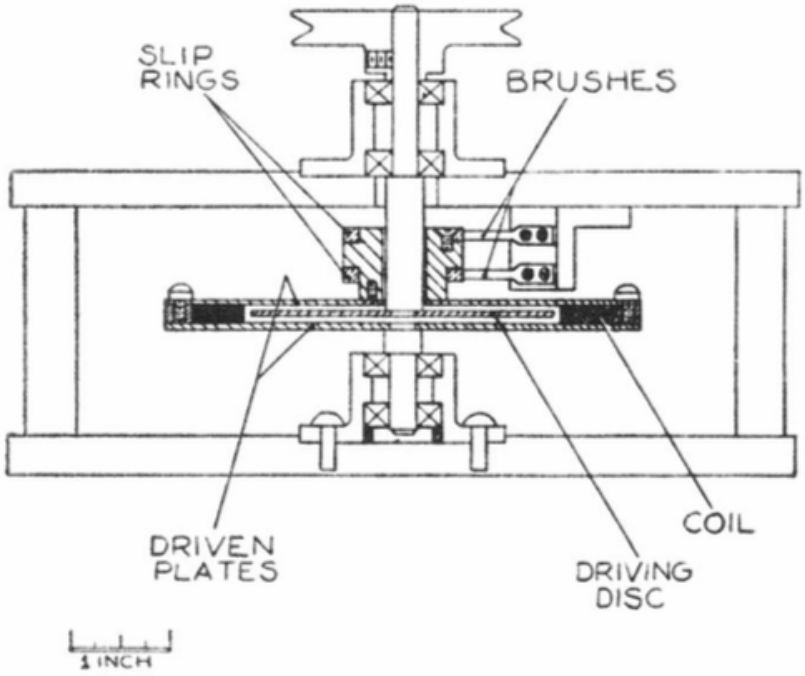

Figure 1. The magnetic fluid clutch designed by Rabinow is 1948 [5].

MRFs are suspensions of micron-sized magnetizable particles in a carrier fluid such as silicon oil, mineral oil, hydrocarbon oil, or water. The carrier liquid acts as a dispersing medium and ensures the homogeneity of the particles in the fluid. The MR effect is due to a magnetic field, which transforms each metal particle in a dipole with ferromagnetic properties that attract neighboring particles, producing chains or the so-called MR structures [7]. There are many factors that influence MRF performance such as particle size, shape distribution and density of particles. Different additives are used to prevent gravitational settling and to reduce the friction between particles, in order to stabilize the particles suspension in the fluid.
In general, the application of MRFs to devices is now limited by the drawback of their stability in terms of sedimentation behavior: when the external magnetic field is removed, particles tend to agglomerate due to residual magnetization and then they sediment [8].

MRFs are widely used nowadays in many different devices for civil engineering, automotive, and biomedical applications. Apart from the use of MRFs in the industrial optical polishing process by QED_{tm}, very few manufacturing applications are on the market at the moment.
This is mainly due to some drawbacks of these fluids, among which sedimentation is the most important.

The aims of this thesis are

1. to put the basis for the development of an innovative device based on MRFs that can be used for manufacturing applications, with particular reference to its capability of damping external forces characterized by different frequencies and intensities;
2. to design an innovative MRF with improved response to the sedimentation drawback to be employed in the damping device for manufacturing applications.

This study starts from an accurate bibliographic investigation on:

1. MRF based devices, in order to deeply understand the different devices and their design features;
2. the chemical features of MRFs and MRF formulation;
3. the combination of a specific MRF formulation with a MRF based device, to understand how the performances required to an MRF-based device are influenced by the device design and by the chemical formulation of the MRF contained inside the device.

The designing process for a novel device based on MR technology moves from the functional requirements of the device and invests both:

- the physical characteristics of an MRF in terms of on-state and off-state viscosity, yield stress and sedimentation behavior,
- the operational characteristics of the device itself in terms of operational mode and magnetic circuitry design.

Then novel three-dispersed MRFs were formulated and tested from the point of view of:

- sedimentation;
- magnetization behavior.

In fact, these features are critical to the scope of the development of innovative devices for manufacturing applications, as it will be shown in the design section of the thesis.

2. Basic functioning principles

An MRF is typically made of a suspension of micron-sized (20-50 μm range) magnetizable particles in a carrier fluid, with a typical particle volume percentage of 30%$_v$-40%$_v$. Additives may enrich the mixture to keep the fluid stable over time, preventing it from losing its operational properties such as, for instance, through the reduction of the transmitted force due to particle sedimentation.
The main property of an MRF is the capability of swiftly changing its rheological behavior. Without magnetic field action, the fluid behaves as a regular fluid with properties close to those of the carrier fluid of which it is made of. In presence of a magnetic field, the MRF starts behaving like a semi-solid as a function of the field intensity. This change is completely reversible: when the magnetic field is removed, the MRF behaves like the carrier fluid again [2]. The condition in which the MRF is subjected to the action of an external magnetic field is called on-state, while the condition in which the MRF is not activated by the magnetic field is called off-state.

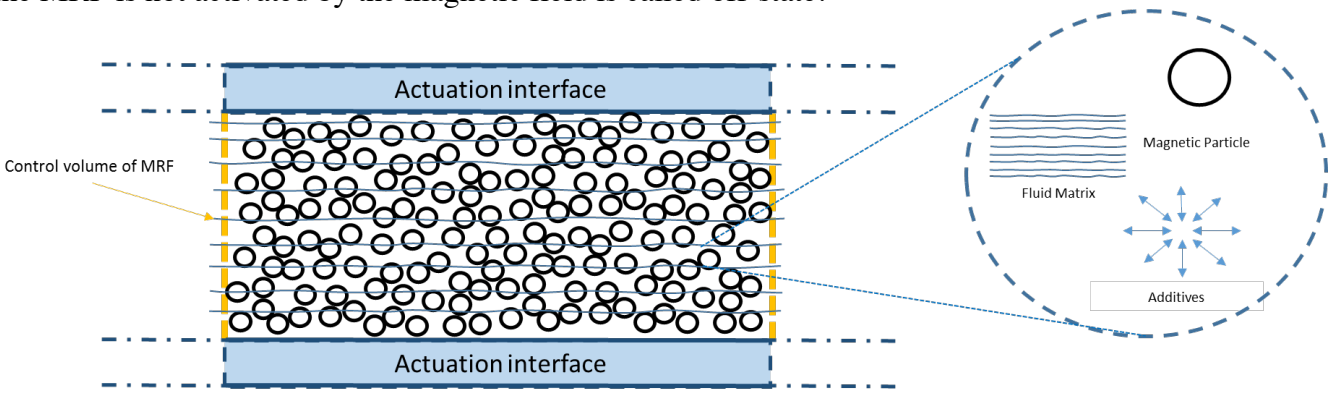

Figure 2: Schematic representation of an "MRF system" acting between two actuation interfaces [9].

To explain principles of MRF functioning, the concepts of 'actuation interface' and 'MRF System', can be used as in Figure 2 [9]. A MRF System can be defined as a set of elements (magnetic particles, carrier fluid and additives) performing different roles under magnetic field control. The actuation interface is the locus of points representing the physical separation between the inner and outer part of an MRF system through which actions are exchanged with the external environment.
The magnetorheological performance of MRFs is the result of the magnetic dipole induced on each particle in the fluid by the application of the external magnetic field. Each dipole is represented by its magnetic moment vector. In absence of magnetic field, particles are randomly oriented and so dispersed in the carrier fluid, because of thermal motion (see Figure 3.a) and the overall magnetic moment is null [10]. When the interaction energy between magnetic moments and the applied magnetic field exceeds the Brownian thermal energy [2], the dipoles align head-to-tail and consequently particles are dragged in proximity. In this way, chain and structures are formed (see Figure 3.b) [9].

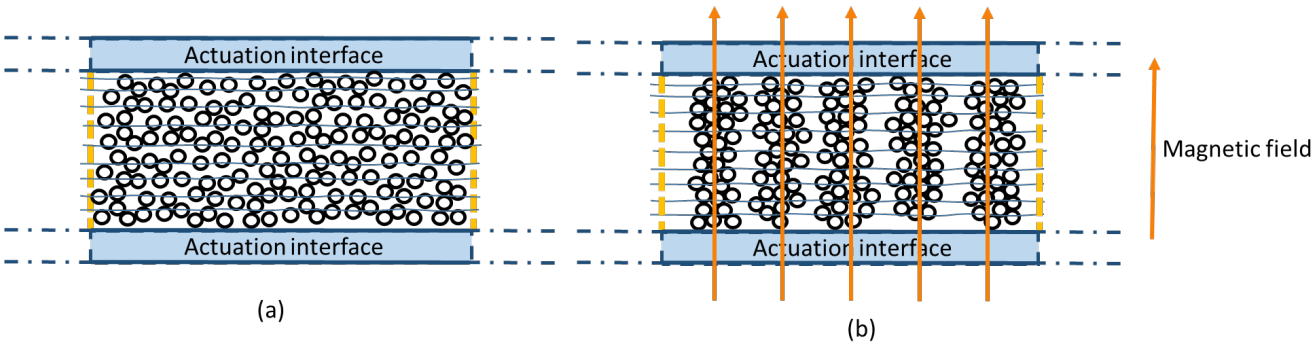

Figure 3. Generic MRF without presence magnetic field (a), with presence of magnetic field (b) [9].

This happens because when the magnetic moments are aligned to the magnetic field lines, the potential magnetic energy of the system is minimized, being minimized the angle formed between them. The more intense is the applied magnetic field strength, the more the magnetic moment on each particle aligns to the magnetic field [11]. Figure 4.a shows the behavior of two particles not subjected to external magnetic fields; Figure 4.b shows particles subjected to a "weak" magnetic field in terms of intensity, while Figure 4.c shows the interaction with a "strong" one. The most regular chains are reached when all the dipoles are aligned with the external magnetic field lines [10]; this happens when the threshold of magnetization saturation (M_s) is reached. In this condition, the MRF results in a "*weakly solid network of particles*" [12], [13], [14], [3], [2].

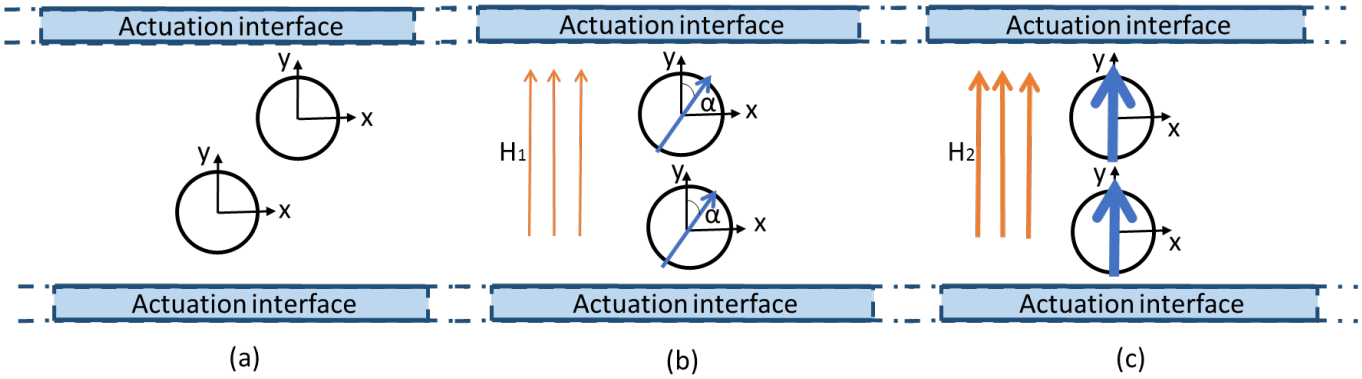

Figure 4. Representation of particles with their own magnetic moment orientation in different conditions: (a) no magnetic field, (b) presence of a magnetic field H_1, (c) presence of a magnetic field $H_2 > H_1$ [9].

The presence of induced chain structures explains the different behaviors of MRFs in the on-state and off-state conditions. In the on-state condition the MRF is subjected to the application of a magnetic field; on the contrary, the off-state condition is associated with the absence of the externally applied magnetic field to the MRF. When the fluid is in its on-state, and it is mechanically deformed like in Figure 5, the induced chains in the fluid oppose to the motion, thus determining the change of the flow behavior of the fluid.

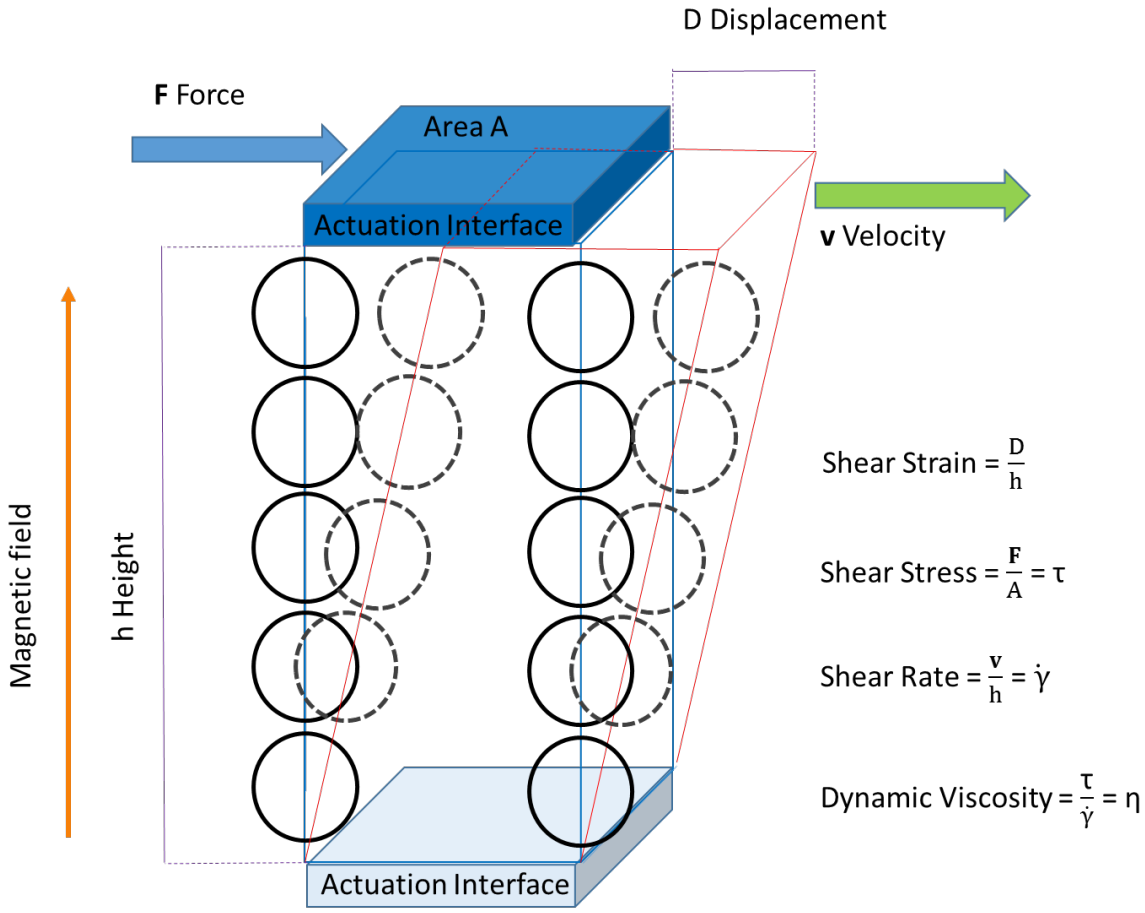

Figure 5. Schematic representation of a mechanically deformed MRF [9].

Figure 6 shows the two commonly used models describing the MRFs behavior: the Newtonian model for the off-state condition and Bingham-plastic model for the on-state condition, instead. In the off-state the relation between shear stress and shear rate is linear and the dynamic viscosity is independent of the stress (Forte, Patern, e Rustighi 2004). The Bingham-plastic model, instead, describes the fluid flow in his on-state condition: differently from the Newtonian model, to obtain the fluid movement it is necessary to exert on it a certain amount of shear stress that causes a plastic deformation without any change in viscous behavior. The maximum shear stress that an activated MRF can resist before starting to flow again is called yield stress (τ_y) and it is a function of the strength of the magnetic field [2]. Once the threshold of the yield stress has been overcome the MRF behaves according the Newtonian model again.

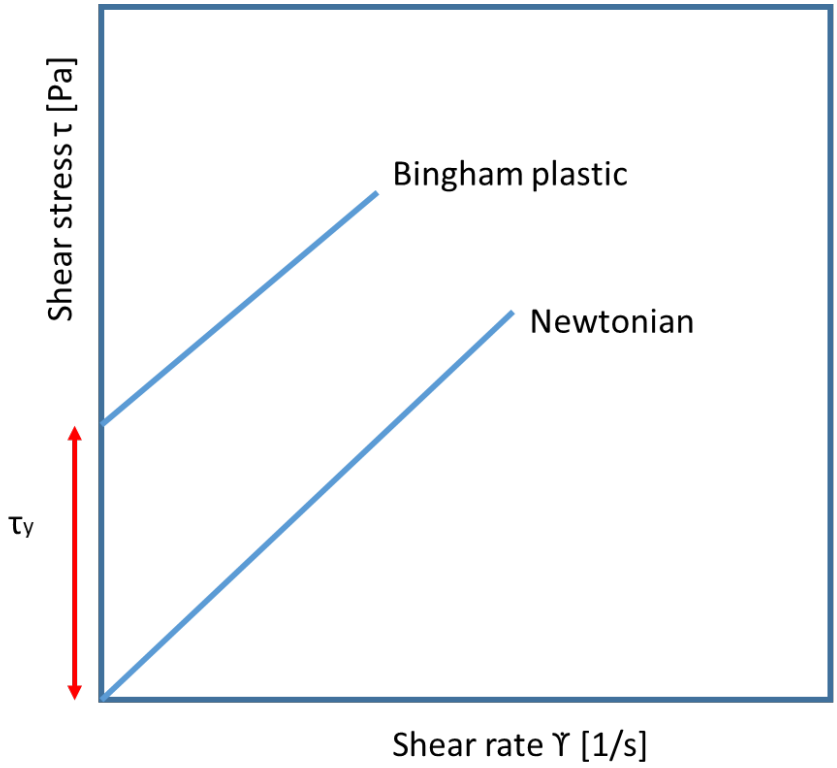

Figure 6. The two models used to descrive MRF rheological behavior: Newtonian model for the off-state condition and Bingham plastic model for the on-state condition being τ_y the maximum yield stress [9].

The value of the yield stress (τ_y) of the fluid increases with the intensity of the externally applied magnetic field. Once magnetic saturation M_s is reached, the yield stress no longer increases upon increase of the magnetic flux density, but remains constant [12]. Since the value of M_s depends on the magnetic properties of the particles inside the MRF, one way to enhance the maximum yield stress reachable is to select particle materials with large saturation magnetization [16] [12].
This change in rheological behavior happens in few milliseconds [17]. The chains have a mechanical resistance to the flow of the fluid, changing their yield stress [2]. As the shear stress reaches its maximum value (the yield stress) chains start breaking and the fluid flows easily even in presence of the magnetic field. The yield stress can be controlled through the value of the magnetic field applied to MRF. Using Bingham plastic model dynamic yield stress can be expressed as:

$$\tau = \tau_{ys} + \eta \dot{\gamma} \quad (1)$$

where τ is the shear stress, η is the viscosity, τ_{ys} is the dynamic yield stress and $\dot{\gamma}$ is the strain rate [18].
The relationship between magnetic flux density and yield-stress can be described by using the models developed by Ginder et al. [7] [12]. With low levels of external magnetic field H, M (magnetization) is expected to be linearly related to H and the relation between the yield stress and the applied field is given by:

$$\tau_{ys} \propto \varphi \mu_0 H^2 \quad (2)$$

where φ is the particle volume fraction, H is the applied field and μ_0 is the permeability of the free space ($4\pi \times 10{-}7$ H/m).
With flux densities above the linear region, but lower than those needed to achieve complete saturation, the yield stress can be evaluated as follows:

$$\tau_{ys} = (6^{1/2})\varphi\mu_0 (M_s)^{1/2} H^{3/2} \quad (3)$$

It is important to know $\mu_0 M_s$ which is the saturation magnetization of the solid fraction and depends on the material selected to formulate the MRF.
At flux densities that can induce complete magnetic saturation, the yield stress depends only on the saturation magnetization of the magnetically dispersed phase and the relationship is the following (ξ = 1.202 is a constant):

$$\tau_{ys}{}^{sat} = \left(\frac{4}{5\frac{5}{2}}\right) \xi\varphi\mu_0 (M_s)^2 \quad (4)$$

A significant contribution to the yield stress is given by the interaction between the MRF and the actuation interfaces in terms of magnetic properties of the material and roughness characteristic. For a fixed magnetic field and with fixed roughness, when the actuation interface material is ferromagnetic, there is an attracting magnetic force between the particle chains in the MRF and the interfaces (Figure 7.a), so the value of the yield stress is higher. On the contrary, when the material is paramagnetic there is no magnetic force between the chains and the interface, resulting in a lower value of the yield stress. The other factor influencing the yield stress is the surface roughness: decreasing it is detrimental in terms of yield stress, because when the asperities in the material are smaller than the particle size, particles slip tangentially on the interfaces without any force retaining them, even in case of ferromagnetic materials (Figure 7.b). The worst case is that of polished surfaces made in paramagnetic material [19].

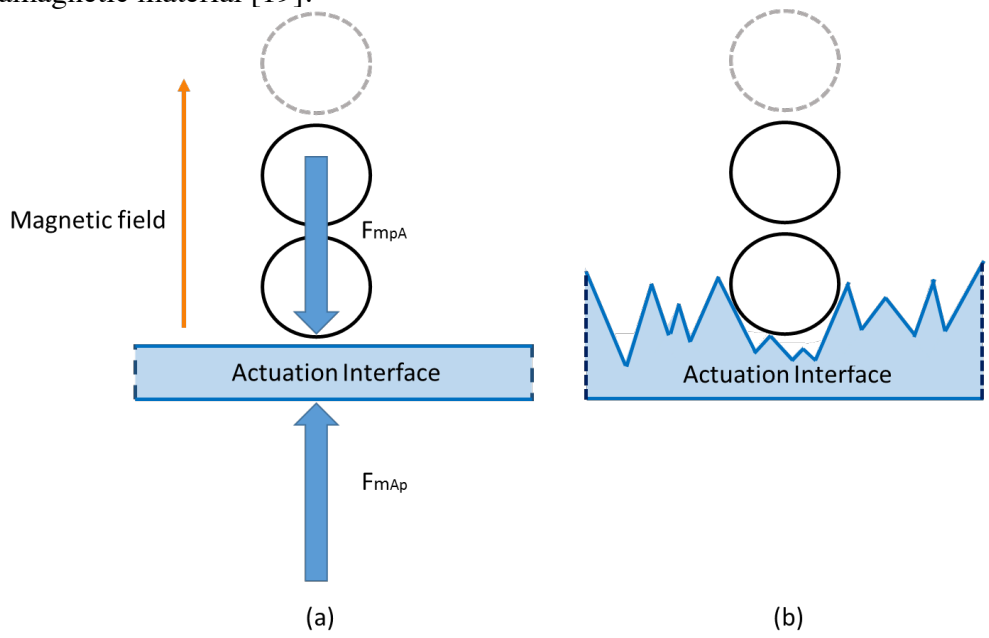

Figure 7. Schematic representation of the interaction between particles and Actuation Interface. In (a) F_{mpA} is the magnetic attracting force exerted by particles on Actuation Interface, and F_{mAp} is the force exerted by the Actuation Interface on the particles.

In general, the interaction between particles results also in a friction force, which contributes to the overall shear stress in reason of one third, in large shear-strain conditions. This causes wearing on the actuation interfaces. Of course, it is important to take into account this effect when designing MRFs and MRF based devices [20]. The friction, in fact, depends on the viscosity of the carrier fluid. In case of low viscosity (10 mPa*s), friction is constant, and particles are entrapped in the asperities in the walls of the MR system. In case of intermediate viscosity, friction firstly decreases because particles slip one over the others, and then increases because particles get embedded in asperities again. At high viscosities (200 mPa*s), particles accumulate around the contact zone reducing the

boundary lubrication (see e.g. [21] [22]). Particle concentration influences friction force too. Without magnetic field, MRFs with higher particle concentration have higher friction force due to more solid particles being trapped in the asperities of surfaces [23]. This is explained by the fact that under operation, particles in the contact zone are plastically deformed and tend to aggregate, creating a thin layer that protects the walls of the actuation interface, reducing their effective roughness and so the possibility for particles to fill the asperities. Finally, the higher the wall roughness the higher the yield stress exerted, due to the larger number of particles mechanically entrapped in the asperities [24] [25].

2.1 Modelling MRF behavior

The crucial property for MRFs subjected to a magnetic field is the maximum yield stress τ_y, which is the maximum stress a MRF can resist in its activated condition. The challenge in formulating new MRFs is to maximize this performance: the yield stress. To this aim, models describing the rheological behavior of MRFs are critical in both on-state and off-state.

As already mentioned, the rheological behavior of an MRF in off-state mode is explained by the Newtonian fluid model (see Figures 6 and 8): in this mode, the relationship between shear stress and shear rate is linear and thus viscosity η is constant (Forte, Patern, e Rustighi 2004). The model that is usually used to explain the rheological behavior for the on-state mode is the Bingham-plastic model. This model is particularly adopted for designing dampers [26] [1] [27]. Bingham-plastic model explains how MRFs return to behave as Newtonian fluid above a definite shear stress τ_y (the yield stress). Bi-viscous model [28] and Herschel-Bulkley model [29] are also adopted to explain MRF behavior. Figure 8 shows the models just recalled.

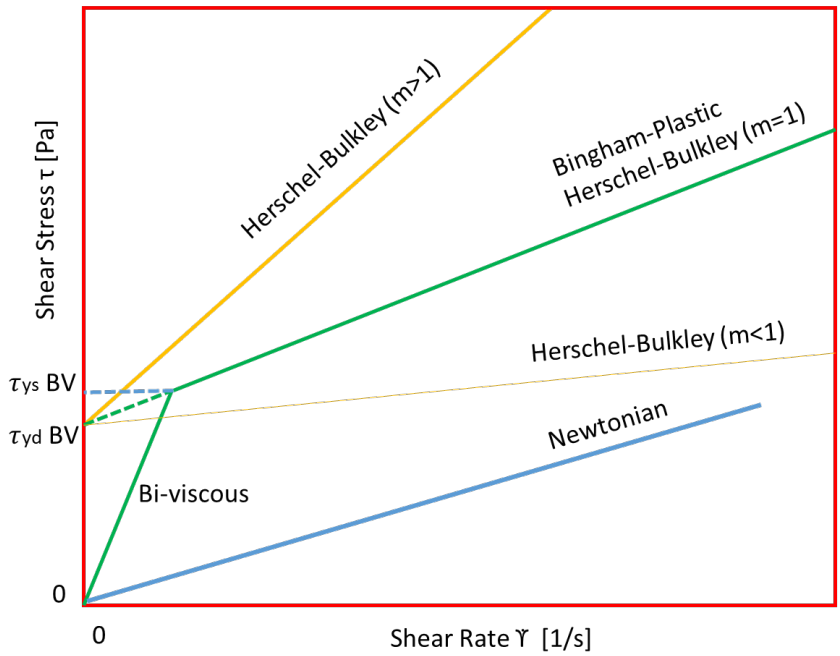

Figure 8: Representation of Newtonian, Bingham, Bi-viscous and Herschel-Bulkley models [9].

2.1.1 Bingham-plastic model

According to the Bingham-plastic model, the MRF is able to resist without changing the viscous behavior up to the yield shear stress τ_y. When the stress level imposed to the fluid is higher than τ_y,

the fluid starts flowing and is characterized by a post-yield viscosity η; while when the stress level is lower than τ_y, the behavior is rigid, and no fluid flow is registered. The stress-rate constitutive relationship for this model is stated in equation 5, where $\dot{\gamma}$ is the shear rate.

$$\begin{cases} \tau = \tau_y + \eta\dot{\gamma} & \tau > \tau_y \\ \dot{\gamma} = 0 & \tau \leq \tau_y \end{cases} \quad (5)$$

2.1.2 Bi-viscous model

This model takes its name from the presence of two different viscosities: pre-yield viscosity η_{Pr} and post-yield viscosity η_{po} and so two yield stresses: static yield stress (τ_{ys}) and dynamic yield stress (τ_{yd}). When the shear stress τ is smaller than the threshold of the static yield stress τ_{ys}, the MRF behavior is Newtonian, and the pre-yield viscosity η_{Pr} is larger than post-yield viscosity η_{po}. This second value characterizes the flow once the threshold of the static yield stress has been overcome τ_{ys}.

The bi-viscous model is shown in equation 6, where $\dot{\gamma}$ is the shear rate.

$$\tau = \begin{cases} \tau_{yd} + \eta_{po}\dot{\gamma} & \tau > \tau_{ys} \\ \eta_{Pr}\dot{\gamma} & \tau \leq \tau_{ys} \end{cases} \quad (6)$$

The Bi-viscous model is mainly used when modeling the MRF behavior in dampers [30] [31].

2.1.3 Herschel-Bulkley model

The Herschel-Bulkley model is similar to the Bingham-plastic model but takes into account both shear thinning and shear thickening effects. In fact, this model can be used to design magnetorheological brakes [32] and dampers [33]. The similarity with the Bingham-plastic model is given by the pre-yield behavior which is rigid in both the models. The constitutive relation is shown in the following equation 7, being $\eta_{eq} = K_H(\dot{\gamma})^{m-1}$ with m the flow behavior index, and K_H the consistency index. Above the yield stress and depending on the value of the m parameter, the MRF behavior is shear thinning (m>1), linear (m=1) or shear thickening (m<1), explained by the value of m. When $m = 1$ this model coincides with the Bingham-plastic model [34], as in Figure 8.

$$\begin{cases} \tau = \tau_y + \dot{\gamma}\,\eta_{eq} & \tau > \tau_y \\ \dot{\gamma} = 0 & \tau \leq \tau_y \end{cases} \quad (7)$$

2.2.4 Viscoelasticity

Magnetorheological fluid-based devices usually operate to contrast vibrations, such as in seismic dampers or in suspensions. In this case, MRFs work with oscillating load cycles. For this reason, testing MRFs cannot be limited to unidirectional flow testing to determine yield stress. Oscillatory flow tests give complementary information on the structures formed by particles when the MRF is activated, since frequency oscillation and then time information are involved [35] [36].

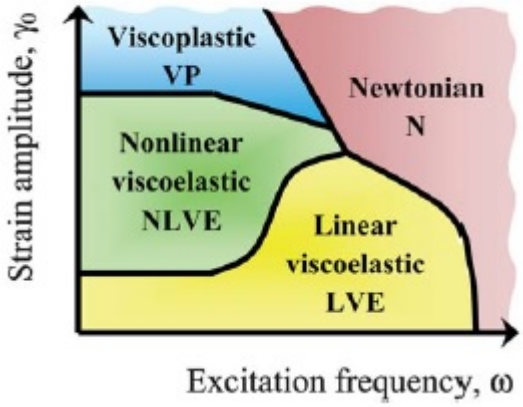

Figure 9. Pipkin diagram of the dynamic rheological behavior of MR. [https://goo.gl/rWjlVC access on 03/01/2021]

Figure 9 shows the Pipkin diagram first introduced for ERF [37]. This diagram is used to show the relationship between strain amplitude and excitation frequency and is used to summarize the MRFs behavior. Small strain amplitudes correspond to a linear viscoelastic (LVE) behavior, while larger strain amplitudes imply a nonlinear viscoelastic response (NLVE). At higher frequency and high strain amplitudes, the fluid behaves as a Newtonian fluid (N). The transition from LVE to NLVE is characterized by a first critical strain amplitude ($\gamma_{c,1}$), while the transition from NLVE to visco-plasticity (VP) is associated with a second critical strain amplitude ($\gamma_{c,2}$).
Researchers have focused on the viscoelastic behavior regime, defining a storage modulus *G'* and a loss modulus *G"*. The storage modulus indicates the amount of deformation energy stored in the elastic behavior and represents the elastic solid-like behavior; on the other hand, the loss modulus represents the energy dissipated as heat and it is the viscous response. In MRFs, the difference between storage and loss moduli is of one order of magnitude. This means that MRFs have the capability to store deformation energy returning to the pristine configuration. In doing so, they behave like elastic solids, but not perfectly. This is due to dissipation of part of the mechanical energy.
When the applied force is higher, the MRF chains collapse and all the mechanical energy is dissipated, i.e. the MRF flows: in this latter case, *G*" becomes much larger than *G*'.
The storage modulus associated with the MR chain structures under the magnetic field action is [38]:
$G' = 1.7\varphi\mu_0\beta^2 H^2$ (8).
When magnetic field strength increases, saturation phenomenon occurs, and the storage modulus is:
$G' = 3\varphi\mu_0 M_s H$ (9)
where M_s is the saturation magnetization of the particles. When saturation magnetization is reached, storage modulus becomes constant with the magnetic field in the same way of yield stress and it is given by [12]:
$G' = 0.3\varphi\mu_0 {M_s}^2$ (10)

2.2 Force evaluation

To fully understand how MRFs work, it is needed a deep knowledge of the forces governing the interaction between particles within the carrier fluid, between particles and the carrier fluid and finally between the MRF and the actuation interfaces.
The main type of forces involved in the interaction between the two particles i and j in a MRF are the magnetic force, the hydrodynamic force and the Brownian thermal force.
Using a Stokesian dynamics approach [39], and starting from the equation of motion for one single magnetic particle dispersed in the carrier fluid, it is possible to express all the contributions to the force acting on the single particle [40]:
$m\frac{dv}{dt} = \mathbf{F^H} + \mathbf{F^{ext}} + \mathbf{F^I} + \mathbf{F^B}$ (11)

In equation 11 $\mathbf{F^H}$ and $\mathbf{F^{ext}}$ represent two hydrodynamic contributions, $\mathbf{F^I}$ is the inter-particles force coming from the dipole-dipole interaction and $\mathbf{F^B}$ represents the Brownian random force directly related to the thermal energy of the fluid.
In general the hydrodynamic force is due to the interaction between the moving particles and the media [20]. The two hydrodynamic forces in equation 11 have two different meanings: $\mathbf{F^H}$ represents the action of hydrodynamic friction among the particles as a function of their velocity in the fluid, while $\mathbf{F^{ext}}$ represents the hydrodynamic force related to the linear deformation velocity.
The hydrodynamic friction force $\mathbf{F^H}$ is proportional to the actual fluid velocity field $\mathbf{v}$:

$$F^H \propto -\xi(\mathbf{v} - \mathbf{v}^0(x)) \qquad (12),$$

where $\xi = 6\pi\eta a/2$ [40], being η the carrier fluid viscosity, a the particle diameter and $\mathbf{v^0}(x)$ the imposed velocity field at the location x of the particle.
The second hydrodynamic term in (1), $\boldsymbol{F^{ext}}$, represents the hydrodynamic friction force due to the symmetric part of the velocity gradient tensor, which is related to the velocity of linear deformation. It scales as $6\pi\eta\Upsilon a^2$, in the case of a pure shear characterized by the shear rate Υ [40].
The term $\boldsymbol{F^I}$ in 11 represents the magnetic interaction between two particles i and j. The magnetorheological behavior of an MRF, due to the induced magnetization, can be explained recurring to the Particle Magnetization Model. This is a "macroscopic" model, since it takes into account magnetic energy minimization principles and homogeneous structures [36].
The magnetic force between two particles i and j is expressed in equation 13. The position of the two particles is represented in spherical coordinates in a Cartesian space, with θ measured in relation to the applied magnetic field, $\mathbf{r}$ the separation vector between them, $\mathbf{e_r}$ the versor for the vector $\mathbf{r}$, $\mathbf{e_\theta}$ the versor as shown in Figure 10.

$$\mathbf{F_{ij}}^{\mathbf{mag}} = F_0(a/r)^4[(3\cos^2\theta_{ij} - 1)\mathbf{e_r} + \sin 2\theta_{ij}\mathbf{e_\theta}] \qquad (13)$$

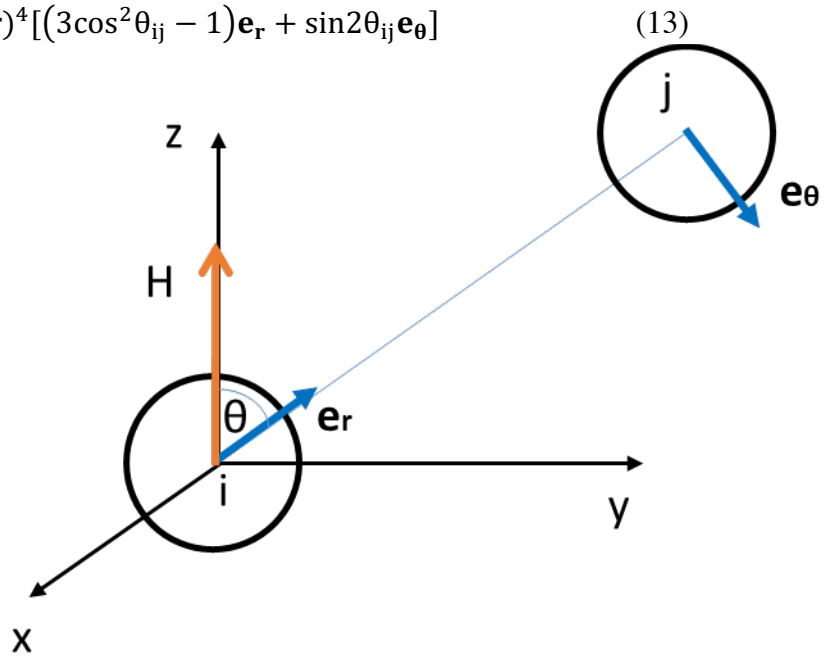

Figure 10. Two particles (i and j) interacting with each other in a magnetic field [9].

In expression 13, F_0 [N] is the magnetostatic force 14:

$$F_0 = \begin{cases} \frac{3}{16}\mu_0\mu_f\ a^2\beta^2\ H^2 & \text{for linear magnetization} \\ \frac{\pi}{48}\mu_0\mu_f\ a^2\ M_s{}^2 & \text{for saturation magnetization} \end{cases} \qquad (14)$$

where $\beta = (\mu_p - \mu_f)/(\mu_p + 2\ \mu_f)$ is the coupling parameter for the relative permeabilities of the continuous phase and the particle [36] [41].

In 11 the last term $\mathbf{F^B}$ represents the Brownian random force, which is proportional to 2kT/a, where k=1.38064852x10^{-23} [J/K] (Boltzmann constant) and T is measured in K. This force contribution is related to thermal motion which is the random movement of a particle in a fluid. This movement is associated with the particle thermal energy directly related to the system temperature [42]. This is why $\mathbf{F^B}$ is proportional to the MRF temperature T.

A set of parameters is used to confront different MRFs characteristics: **λ, Mn, Pe**.
The first one is the so called "λ parameter", which has been introduced by Hagenbüchle and Liu [10] to represent the ratio between the thermal energy and the interaction of two magnetic moments in the linear regime in repulsive configuration [36] :

$$\lambda = \frac{\pi\mu_0\mu_f\beta^2\left(\frac{a}{2}\right)^3 \mathbf{H_0}^2}{2k_BT} \qquad (15)$$

For large values of λ (λ>>1) the thermal motion is dominated by magnetic force: particles interact leading to chain-like structures in the fluid subjected to the magnetic field. On the other hand, small values for λ (λ<<1) imply the prevalence of Brownian motions over magnetic force, leading to absent or weak aggregates. Ferrofluids are usually characterized by small values of λ, MRFs by large values [43].
When a MRF flows, hydrodynamic drag and magnetostatic forces act on magnetic particles.
To represent the ratio between hydrodynamic drag and magnetostatic forces acting on the particles, the second parameter (dimensionless), Mason number (Mn), is introduced as follows:

$$\mathrm{Mn} = \frac{8\eta\,\dot{\gamma}}{\mu_0\mu_f\,\beta^2\,\mathbf{H_0}^2} \qquad (16)$$

In (16) η is the dynamic viscosity of the carrier fluid and $\dot{\gamma}$ is the shear rate.
Mn and λ parameters are related through Peclet number

$$\mathrm{Pe} = \frac{6\pi\eta\dot{\gamma}a^3}{k_BT} \qquad (17)$$

since

$$\mathrm{Mn}\lambda = 2\mathrm{Pe}/3 \qquad (18)$$

In general, the time for a micron-scaled particle to reach a constant velocity is very short: 1.7 μs for an iron particle of radius 1μm in water. In this condition, equation 11 can be rearranged by setting the left-hand term to zero. All the remaining terms are divided by their scaling factors and the resulting dimensionless equation is:

$$\frac{(\boldsymbol{v}-\boldsymbol{v}^0)}{\dot{\gamma}a} = \frac{[\boldsymbol{F^I}]}{Mn} + \frac{[\boldsymbol{F^B}]}{Pe} + [\boldsymbol{F^{ext}}] \qquad (19)$$

Equation 19 represents the equilibrium situation for a system and depends on two quantities: Mn and Pe or Mn and λ, since is valid equation 18. This means that, at the equilibrium, two MR systems starting with the same initial conditions and characterized by the same volume fraction φ, are characterized by the same properties if their Mn and Pe are the same [40].

Microscopic models can be used to complement the macroscopic Stokesian drag model represented in expression 11. In fact, along with the dipole-dipole interaction, Brownian and hydrodynamic forces governing the on-state condition, there are other forces influencing the off-state properties (short-range repulsive force, van der Waals force, acid–base, frictional and body forces, as in [36] [44] [45]). Off-state viscosity and sedimentation depend on short-range forces that can be controlled using various additives; at the same time van der Waals forces and remnant magnetization can influence again sedimentation behavior and re-dispersibility of fluids.
In particular, short-range repulsive force of equation 20 represents the tendency of particles to repulse each other when their surfaces stay close:

$$\boldsymbol{F_{ij}}^{\boldsymbol{rep}} = -F_0\, exp[-100\,\frac{h_{ij}-h^*}{a}]\boldsymbol{e_r} \qquad (20)$$

In equation 20 $h_{ij} = r_{ij} - a$ represents the distance between the particle surfaces. The h^* represents the steric barrier, which is the shortest distance dividing two molecules due to the electrostatic

repulsion between electrons cloud surrounding the atoms in the molecule; so this steric barrier models the effect of particle surface treatment (see chapter 3). It is important to notice that, since particles involved in MRFs are magnetic, the magnitude of the magnetostatic force still gives contribution to short-range forces even in the off-state condition.

Van der Waals force represents the long-distance attracting forces between two particles and is directed along the vector **r** that joins the centres of the two particles (equation 21):

$$\boldsymbol{F_{ij}}^{\boldsymbol{vdw}} = \begin{cases} \frac{A}{24}\frac{a}{{h_{ij}}^2}\boldsymbol{e}_{\boldsymbol{r}} & for\ h_{ij} > h_{min} \\ \frac{A}{24}\frac{a}{{h_{min}}^2}\boldsymbol{e}_{\boldsymbol{r}} & for\ h_{ij} \leq h_{min} \end{cases} \qquad (21)$$

The key role is played by the reciprocal distance between the two particles surfaces h_{ij}. In these equations, A is the Hamaker constant for the body-body interaction and in both cases the force decreases with the increasing of the distance between the particle surfaces [46]. A cut-off distance h_{min} is defined corresponding to the lowest energetic condition for two particles in proximity [47].

2.3 MRF operational modes

When it comes to the use of MRFs in devices, these fluids can be operated in three basic modes: valve, shear and squeeze mode (Figure 11). The difference among these modes depends on the level of stress induced in the fluid as well as on how the fluid flows (see [2] [48] [49]). In real applications mixed operational modes are possible.

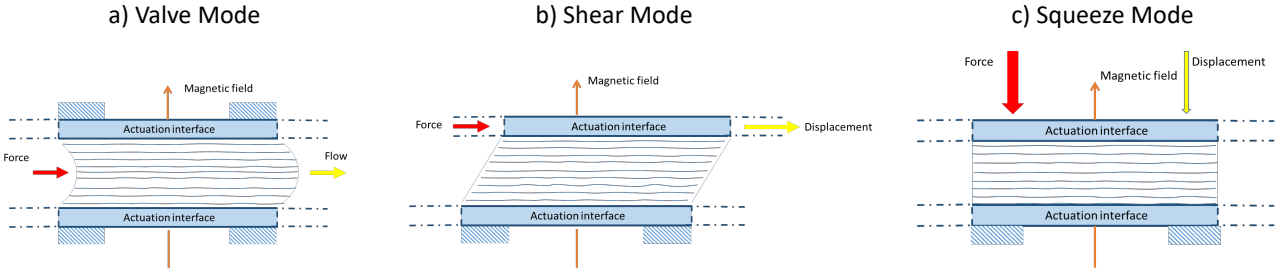

Figure 11. The three operational modes for MRFs: a) valve mode, b) shear mode, c) squeeze mode [9].

2.3.1 Valve mode

In valve operational mode, the MRF flows between two fixed actuation interfaces that create an orifice: the magnetic field is orthogonal to the flow direction (see Figure 12). The viscosity of the fluid is modified by changing the applied magnetic field and the resulting force exerted between interfaces is in the same direction of the fluid flow. The direct consequence is a resulting pressure drop directly proportional to the magnetic field intensity. The pressure control is the basic phenomenon endeavored in devices that resist an output force [50] [51] The pressure drop between the input and output of the orifice has two components: ΔP_{η} is the pure rheological component, while ΔP_{mr} represents the Magnetorheological component [52].

$$\Delta P = \Delta P_{\eta} + \Delta P_{mr} = \frac{12\eta QL}{g^3\, w} + \frac{c\tau L}{g} \qquad (22)$$

In 22 η [Pa*s] is the dynamic viscosity of the fluid in absence of magnetic field, τ [N/mm2] is the yield stress in response to an applied magnetic field, Q [m3/s] is the volumetric flow rate of the MRF. L, g, and w [m] are the length, the gap size, and the width of the orifice as shown in Figure 12 [3].

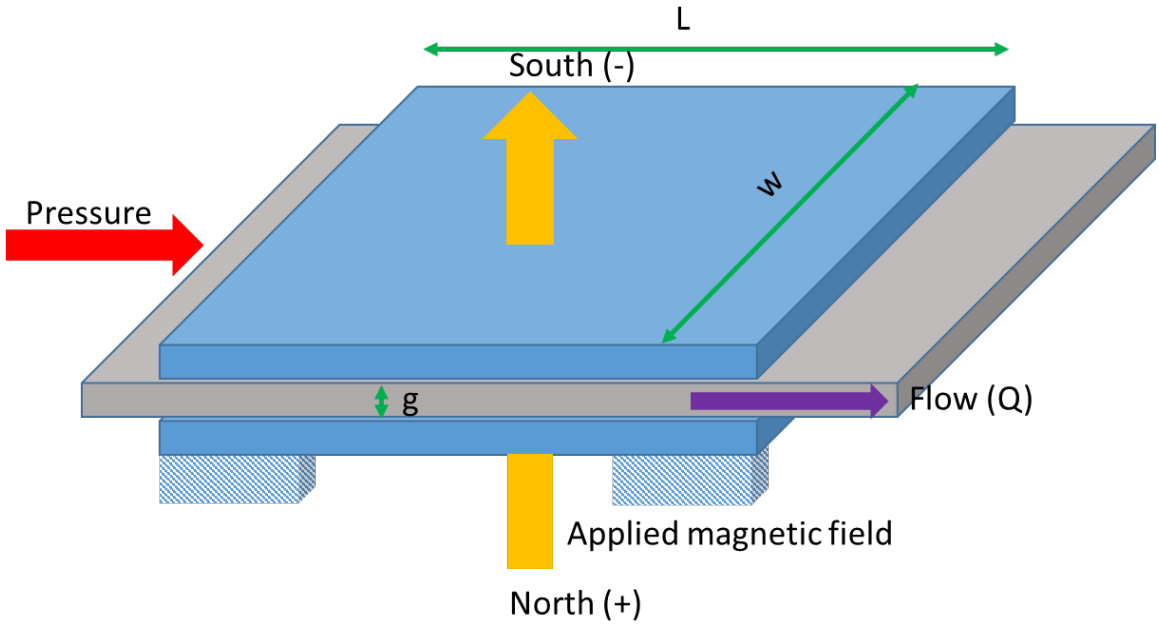

Figure 12. Valve mode [9].

The parameter *c* (unitless) is an empirical factor determined and depends on the flow velocity profile and ranges from 2 (when $\Delta P_{mr}/\Delta P_{\eta} < 1$) to 3 (when $\Delta P_{mr}/\Delta P_{\eta} > 100$) [2].

2.3.2 Shear mode

In the shear operational mode, MRFs transmit forces between two actuation interfaces because of their linear or rotational relative movement (see Figure 13). Magnetic field direction is orthogonal with respect to the moving actuation interfaces; this changes the fluid viscosity accordingly to the theory of the chain-like structures previously recalled. The shear mode is endeavored in applications such as dampers, brakes or clutches [53] [54] [55]. Just like in the valve mode, also in shear mode the total force has two components: a pure rheological component F_{η} and a magneto-rheological component F_{mr} as in equation 23:

$$F = F_{\eta} + F_{mr} = \frac{\eta * S * A}{g} + \tau_y * A \qquad (23)$$

where η [Pa*s] is the dynamic viscosity of the fluid independent from magnetic field; S [m/s] is the relative speed; A = L * w is the area of the working interface; τ_y [N/mm2] is the yield stress dependent from the applied magnetic field; *L*, *g*, and *w* [m] are the length, the gap size, and the width of the flow channel (Figure 13).

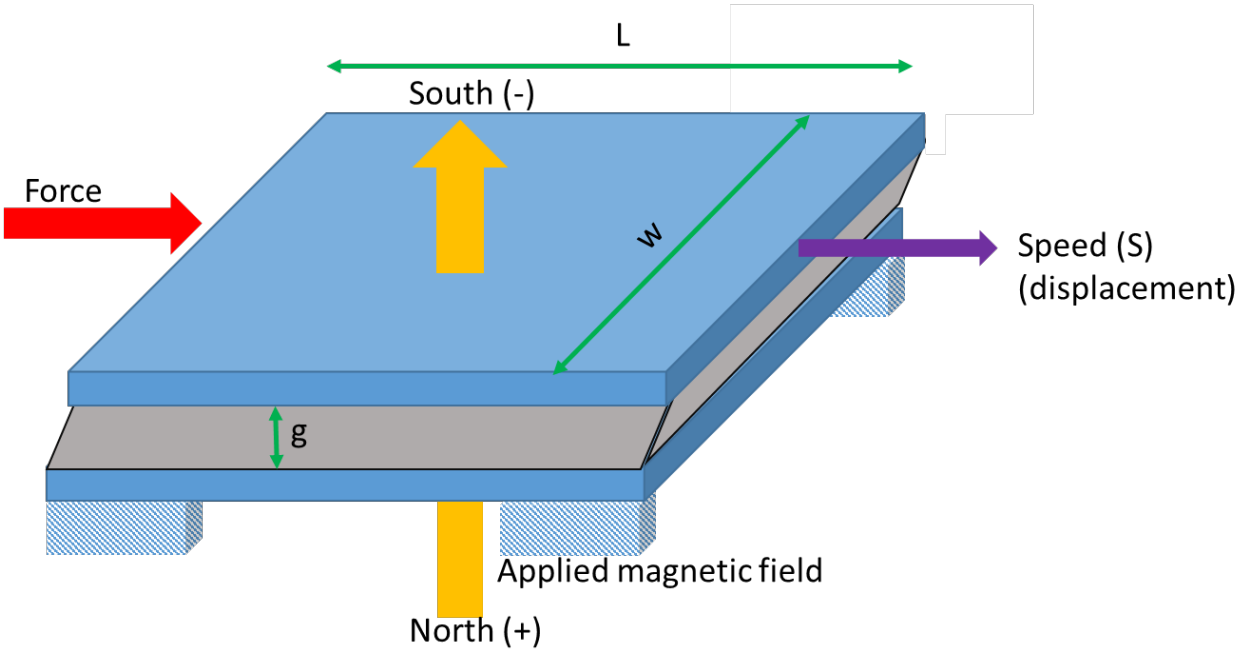

Figure 13. Shear mode [9].

The minimum active volume for shear mode-based applications represents the minimum amount of MRF necessary to be activated in order to obtain a required MR effect $\frac{F_{mr}}{F_\eta}$ at a given speed S and is expressed in equation 24:

$$V = L * w * g = \frac{\eta}{\tau_y{}^2} * \frac{F_{mr}}{F_\eta} * S * F_{mr} \quad (24)$$

Minimum active volume

The minimum active volume can be also calculated from equations 22 and 23 and this case it represents the minimum amount of MRF necessary to be activated in order to gain a desired amount of magnetorheological force at a given speed S:

$$V \geq k_{om} \left(\frac{\eta}{\tau_y{}^2}\right) \varkappa F_{mr} S \quad (25)$$

In equation 25 k_{om} is a constant whose value changes on the basis of the operational mode: 2 for valve mode and 1 for shear mode; V = L*w*g is directly proportional to the fluid viscosity of the fluid η and inversely proportional to the square of the yield stress τ_y [49].

The minimum active fluid volume in order to achieve the desired control ratio $\varkappa$ in correspondence to a given mechanical power W_m is given by:

$$V = k_{om} \left(\frac{\eta}{\tau_y{}^2}\right) \varkappa W_m \quad (26)$$

For valve mode: k_{om} =12/c^2, $\varkappa$=$\Delta P_{mr}/\Delta P_\eta$ and W_m=QΔP_{mr}. For shear mode: k_{om} =1, $\varkappa$=F_{mr}/F_η and W_m=F_{mr}S [52].

2.3.3 Squeeze mode

In squeeze mode, the fluid is placed between two surfaces that linearly move one towards/depart from the other (see Figure 14): the magnetic field paths (and so the MRF chains) are parallel to the motion. In devices based on squeeze mode usually there is no motion of MRF. Squeeze mode is in some way quite neglected and less studied with respect to other operational mode. It has been investigated in some experimental vibration isolation systems [56] [57].

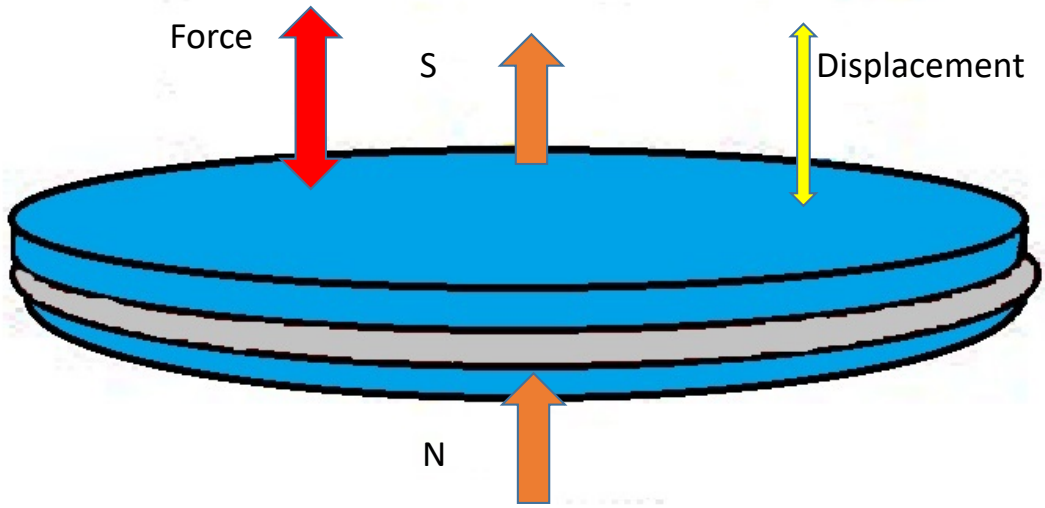

Figure 14. Squeeze mode [9].

3. How to design MRFs

Since the overall performance of a MR based device depends mainly on the MRF included in the device, it is important to review the physical characteristics of MRFs in order to fully understand how these fluids are formulated and how they should be selected on the basis of the functional requirements the MRF based device has to meet.

The selection of MRF formulation depends on the characteristics of the combination of the carrier fluid with additives, but also on the volume percentage of solid particles. As a consequence, the main criteria of selection are:

- yield stress;
- viscosity (on-state and off-state),
- sedimentation and redispersion behavior.

3.1 MRF components

A typical MRF formulation is based on a ternary system, composed of *a*) magnetizable powders (dispersed phase), usually consisting of 20-40 $\%_v$ of micrometric ferrimagnetic and/or ferromagnetic particles, suspended in *b*) a carrier fluid (continuous phase) such as mineral oil, synthetic oil, water or glycol, with the addition of *c*) a variety of additives.
Different combinations of micrometric particles, carrier fluids and additives result in different MR behavior both in the on- off-state, for several industrial applications such as automotive devices (clutches, linear dampers, rotor dampers and rotary brakes), prosthetic knee dampers or shock absorbers, advanced and intelligent polishing tool [58] [59]. MRFs have been applied in medical devices for tumor medical methodology allowing drug delivery and denying blood supply to the cancer cells [60]. The combination of different continuous phases, dispersed phases and additives in their preparation confers to MRF engineered characteristics for different applications. In table 1 are listed three examples of MRF commercial products with the corresponding formulation and used for particular applications.

Product code	MRF formulation			Applications
	Continuous phase	Dispersed phase	Additives	
MRF-132AD	Synthetic hydrocarbon base oil	Carbonyl iron particles (32 $\%_v$)	Dispersants and thixotropic agents	Dampers, valves
MRF-241ES	Water	Carbonyl iron particles (41 $\%_v$)	Dispersants	Polishing tools
MRF-336AG	Silicon oil	Carbonyl iron particles (36 $\%_v$)	Dispersants	Brakes

Table 1. Examples of MRF formulations with relevant applications [61].

In the following paragraphs, the chemical features of MRF components are discussed in detail.

3.1.1 Solid fraction

The magnetizable particles, generally used as dispersed phase in the MRF preparation, are iron-based materials. Iron has the highest saturation magnetization (M_s = 217.6 emu/g) among elements. Since the maximum magnetorheological effect is reached when the inter-particle attraction is maximum, this condition is achievable choosing magnetizable particle with high M_s. Particles sizes range from 0.1 μm to 10 μm. Micron-sized particles directly affect the stabilization and the high magnetization

of the MRF, as well as the reversibility of the structure aggregation process of the magnetizable particles, obtaining a MRF shear stress which can be regulated in milliseconds. Even though increasing particle sizes over 10 μm augments shear stress of MRF, the use of particles larger than 10 μm could be detrimental for the MRF stability due to sedimentation problems. Smaller particles (less than 0.1 μm) settle more slowly, but Brownian motion hinders magnetic field-induced structuration.

As mentioned above, presently high purity carbonyl iron (CI) powder is commonly used for MRFs, which meets the requirements of magnetorheological performance for industrial applications. However, due to the very high density of CI powder (d = 7.91 g/cm^3), sedimentation problems have limited its widespread use in commercial applications, unless it is subjected to particular treatments. Different methods have been proposed to avoid undesired contact between CI particles, and to reduce the CI powder density for slowing down its settlement. The shape of the magnetizable particles could be an important feature in this regard. Typically, the dispersed phase is composed of spherical magnetizable particles. However, due to their high wetted area and wire-to-wire interactions, the use of wire magnetizable particles enhances the magnetorheological effect and prevents MRF from settling. Because of the shape of the wire particles, the iron loading is not as high as that of the spherical particles. As a consequence, the yield stress of spherical-based MRFs, which is proportional to the magnetizable particle loading, is higher than that of wire-based ones. Therefore, a combination of spherical and wire particles could be a solution for the stabilization of MRF with promising magnetorheological effect [62]. The number of magnetizable particles in an MRF can range from 10 $\%_v$ to 70 $\%_v$, depending on the magnetorheological effect required, as well as on the allowed sedimentation range.

For the dispersed phase of an MRF, the selection of parameters of critical variables such as chemical nature of the particles, loading in particles, particle size distribution and particle composition, and shape of the particles are important in order to obtain a performing MRF for the selected application.

3.1.1.1 Chemical nature of the particles

Typically, the iron-based materials used in the MRF formulation are carbonyl iron powder (CI, obtained by the thermal decomposition of iron pentacarbonyl), iron powder and iron/cobalt alloys [63] [64]. In fact, while most of the conventional and commercially available MRFs utilizes CI microparticles, ferromagnetic binary alloys, due to their high magnetic permeability and M_s, represent a viable choice for MRFs as alternative magnetizable particles in terms of enhanced magnetorheological effect and improved stability.

Among the magnetic alloys, FeCo is interesting because of its high M_s, permeability and low coercivity. In fact, in an MRF, the yield stress increases with the magnetic field, but, if M_s is reached, the yield stress remains constant even if the magnetic field is still increasing. That is why particles with a high M_s are best suited in the formulation of a MRF. Another way to improve the yield stress is changing the chemical nature of the particles [64] replacing the conventional carbonyl iron powder with iron alloys (such as iron-nickel and iron-cobalt, due to their higher magnetic saturation). At a magnetic field strength of 0.600 T, the yield stress exhibited by the magnetorheological material containing FeCo alloy particles is about 70% greater than that exhibited by the reduced iron-based magnetorheological material.

In the past, non-toxic and easily obtainable magnetite (Fe_3O_4) magnetic particles have been extensively used for the preparation of MRF. However, their application has been limited due to their low M_s and the related problems of sedimentation and aggregation after use [65]. The use of magnetite rod-like particles, with average diameter and length of 560 nm and 6.9 μm respectively, showed a significant performance improvement for elongated magnetic particles, suggesting that particle shape strongly affects the structuration under an external field [35]. However maghemite (γ-Fe_2O_3) together to magnetite, due to their lower density than the CI, have been applied in the MRF formulation. In order to overcome sedimentation problem, recently, Pickering emulsion polymerization method [59] has been applied to prepare core-shell-structured particles where γ-Fe_2O_3 nanoparticles consist of the

surfactant instead of conventional organic surfactants. In fact, in the Pickering emulsion polymerization method the main body is composed of magnetic nanoparticles (shell) of γ-Fe_2O_3 attached to a particle (core) of a light polymer surface such as polystyrene. The density of this core-shell structured particle is much lower than that of the metal particle and this magnetizable particles can be used for small devices due to their small yield stress values.
The possibility of synthesizing magnetizable colloidal particles of ceramic metal ferrite, with different shapes such as spheres or rods and narrow size distribution, has opened new horizons in the MRF formulation. The lower cost, outstanding erosion resistance and possibility of application at higher temperatures with no physical change are some of the main advantages that make metal ferrite-based MRFs more desirable. In this regard, the effect of the particle size of cobalt ferrite-based MRFs with solid particles produced by co-precipitation, upon the magnetic behavior, structural properties and fluid viscosity has been described [66] [67]. Recently rod shaped Li-Zn ferrite particle are used in MRF formulation as magnetizable particles [68]. Due to the low density of these soft ferrimagnetic particles MRF preparation can be formulated without a stabilizing-agent or de-agglomerating-coating. Moreover, the excellent resistance to oxidation and corrosion exhibited by ferrite-based particle makes these MRFs highly versatile and economical.

3.1.1.2 Particle loading

The properties of an MRF depend on the volume fraction of magnetic particles in the fluid (also called loading). The first and most obvious property depending on the loading is the viscosity of the fluid: the more the loading is, the higher the viscosity is. The loading is also important for the yield stress. Various studies shown that when the particle weight fraction increases, the yield stress also increases (Figure 15).

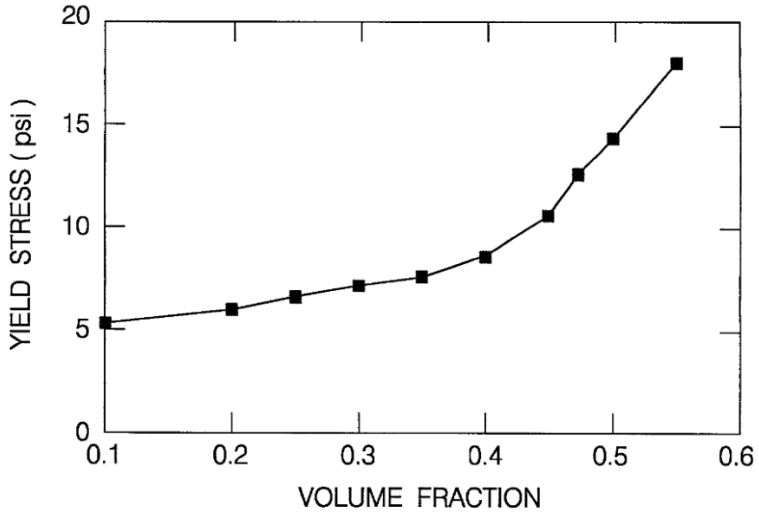

Figure 15. Yield stress (psi) vs. volume fraction of monomodal size distribution CI particles and an MRF mixture with a magnetic flux density of 1 T. (Image adapted from [69]).

3.1.1.3 Particle size distribution and particle composition

Genç et al. [18] studied the effects of dispersed phase M_s and applied magnetic fields on the rheological properties of MRFs based on two different grades of carbonyl iron powder, Grade A and Grade B, with two different average particle size of 7-9 μm and 2μm respectively. A decrease in yield stress for finer particle based MRFs is observed, due to the relatively smaller magnetization of the finer particles. The relationship between yield stress and the particle size distribution has been reported by [70]. It is possible to increase the yield stress by raising the proportion of iron powder but there is also an increase in the off-state viscosity. The solution proposed by the authors to overcome the drawback is to use an MRF formulated with a bi-dispersed distribution of particles.

Then, the yield stress increases whereas the off-state viscosity is reduced. Although most MRFs utilize a substantially non-magnetic carrier fluid (mineral oil or silicone oil), Ginder [12] employed a magnetizable carrier fluid, such as a ferrofluid, to obtain a synergistic rheological effect. The use of a magnetizable carrier medium enhances the force between magnetizable particles and thus increases the stiffness and viscosity of the MRF. In the same way, Wereley et al. [26] showed that the introduction of nanometeric particles in small concentrations enhances the yield stress and reduces the particle settling rate.

Bi-dispersed MRFs with nano-sized smaller particles were proposed ([70] [12]) in order to circumvent the problem of sedimentation and also to increase the magnetic field induced yield stress. The increase of yield stress is due to the increased force between two iron particles. Magnetic nanoparticles greatly reduce gravitational settling by increasing the viscosity and density of the medium. The percentage of particles dispersed in the carrier fluid may alter dramatically the MRF behavior. For instance, in an MRF formulation proposed from Foister in a patent [70] the effect of particle size and particle size distribution in bi-dispersed micro-sized iron particles results in a good magnetorheological performance, in terms of high values of yield stress, at a composition of 75 $\%_v$ of large magnetizable particles with size of ca. 7 μm and 25 $\%_v$ of small magnetizable particles with size of 1 μm for a total iron concentration fixed at 55$\%_v$ (see Figure 16).

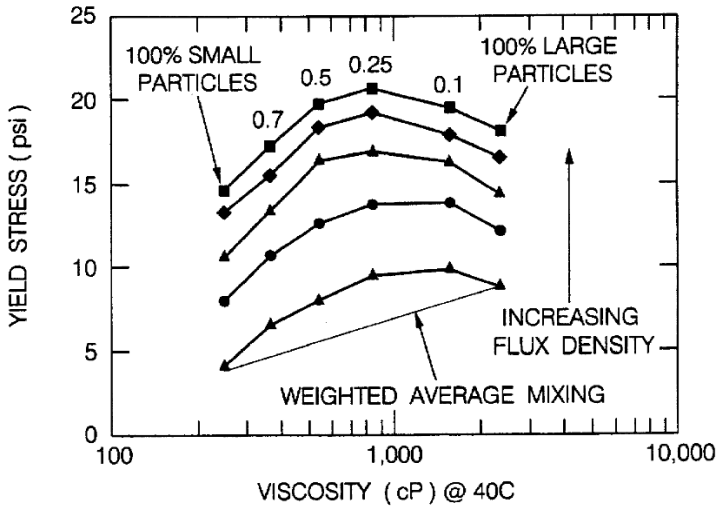

Figure 16. Yield stress versus viscosity for large particles, small particles and mixtures of large and small particles in a 55 %v total solid MRF at an increasing magnetic flux density [70].

However, this increase in yield stress is accomplished by a decrease of viscosity of the fluid at the off-state . Good results in terms of magnetorheological performance were also obtained either using a dispersed phase made up of spherical CI particles of 4 μm with a monomodal average particle size distribution or using 75 $\%_v$ of spherical CI particles of ca. 7 μm, along with 25 $\%_v$ of CI particles of about 1 μm, with a bimodal average particle size distribution. CI particles need to be processed in order to prevent undesired sedimentation.

3.1.1.4 Shape of the particles

A significant further advance in improving the stability and increasing the yield stress of MRFs is the use of magnetic fibers instead of spherical ferromagnetic particles. López-López et al. [71] synthesized cobalt wires and iron filaments (approx. 60 μm in length and 4-16 μm in width) and dispersed them in silicon oil. The MR properties of suspensions of magnetic fibers, in particular the Bingham yield stress is about three times greater compared to that measured for similar suspensions of spherical particles. Generally, MR materials use spherical particles, but such particles do not provide the requisite packing density and interaction area for yielding the necessary attractive forces

between particles at moderate magnetic fields. Then, Starkovich et al. [72] studied the use of controlled-shaped particles, more precisely disk, rod, cube, prismatic, tetrahedral and hemispherical shaped particles in magnetorheological materials to increase yield-stress of the material. They found that the forces which are proportional to the yield stress of an MRF having cubic particles provide 170 times increase over conventional spherical particles and a 10 times increase over cylindrical particles.

3.1.1.5 Synthesis of CI magnetizable particles

As mentioned above, among ferromagnetic materials selected as dispersed phase in the MRF preparation Fe and FeCo alloy particles are mostly used due to the high M_s requested in the application. These metallic particles suffer from oxidation process making difficult the obtainment of a single-phase crystals containing metallic elements. Therefore, syntheses of these metallic magnetic particles usually require stringent control of synthesis parameters. FeCo-based alloys have been prepared by means of synthetic methods including thermal decomposition, sonochemical reduction, aqueous reduction by borohydride derivatives and solvothermal synthesis. For example, oxide phase-free FeCo nanoparticles can be prepared using the polyol process ethylene glycol (EG) as a solvent and a mineralizer such as sodium hydroxide (NaOH) under refluxing conditions, and in some cases under inert atmosphere to reduce oxidation.

In order to overcome oxidation drawbacks inexpensive, non-toxic, chemically stable iron oxides such as Fe_3O_4 and γ-Fe_2O_3 have been used in the MRF formulation, due to their lower density than the ferromagnetic metals or alloys, even if their low values of M_S have somehow limited their applications.

On the other hand, the ferrimagnetic oxide particles such as spinel ferrites have excellent chemical and thermo-oxidative stabilities and low mass-density. The low density of ferrite particles makes the MRFs stable and could be considered as good magnetizable particles as the most used CI particles. For example, Li-Zn ferrite particles have been synthesized by a combustion synthesis method obtaining particles with a rod-shape morphology and high values of M_s [68].

Despite research studies are projected towards the use of new magnetizable particles with high chemical and thermo-oxidative resistance for achieving highly stable and efficient MRFs, CI particles are the typical magnetizable particles considered in the MRF formulation by the most important MRF provider. Figure 17 shows the pathway for the production of finished CI magnetizable particles suitable for the preparation of MRFs. CI powder is produced by thermal decomposition of liquid iron pentacarbonyl [$Fe(CO)_5$], which, in turn, is prepared by reaction of carbon monoxide with iron, and purified by distillation. In the course of the decomposition process, spherical iron layers form upon a nucleus, thereby achieving raw CI powder with an onion-like structure, which confers to raw CI powder a “hard” nature. The decomposition conditions determine the main properties of the intermediate products, including the particle size distribution. The finished CI powder suitable for MRF preparation is processed with subsequent treatments in order to reduce its high-density due to the onion-like structure. In particular, annealing under hydrogen and coating with specific compounds are the commonly used techniques for the preparation of finished CI powder with “soft” nature.

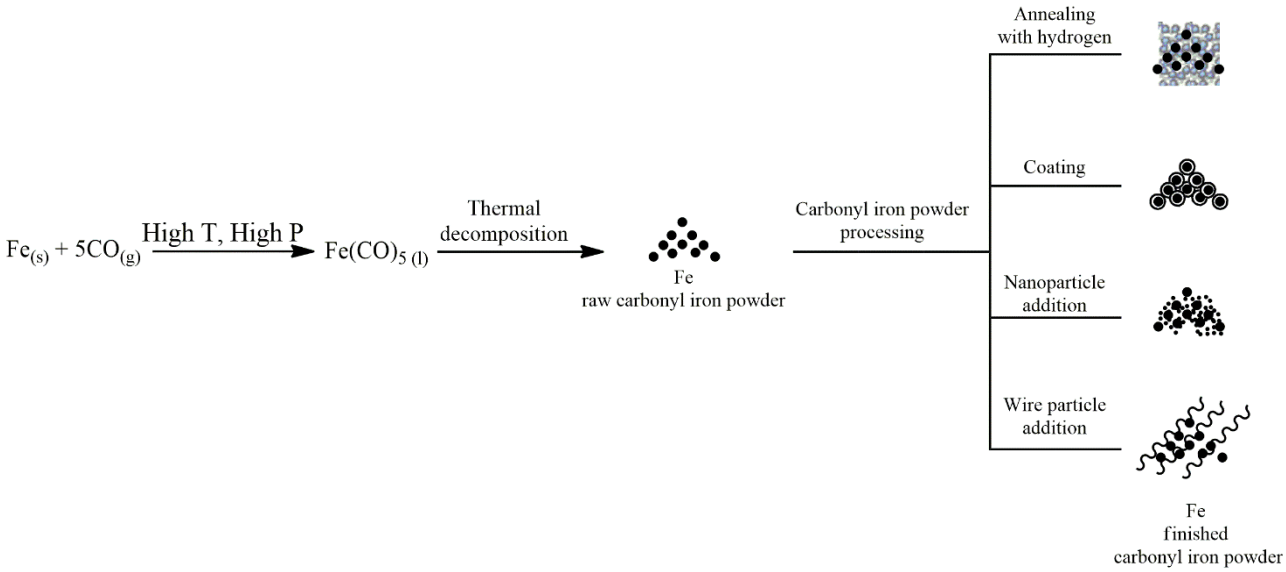

Figure 17. Pathway for the production of finished CI magnetizable particles suitable for the preparation of MRFs [61].

To overcome sedimentation problems of magnetizable particles in the MRF formulation, other methods such as coating with polymeric film onto the surface particle and the addition of nanoparticles or wire particles have been proposed [62] for CI magnetizable particles. These issues will be discussed in the following sections.

3.1.1.6 Coating process of CI magnetizable particles

Recent work on stabilization of MRF focused on the coating of CI particles with formation of composite particles with core-shell structure to overcome sedimentation problems [73]. Since coating materials have low or no magnetic susceptibility, coating process can affect the magnetic behavior of CI particles. The shell part is chosen so to efficiently prevent agglomeration of particles and to protect core materials from external oxidation. Organic polymers are the commonest coating shells used for the magnetizable particles of MRF. Figure 18 shows two pathways commonly followed for the coating of CI particles. The coating route *a*) consists of the polymerization of suitable monomers onto the surface of activated CI particles. Monomers represent small molecules which combine themselves chemically to produce a polymer, *i.e*. a very large chainlike or network molecule. The first step of the coating process is the surface treatment of the magnetizable particles, in order to activate their surface and also to enhance the compatibility between particles and monomer. The coating is obtained after polymerization of the as-modified magnetizable particles with the monomer and the stabilizer. The coating route *b*) of Figure 18 involves the activation of the CI particle surface by adsorption of the polymer, dispersed in an organic solvent, with subsequent stabilization of the polymeric coating by water extraction in the presence of emulsifiers and stabilizers. The interaction between the polymer and the CI particles is represented by the adhesion of polymeric molecules to the CI particle surface. This process is a surface phenomenon which creates a film of the polymer on the surface of the CI particle.

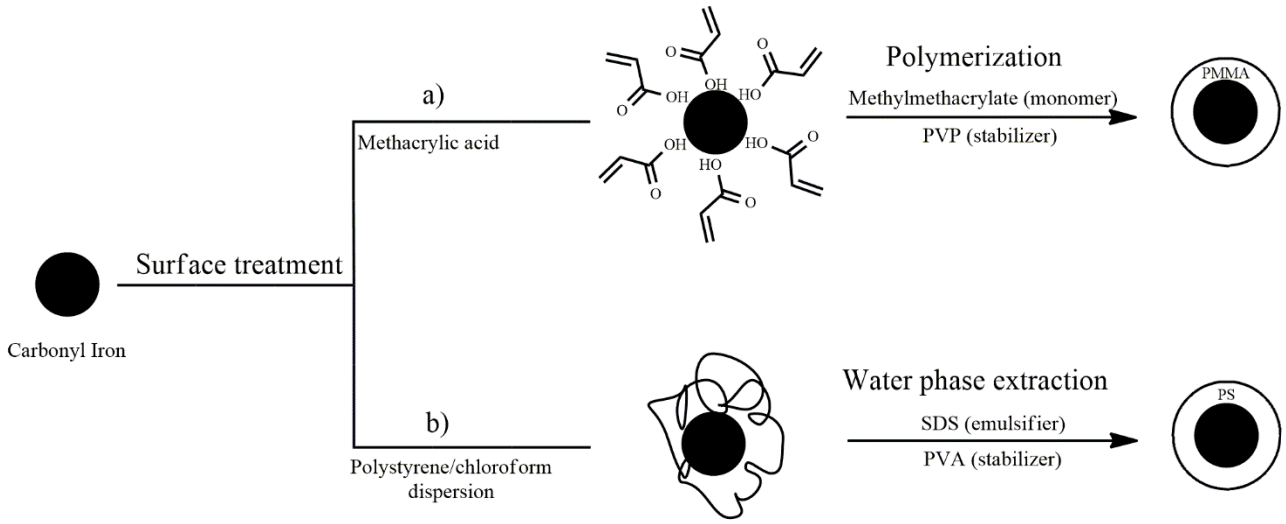

Figure 18. Pathways for the coating of CI magnetizable particles suitable for the preparation of MRFs. PVP = polyvinylpyrrolidone; SDS = sodium dodecyl sulphate; PVA = polyvinyl alcohol [61].

Coating of the activated CI particles results in lower sedimentation of the MRFs, due to the reduced density difference between the dispersed phase and the continuous phase. The coating parameters, which affect the magnetorheological effect and the MRF stability, are the surface morphology of the magnetizable particles and the mass ratio of the polymeric layer. For mineral oil based MRFs, CI particles are coated with polymers such as polymethylmethacrylate (PMMA) [74] or polystyrene (PS) [75]. In MRFs prepared with CI coated with PMMA, a significant improvement of stability has been observed, together with a detrimental decrease in the yield stress when a magnetic field is applied to the MRFs. CI/PS composite magnetic particles enhance significantly the sedimentation stability of the MRF suspension which also possesses good MR performance. For silicon oil based MRFs, CI particles are coated with a natural polymer such as guar gum [76], which leads to an increase in the MR effect and an MRF stability due to the lesser aggregation of the particles. In addition to organic polymers, other compounds such as silica [77], cholesterylchloroformate [78] and carbon nanotubes [79] can be used as coating shells for CI particles. MRFs based on CI/SiO_2 particles showed good resistance to oxidation and lower density than uncoated CI particles. All coated MRFs are characterized by a smaller magnetorheological effect. Coating using carbon nanotubes improves MRF stability but, at the same time, it affects yield stress and elastic properties of the composite based MRF.

3.1.1.7 Addition of wire particles to CI particles

The magneto rheology of magnetizable spherical particles-based MRF has attracted more attention in comparison with wire-shaped ones. Fibers significantly enhance the MR effect, due to their shape anisotropy and to the existence of higher friction, but volume fraction of iron particles is limited owing to the large wet area of tubular microwires and reciprocal interaction of the wires. Therefore, the yield stress of these fluids is lower than that of conventional MRFs which are made with a greater content of spherical particles. It should be noted that if the same percentage of particles is considered, the microwire-based MRFs show higher yield stress and slower sedimentation in comparison to spherical-based ones. Thus, a combination of CI spherical particles and iron nanowires has been applied to increase yield stress and overcome the sedimentation problem. FeSiB alloy microwires (instead of CI microspheres) in combination with mineral oil have been used to prepare a new MRF [80] which showed a correlation between the redox potential of the magnetizable particles and the size of the FeSiB microwires. In fact, the smaller particles were endowed with a lower magnetic saturation and hence with a lower yield stress in magnetic field. An amorphous magnetorheological

fluid composed of CI particles and Fe nanowires showed an increase in the yield stress and stability of MRF with the increase of the weight percentage of iron nanowires [81].
Another method to achieve an improvement of viscoelastic characteristics and of the stability of MRFs consists of the addition of carbon nanotubes to CI-based MRF (Fang, 2009). Using nanowires in MRFs is a good practice for enhancing their stability, but respect to the addition of nanoparticles, wire-particles are difficult and expensive to produce, restricting their wide usage.

3.1.2 Carrier fluids (continuous phase)

The second component of the formulation of an MRF is the carrier, which represents the continuous phase in which the magnetizable particles are dispersed. The carrier fluid plays an important role for the MRF properties and applications [82]. Significant features of the carrier are: compatibility with the magnetizable particles, chemical stability, density, viscosity and vapor pressure. The polarity of the carrier fluids characterizes the affinity with the magnetizable particles. Viscosity is one of the most important characteristics of the continuous phase in MRFs: a low viscosity of the carrier fluid can lead to instability and sedimentation issues, whereas a high viscosity of the carrier fluid can solve sedimentation problems but can also result in MRFs which result too viscous (even in the absence of a magnetic field) to be used in some applications. Low vapor pressure carrier fluids are preferred for the preparation of the MRF because they can be hardly vaporized and thus used in a wide range of temperatures. The commonest carrier fluids used for MRF preparation, grouped according polarity and viscosity, are:
a) Petroleum-based oils and mineral oils, synthetic hydrocarbon oils, which are a-polar and present a wide range of viscosity.
b) Silicone oils, which are polar and poorly viscous.
c) Polyesters and polyethers, which are polar and highly viscous.
d) Water, which is polar and with a low environmental impact, in combination with glycol, which is polar and with thickening feature together to silica nanoparticles.
e) Ionic liquids, which are highly viscous and with a low environmental impact.
Petroleum-based oils are hydrocarbon mixture obtained from crude oil refining by means a distillation process. Hydrocarbon oils are obtained, depending on the chosen distillation fraction, with different kinematic viscosity grades which range from roughly 10 cSt to 600 cSt at 40 °C and a working temperature between –40°C to 150°C. Synthetic oils are artificially made and produced using chemically modified petroleum components, but can also be synthesized from other raw materials. For instance, poly-α-olefin (PAO) is a polymer obtained by a catalyzed polymerization of a α-olefin. Synthetic base oils can be produced with the same rheological properties of mineral oils, even if permit a good low- and high-temperature viscosity performance at working temperature together to a good resistance to the oxidation processes. MRF-based hydrocarbon oils are typical of the type of fluids used in dampers having a dynamic shaft seal. In fact, for magnetorheological dampers and valves, a synthetic hydrocarbon-based oil is the widely adopted carrier fluid because it offers the best performance for the MRF-based device. In addition, this MRFs are formulated to have a very low viscosity as a very low off-state is necessary in order to effectively implement semi-active control in this application. The combination of carefully chosen particle morphology and highly effective anti-wear ingredients allows MRFs to be used reliably in conjunction with dynamic seals. This linear MR damper has also served to demonstrate that the stability of the MRF suspension is not an issue for this class of devices. Even though the MRF used in this damper was formulated to have a very low plastic viscosity, particle separation and settling do not represent a problem. The additives in the fluid are very effective in preventing caking or particle sedimentation.
Silicone oils is versatile because of its high operating temperature range (from –50 to 200 °C), low thermal coefficient of viscosity, non-flammability, high lubricity, electrical insulating behavior. It provides non-oxidizing environment, is non-toxic and is endowed with high shelf-life and represents the widest choice of viscosity [83]. MRF-based silicone oils exhibit nearly an order of magnitude greater viscosity at low shear rate as compared to the other MRFs. For brakes and for all the

applications which used MRF in the off-state for most of the time and where the difference between the viscosity in the off-state (low viscous fluid) and in the on-state (high viscous fluid) is a crucial parameter, oils with low viscosity, like silicone oil, are preferred as carrier fluids.
Polyesters are condensation polymers formed by the reaction of polyols, organic molecules with multiple hydroxyl (-OH) functionalities, with saturated or unsaturated diprotic organic acids. Polyethers are synthesized by a condensation polymerization of monomers through an ether linkage (C-O-C). A variety of polyesters and polyethers are manufactured, ranging from engineering fluids to elastomers, with high viscosities. The use of these highly viscous polymers as carrier fluids in the MRF formulation are indicated in the shock absorbers application.
Water has the lowest environmental impact in the preparation of MRFs. The working temperature range from 5 °C to 90 °C, and this range can be extended by addition of suitable amounts of glycols. Water-based MRFs should not be used in an unsealed system. Water-based MRFs manufactured in order to have a consistency of a light thixotropic paste can be applied exceptionally well in small sealed devices. However, they are better suited for high shear rate applications. In polishing tools, the concentration and the type of the dispersed phase of the MRF are the parameters which affect the quality of the polishing operation. Considering costs, environmental issues and cooling characteristics of the surface, which is to be polished, water is the best candidate as carrier fluid for magnetorheological polishing processes.
A new class of carrier fluids used for the synthesis of MRFs is represented by ionic liquids. Ionic liquids are mainly constituted by ions and their physical-chemical features depend on the nature of these ions. An ionic liquid is a salt in which the ions are poorly coordinated, which makes these solvents liquid below 100°C, or even at room temperature (in this case they are referred to as RTIL, room temperature ionic liquids). The main characteristics of the ionic liquids are the stability and the environmentally friendly impact associated to their negligible vapor pressure and flammability. Ionic liquids as carrier fluids lead to an improvement of MRF stability, since a decrease of particle aggregation is obtained due to physical adsorption of the ions on magnetizable particle surfaces giving rise to steric repulsion between the dispersed particles. However, investigations concerning compatibility of the dispersed phase with ionic liquids as continuous phase, as well as studies on the relationship between particle surface and constituents of the ionic liquids, are still currently under way [84][85]. Despite the number of researches carried out to date to determine the effect of the new polymer- and ionic liquid-based carriers on the MR effect and stability of the MRF, no material or composition has been still found satisfactory enough for industrial applications. Further studies are needed in this direction, while silicon oil or mineral oil are still used in most applications of magnetorheological fluids as the carrier fluid.
Testing of new carrier fluids as continuous phase for the preparation of MRFs is directed toward materials that allow to overcome sedimentation problems, still maintaining the MRF off-state viscosity low. Polyethyleneoxide in water [86], polyethyleneglycol [87] and polyacrylic acid in water [88] have been used in MRF formulation as polymeric carriers, while for hydrocarbon-based MRFs poly-α-olefins and polyisobutylene/polybutene systems (Kim, 2011) have been utilized. These polymeric fluids render MRFs more stable and enhance considerably the MR effect but have a detrimental effect on the “off-state viscosity” (which undesirably increases). Only high molecular weight polyacrylic acid leads to the reduction of system stability since hydrophilic adsorption acts against spatial repulsion. The MRF can be stabilized using a correct concentration of the polymer with low molecular weight.

3.1.3 Additives

The continuous and dispersed phases of MRFs are usually added of apposite substances that provide supplementary rheological properties, such as the viscosity of the carrier and the inter-particle friction that prevent sedimentation and agglomeration. Erosion is another problem caused by inter-particle contact friction in fluid flow which leads to an irreversible thickening of the suspension and to a decreased MRF performance. For this reason, together to dispersant and thixotropic agents, anti-

friction and anti-abrasion/erosion compounds are usually added to protect the magnetizable particles and to modify the rheological features [89]. The used additives are similar to those found in commercial lubricants, aimed at inhibiting gravitational settling, promoting particle dispersion, enhancing lubricity, modifying viscosity and limiting wear.
Additives used as dispersants, such as surfactants, which are amphiphilic molecules constituted by a hydrophobic and hydrophilic part, can modify a particle-surface interaction force. Adsorbed surfactant molecules, as shown in Figure 19, can alter the van der Waals attractive force, electrostatic force, hydrophobic force, as well as provide a steric barrier to contact of solid particles suspended in a liquid. In the case of an MRF, the addition of surfactants increases the particle interaction at the interface between the dispersed phase and the continuous phase and leads to inter-particle repulsive forces. In this way the agglomeration process and the tendency of sedimentation of the particles are reduced.

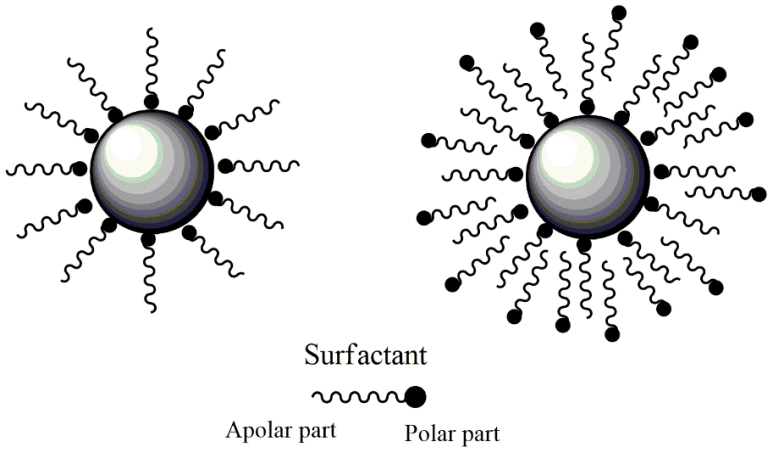

Figure 19. Surfactant interaction on a single-layered and double-layered particle [61].

Iron naphthenate and iron oleate are typical dispersant additives of the MRF composition for decreasing sedimentation of the particles. These two compounds differ for the organic moiety which interact with the magnetizable particles: naphthenate anion is composed by a cycloaliphatic chain while oleate anion is constituted by a long alkyl chain. Both of them form a barrier around the magnetizable particle in order to prevent agglomeration.
The off-state viscosity of an MRF ranges between 0.20 to 0.30 Pa*s at 25 °C, and the operational temperatures between –40 °C (233 K) to + 150 °C (323 K), depending on the nature of carrier fluid. Without a magnetic field, the MRF has a liquid behavior presenting a low viscosity. When a magnetic field is applied, the particles interact each other as dipoles and form chains: the viscosity increases and the MRF behaves like a semi-solid. This phenomenon is reversible and the yield stress of the fluid, which is defined, as above-mentioned, as the stress level at which a material loses its elastic properties after a performed deformation during MRF active state (on-state), can be controlled very accurately by varying the magnetic field intensity. Generally, for an applied magnetic field of 150-250 kA/m (0.188 T – 0.313 T or 2-3 kOe), the yield stress is situated between 50 and 100 kPa. In the MRF formulation thixotropic additives are added as viscosity modifiers for a progressive decrease in viscosity during the on-state phase when the magnetic field is applied, followed by a gradual recovery when the stress is removed. As shown in Figure 20, when the MRF is in the off-state, thixotropic compounds (at rest) form a gel by means of intermolecular secondary bonding. This supramolecular network structure can be broken under shear resulted during the MRF on-state period (sheared).

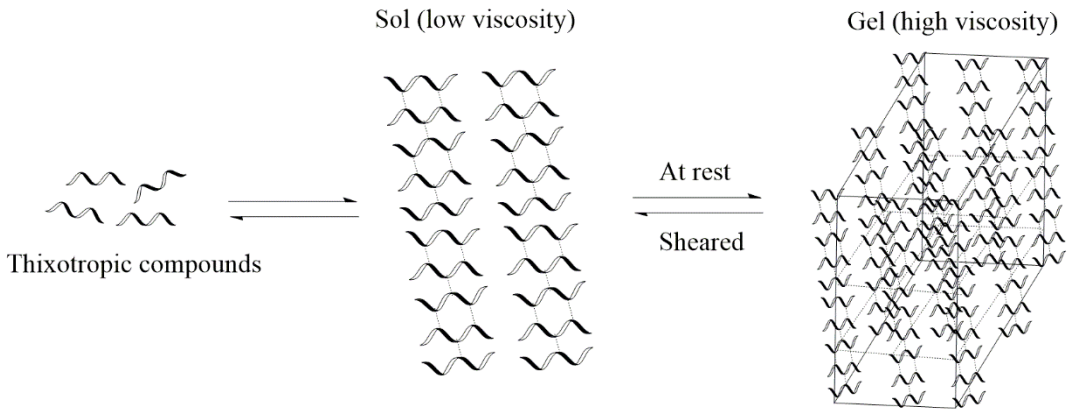

Figure 20.Illustration of the formation of the supramolecular network and thixotropic behaviour [61].

Thixotropic agents such as greases, metallic soaps as lithium stearate and/or sodium stearate, organoclays, silica gel and carboxylic acids [6] [90] are added to produce a stable suspension, fix sedimentation issues and change initial viscosity of the MRF. For instance, stearates produce physical entanglements which increase considerably the viscosity of the MRF at ultra-low shear rates, by entrapping and immobilizing magnetizable particles. As the share rate is raised, these additives permit MRF to maintain the fluid thickness thin and to prevent thickening of the fluid after several cycles of use. The use of fumed silica particles in combination with CI particles successfully prevent sedimentation without any change in the MR effect [91]. Many researchers have pointed their attention to investigate the effect of additives fraction, in particular high viscosity materials such as grease, on the stability of a MRF [92] [93] [94]. It has been found that using grease results in a higher MRF stability without significant change in the MR effect, the influence of particles percentage on the increasing yield stress being more promising at stronger magnetic fields.
The use of additives in the MRF formulation is also a common method to increase of the yield stress. A method to obtain the improvement of the MRF yield stress consists of passing MRF through a porous media [95] [96].
Anti-wear additives are often added to a MRF in order to enhance the performance of the fluid beyond its wear-protection action, through its antioxidant functionality. In fact, the chemical nature of these additives permits the control of the oxidative decomposition of the continuous phase of the MRF, decreasing the rates of chemical reactions with oxygen of the dispersed phase particles of the MRF. Moreover, these additives reduce wear of the magnetizable particles of the MRF adhering to the metal surfaces and forming a protective film.
Some additives are used with the aim of reducing friction and abrasion/erosion processes (see Figure 21) in the MRF based devices. An additive package composed of tolutriazole compound, an ashless dithiocarbamate, and an organomolybdenum dithiocarbamate can be inserted in the MRF formulation in a 0.05-5.00 $\%_w$. Other compounds used as anti-friction and anti-wear agents are organomolybdenum and zinc dialkyl dithiophosphate [97].

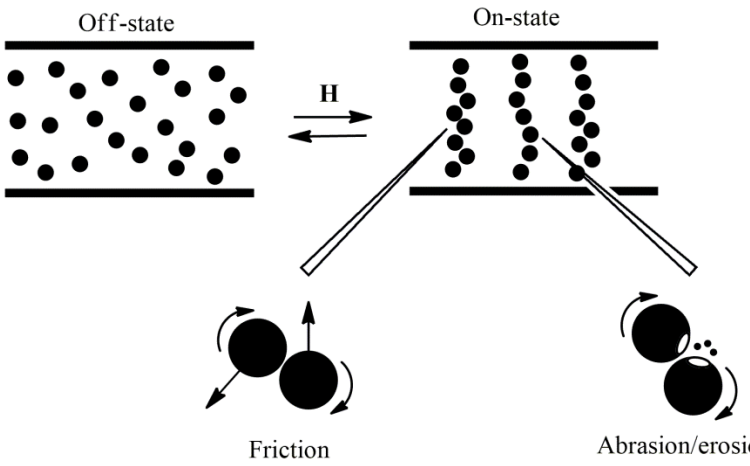

Figure 21.Schematic view of friction and abrasion/erosion processes among CI particles in MRFs [61].

Hydrocarbon carrier fluids, which by virtue of their chemical feature are essentially non-polar, have not suitable lubricant properties for some applications, including shock absorbers. These carrier fluids are thus used in mixtures with known lubricant liquids, such as liquid synthetic diesters. 2-ethyl hexyl sebacate, for the presence of two branched alkyl groups and two ester groups, as shown in Figure 22, is essentially very miscible in nonpolar liquid while having a good polarity and represents the plasticizer agents more used in the formulation of stable MRFs.

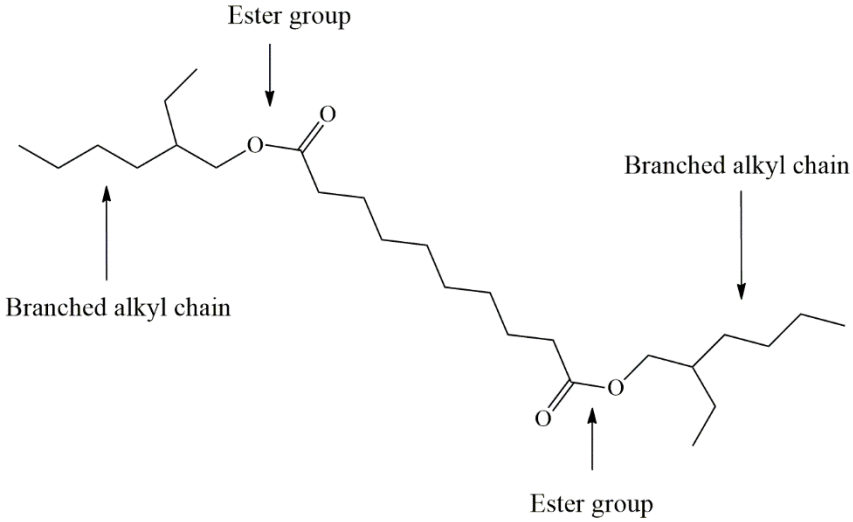

Figure 22. Structure of the 2-ethyl hexyl sebacate plasticizer agent [61].

One can think to formulate MRFs using only anti-friction and anti-wear agents as additives, together with magnetizable particles and the carrier fluids more suitable for the chosen application. Since MRFs are used for long terms, in order to reduce the rate of thickening of the MRF the use of dispersant and thixotropic agents is mandatory. Currently, the compounds commonly used for this purpose are lithium stearate and iron oleate. Furthermore, among the existing methods, it seems that using magnetizable nanoparticles and stabilizing additives such as fumed silica in MRF preparation gives satisfactory results in terms of a higher magnetorheological effect and stability.
The amount of additive used in the MRF is an important parameter to be considered. For instance, an increasing amount of stearic acid added to a MRF resulted detrimental for the yield stress of the MRF [98].

3.1.4 Addition of nanoparticles

The composition of a MRF is similar to that of a ferrofluid, but the use of magnetizable nanoparticles instead of micrometric particles permits to obtain fluids with distinct behavioral differences.

Nanoparticles are characterized by nanometric length scale dimensions (under 100 nm), which confer peculiar physical-chemical properties in comparison to the same materials at a micrometric scale. This is due to the fact that nanoparticles have a high value of the surface to volume ratio [99]. As far as the magnetic properties are concerned, nanoparticles constitute a single-domain magnetic dipole, even when magnetic field is not applied. In the case of MRFs, nanoparticles are used as solid additives so forming a ferrofluid in the continuous phase of CI based MRFs. This leads to an enhancement of MR effect since a nanoparticle "cloud" surrounds each CI microparticles, with part of the nanoparticles disposing themselves in the voids existing among CI microparticles, thus forming anisotropic structures. This phenomenon implies the breaking of CI microparticles aggregates, providing more regular chains when the MRF is subjected to a magnetic field as in Figure 23, and thus considerably increasing the yield stress [26]. In fact, upon application of a magnetic field, the micron-sized particles become polarized and gather in chains or clusters due to dipole–dipole interaction. Formation of these clusters creates microcavities within the structures which are easily occupied by ferrofluid nanosized particles producing a kind of colloidal nanobridges [100].

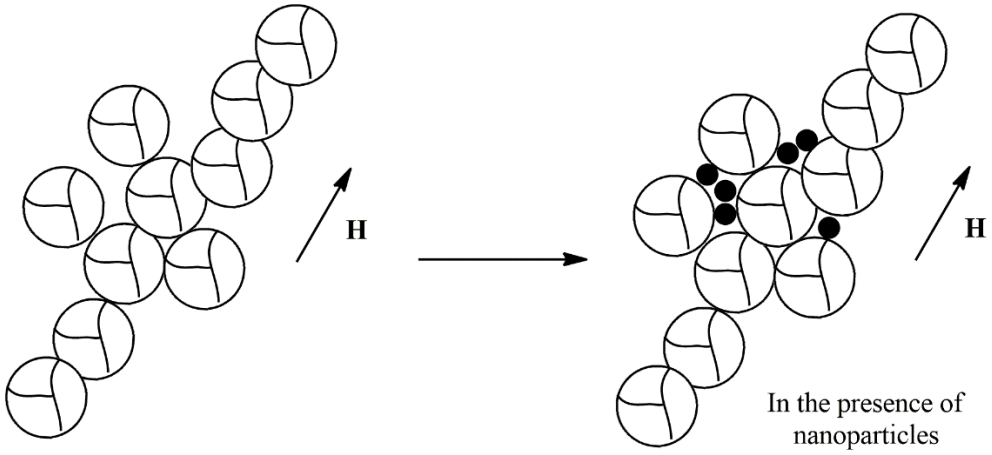

Figure 23. Schematic view of role of nanoparticles in MRFs during the on-state [61].

The improvement in the yield stress is also due to greater magnetic interactions within CI microparticle structures stabilized by the nanoparticle intercalation and characterized by a higher magnetic permeability. At the same time, the addition of nanoparticles, breaking CI microparticle aggregates, improves the MRF stability with respect to sedimentation [77]. The sedimentation can be mitigated also by the presence of nanoparticles which fill the density gap between the continuous and the dispersed phases, due to the lower density of the ferrofluid phase in the MRF.

Typical chemicals for nanoparticles to be used in MRF formulations are: iron and its compounds, fumed silica, organo-clay, graphite fibers, carbon nanotubes, and others. The addition of nanoparticles reduces the instability of the MRFs and could also affect yield stress values, both in a negative and positive way. For example, the yield stress of the MRF slightly increases by adding 1 $\%_w$ CI nanoparticles to the dispersed micro-CI suspension in lubricant oil [101]
[102]. In some cases, the yield stress is reported to be up to four times greater than that of conventional magnetorheological fluids. On the other hand, a decrease of the yield stress is reported when a threshold value of the number of nanoparticles is exceeded [18]. Some researchers tried to find a limit value for the nanoparticles percentage. For MRFs prepared without the use of viscosity stabilizer and/or modifier material, the addition of nanoparticles up to 3 $\%_v$ produces a stable magnetorheological fluid with an increase in the yield stress [103]. For MRFs stabilized with additives, exceeding the nanoparticle amount of 15 $\%_v$ induces an adverse effect and rather decreases the yield stress [26] [104].

Thus, differently from coating methods applied to CI particles, which results in the addition of nonmagnetic additives into the MRF, the addition of nanoparticles with high magnetic saturation such as iron and magnetite is a promising method for improving the performance of CI microparticles based MRFs.

3.2 Performance

The main performance of an MRF is the yield stress that the fluid exerts. It is defined as the threshold value of shear stress above which the fluid start flowing, and thus it indicates the mechanical energy necessary to break MRF chains and columns. As it has already been shown in chapter 2, it is dependent on the magnetic field intensity [52][105].

Another peculiar performance of MRFs is the turn-up ratio, which represents the ratio of the maximum achievable force in the on-state condition over the minimum force achieved in the off-state condition. The maximum force achievable on-state is related to the maximum yield stress, while the minimum force in off-state is directly linked to the carrier viscosity in absence of magnetic field. The higher the turn-up ratio is, the better the quality of the MRF. This parameter is important because it represents the main two conditions in which an MRF operates: on-state (where the yield stress is important) and off-state operability, since in MR devices the fluid persists for longer time in the off-state than in the on-state [1] [106].

Ideally, the higher the magnetic particle loading (the volume or weight fraction of magnetic particles suspended in the carrier fluid), the higher the yield stress, which turn to be detrimental for the off-state viscosity. In this latter case, the overall turn-up ratio is not the highest as possible.

Response time is another interesting performance of MRFs. Typically, as an order of magnitude, few milliseconds are sufficient to form the structures in a MRF subjected to a magnetic field; around 60% of the expected yield stress is reached when it is subjected to a magnetic field for a time greater than 0.6 ms [8].

Another interesting performance of MRF is the versatility attributed to the stably operation in a temperature range: the wider the range the better the MRF is. As an order of magnitude, this parameter ranges from -40 to 150°C, depending on the nature of the carrier fluid [4].

Table 2 summarizes performance data of several commercial and experimental MRFs.

Table 2. Fluids (in columns) and their performance (in rows) [9].

MRF	MRF-122EG http://www.lordmrstore.com/lord-mr-m/lord-mr-products/mrf-122eg-magneto-rheological-fluid	MRF-132DG http://www.lordmrstore.com/lord-mr-products/mrf-132dg-magneto-rheological-fluid	MRF-140CG http://www.lordmrstore.com/lord-mr-products/mrf-140cg-magneto-rheological-fluid	lopez lopez 2008 Preparation and Characterization of Iron-Based Magnetorheological Fluids Stabilized by Addition of Organoclay Particles	lopez lopez 2008 Preparation and Characterization of Iron-Based Magnetorheological Fluids Stabilized by Addition of Organoclay Particles	margida, 1996, MR materials based on iron alloy particles	margida, 1996, MR materials based on iron alloy particles	vicente,2010,Effect of particle shape in magnetorheology	vicente,2010,Effect of particle shape in magnetorheology	vicente,2010,Effect of particle shape in magnetorheology	dong 2012 Properties of magneto-rheological fluids based on amorphous micro-particles	lopez lopez 2005 Preparation of stable magnetorheological fluids based on extremely bimodal iron–magnetite suspensions	chand,201	iglesias,20	Lopez-Lop	Lopez-Lop	Lopez-Lop	liu, 2014,F	wu,2006,The streng
Yield stress [KPa]	32 (200 kAmp/m)	H 45 (200 kAmp/m)	H 58(200 (kAmp/m)	0,045 (9 (kAmp/m))	0,14 (9 (kAmp/m))	45 (200 H (kAmp/m))	26 (560 (kAmp/m))	,01 (120 (k	0,012 (120	0,011 (120	35 (200 kA/m)		13(200 kA	3,5(200 kA	1,3(200 kA	4,154 (2m	52,5 (400mT)		
maximum Yield stress [KPa]	34 (350(kAmp/m))	49 (290(kAmp/m))	58(200 H (kAmp/m)								41	10 (343 mA/m)		4,9 (500 kA/m)	1,7(500 kA/m)				
saturation flux density [T]	1.5	1.67	1.75	0,37	1,38			2	2	3	10		0,6						
Dynamic range	large	large	large																
Temperature range	-40 to +130	-40 to +130	-40 to +130	10 to 60	10 to 60	-50 to +20	-50 to +20	-50 to +20	-50 to +20	-50 to +20	-50 to +20	10 to 60	10 to 60	up to 150	-50 to +20	-50 to +20	-40 to +13	-50 to +200	
Reaction time [ms]	1 - 3	1 - 3	1 - 3																
Sedimentation ratio (1000 min)	2%	1%	1%	57%							5%	30%					1%	2.2% after 3 months	
Solid (weight)	72%	80,98%	85,44	carbonyl i	carbonyl i	48iron-50	38iron-4n	magnetite	magnetite	magnetite	Amorphou	carbonyl i	magnetite	carbonyl i	cobalt wir	cobalt sph	carbonyl i	carbonyl iron	
Carrier	hydrocarbon o	hydrocarbon	hydrocarbon	kerosene	kerosene	silicon oil	silicon oil	silicon oil	silicon oil	silicon oil	silicon oil	kerosene	kerosene	mineral o	silicone o	silicone o	hydrocarb	silicone oil	
additive				organocla	no	steric acid	stearic acid					oleate-co	oleic acid	magnetite nanoparticles (7.9%			(SrFe 12O	guar gum 3%	

3.2.1 Performance decay

The aforementioned MRF system, made up of a fluid matrix, particles and additives, exhibits properties that may change over time or according to the operating conditions experienced by the material. In general, a decay of initial performance can be observed in terms of sedimentation, agglomeration, in-use-thickening (IUT) and oxidation phenomena as below explained. The challenge for MRF designers is to keep the fluid performance stable for a longer time. The presence of one or more additives in the formulation of MRFs is needed to mitigate or even prevent these problems [8]. Depending on the shear rate, the temperature and the operational conditions, MRF duration may be subjected to change. LDE (Lifetime Dissipated Energy) is a parameter which can be used to predict deterioration, in terms of mechanical energy dissipated per unit volume of MRF over the expected life of a device:

$$\mathrm{LDE} = \frac{1}{\mathrm{V}} \int_0^{\mathrm{life}} \mathrm{Pdt} \qquad (27)$$

where P is the mechanical power converted into heat (and so dissipated) and V is the volume of the MRF contained in the device [107].

3.2.1.1 Sedimentation

In sedimentation, magnetic particles inside the MRF settle over time due to gravitational force, which is opposed by Brownian motion of carrier fluid molecules [108]. Since there is a big difference between particle density (7.5 g/cm^3 ca) and carrier fluid density (1 g/ cm^3 ca), the result is a phase separation in the MRF [109] due to the gravitational settling. Particles precipitate creating a neat division between the fluid and a thick layer of solid material which settles on the bottom of the container. Of course, MR effect is not the same as of an un-sedimented fluid.

Sedimentation can be studied in terms of:

- o Sedimentation rate: depending on the rate of use of the MRF, the problem of how fast the fluid sediments can also be critical;
- o Re-dispersibility: at the same time, how easy would it be for the particles to re-disperse after sedimentation is another criticality.

Depending on the application, a certain degree of sedimentation can be accepted, especially if particles are easily re-dispersed in the fluid with the operation. This is not possible when the sediment layer on the bottom of the container is so compact that is very difficult to operate re-dispersion on it. A solution to this problem has recently brought to the development of new class of materials: magneto-rheological elastomers based on a solid matrix [110].

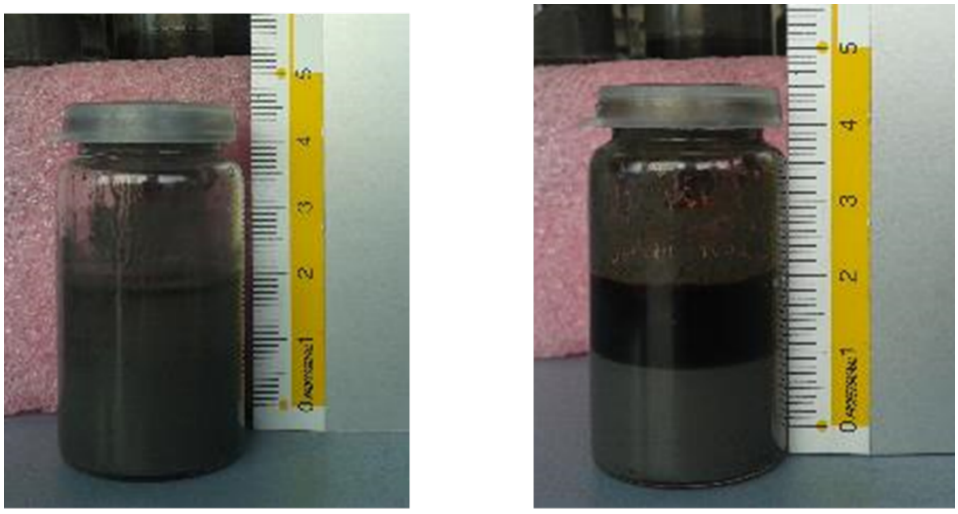

(a) (b)

Figure 24. On the left (a) a new MRF, on the right (b) the same MRF affected by a considerable sedimentation after one month of inactivity [9].

3.2.1.2 Agglomeration

Agglomeration is due to the fact that during MRF operation, or once particles are settled down, the distance between them is smaller and a remnant magnetization is observed, also in the off-state condition [111]. This internal magnetization of one aggregate attracts others creating bigger and heavier aggregates. This makes making MRF performance decay faster also by facilitating the sedimentation phenomenon. When agglomeration begins, fluid thickens, and re-dispersion of the particles becomes very difficult [107].

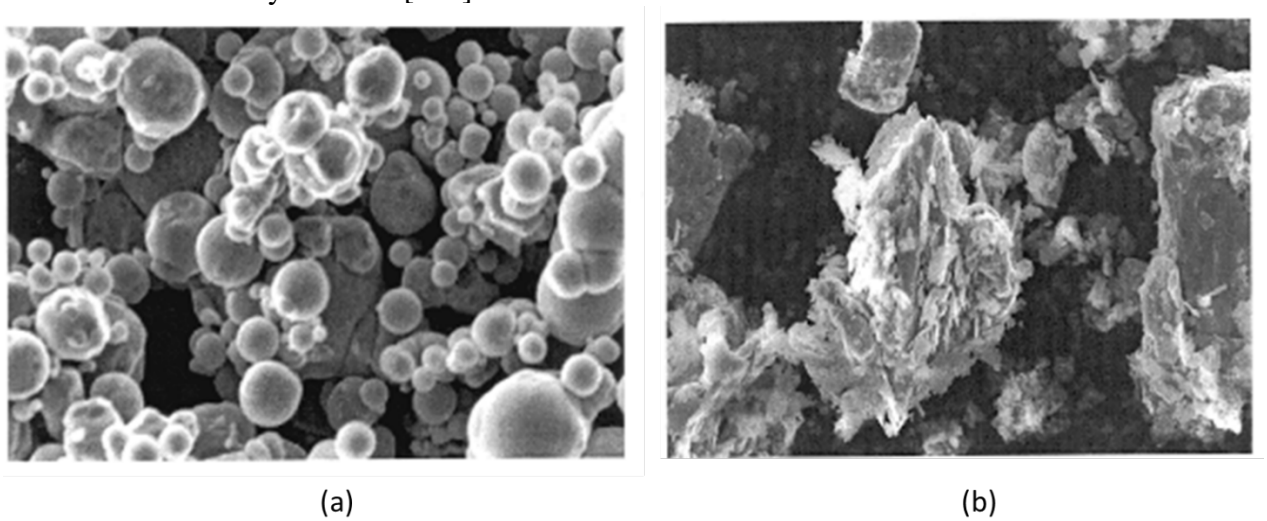

Figure 25. SEM images of unused MRF (a) and MRF after 1 million cycles of durability testing (b); from [112] [image from https://goo.gl/BFKIAo present at 07/01/2021].

3.2.1.3 In use thickening (IUT)

The IUT issue occurs when the MRF undergoes high stress and high shear rate conditions for a long period of time. In this condition, the iron particles are deformed and so their external layer peels away. The resulting fragments get dispersed in the carrier fluid, thus increasing the off-state viscosity of the MRF, degrading its properties until it is no longer usable. A clear signal of IUT is the progressive increase in the off-state force as shown in Figure 26 [49]. The deformed and broken particles adhere to each other under the action of the external magnetic field and do not separate when the field is removed, resulting in agglomeration [8].

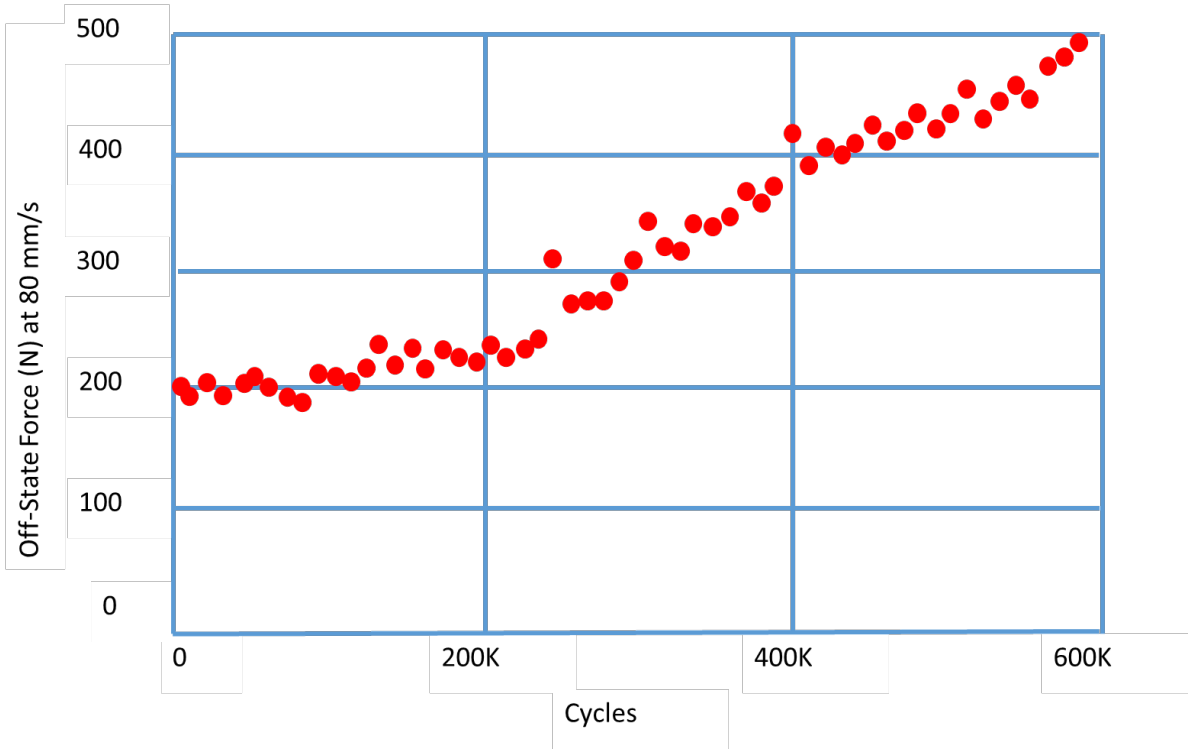

Figure 26. The effect of in use thickening (IUT): the increase of the off-state Force [9].

3.2.1.4 Oxidation

Iron magnetic particles are naturally subjected to oxidation. Depending on the working conditions, particles may oxidise when operating in an MRF-based device, or they can be accidentally used to participate to an MRF composition when they are already oxidised. Oxidation phenomenon is directly related to humidity and temperature: the higher the humidity and the temperature, the higher the oxidation. Particle oxidation directly influences MRF behavior in the real applications, because iron oxides has poorer magnetic properties with respect to pure iron (e.g., lower magnetic saturation levels). Under the influence of the external magnetic field, MRFs with oxidised magnetic particles show a MR effect decreased in reason of 20% [113] [114]. As shown in Figure 27 this is due to the iron oxide layer on the outside of the particle, forming a core-shell structure [69] [115].

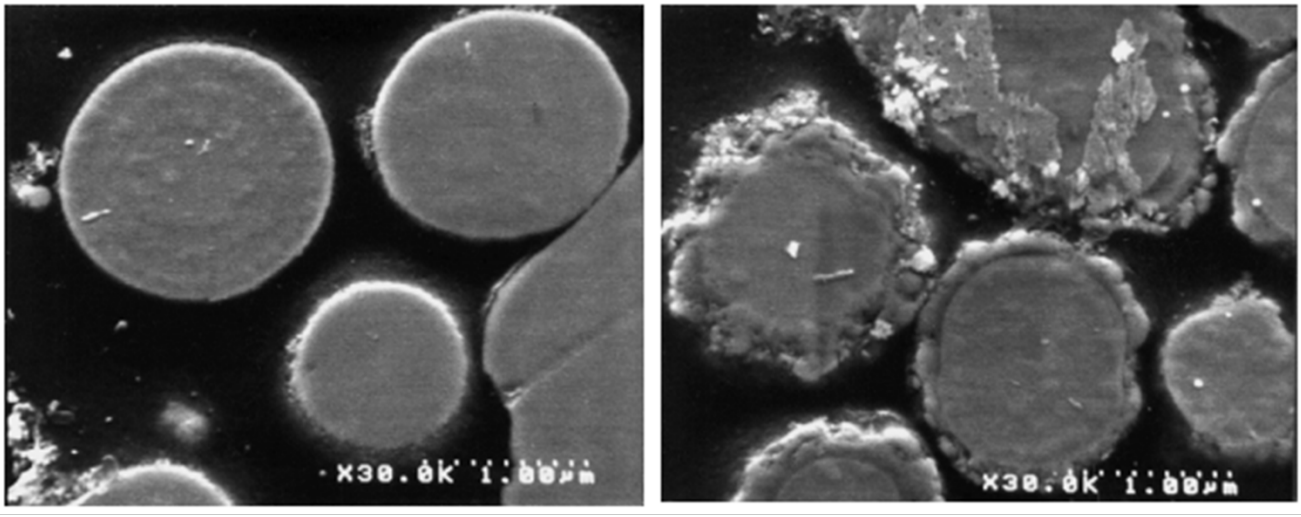

Figure 27. Effect of oxidation on carbonyl iron particles [69]: (a) SEM picture of unused particles [https://goo.gl/UE590T present at 07/01/2021]; (b) SEM picture of particles after 540 h durability test. They are characterized by iron oxide layer [https://goo.gl/6vqL1a present at 07/01/2021].

3.3 Benchmarking MRFs: Figures of merit

In order to design devices based on MRF technology it is useful to refer to Figures of merit since they provide an instrument to compare the nominal behavior of different MRFs.

First, it is useful to define the mechanical power density $\widehat{W}_m$ and electrical power density $\widehat{W}_e$ for a Magnetorheological device:

$$\hat{W}_m = \tau_y \dot{\gamma} \quad (28)$$

$$\widehat{W}_e = \frac{\mathbf{BH}}{2t_c} \quad (29)$$

where τ_y [Pa] is the maximum yield stress, $\dot{\gamma}$ is the shear rate of the fluid, **B** the magnetic flux density and **H** the external magnetic field, being t_c is the characteristic time necessary to the formation of the chains in the fluid [52].

From (28) and (29) it is possible to define the fluid efficiency ratio α as the ratio between the mechanical and electrical power densities (30):

$$\alpha = \frac{\widehat{W}_m}{\widehat{W}_e} = 2t_c \dot{\gamma} \frac{\tau_y}{BH} \quad (30)$$

Now it is possible to define tree Figures of merit as follows.

$$F_1 = \frac{{\tau_y}^2}{\eta} \quad (31)$$

F_1 relates to the concept of the minimum active fluid volume, being F_1 inversely proportional to it. When F_1 is maximized, the device size and electrical power requirement are minimized since $W_e = \widehat{W}_e V$. At the same time if V is fixed, increasing F_1 implies the increasing of turn-up ratio.

The second Figure of merit is F_2, a modification of F_1 and takes into account the weight of the fluid, since fluid density ϱ is incorporated. This is useful when designing devices where it is important to take into account the weight.

$$F_2 = \frac{{\tau_y}^2}{\eta \rho} \quad (32)$$

The third Figure of merit is F_3 and it is related to the power efficiency. Maximizing F_3 implies the minimization of electrical power consumption for a given mechanical power requirement:

$$F_3 = \frac{\tau_y}{BH} \quad (33)$$

Other characteristics of MRFs can also be addressed for benchmarking these fluids, such as stability and temperature range. In particular, these play a key role in the selection of a specific MRF for a defined application [52] [116] [117].

Chapter conclusion

MRFs are comprised in the category of smart material since their rheological properties can be changed under the application of a magnetic field. MRFs are composed of three main components: a) magnetizable micron-sized particles, b) carrier fluid and c) additives. A suitable combination of these three components allows to overcome or at least mitigate possible failures and defects (agglomeration, sedimentation, oxidation process, etc.) of the obtained MRFs as well as to select a MRF for the right application. The most important parameters characterizing an MRF behavior are stability towards agglomeration and sedimentation, yield stress and off-state viscosity of the carrier fluid. All of these parameters are affected by particle loading, particle size and chemical nature and concentration of additives. In chapter 5 a model of the interaction between these parameters and the influence on the MRF performance is presented, along with the relationship with the device characteristics.

In this chapter we tried to focus the opportunities of innovation and the critical parameters recognized in the MRF behaviors, as synthesized in Figure 28.

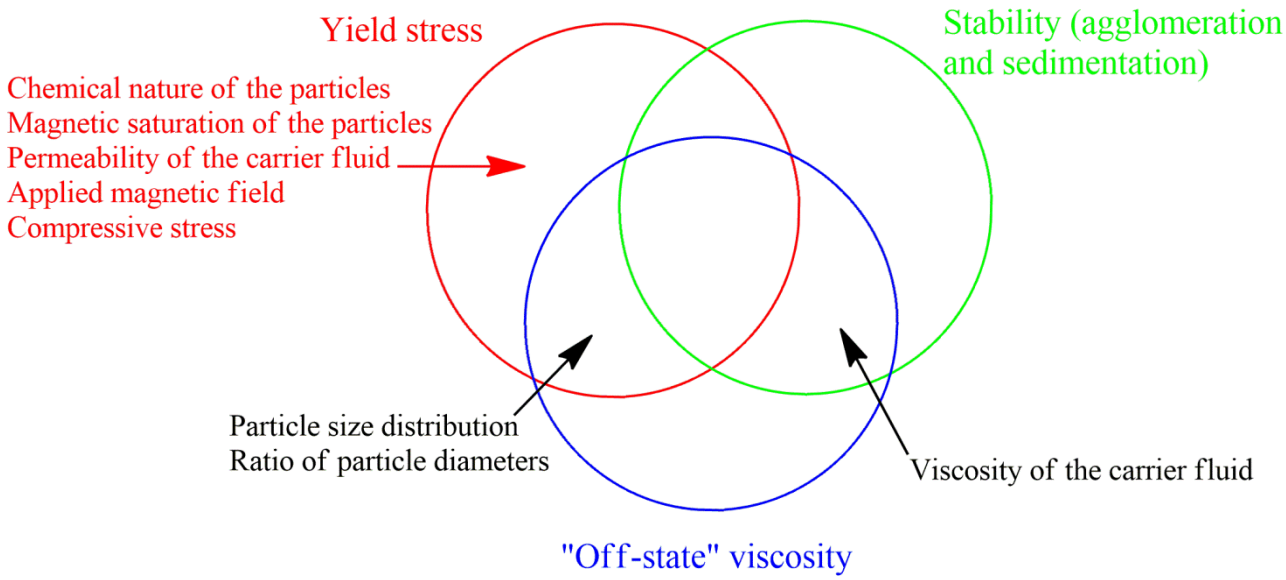

Figure 28.Main parameters characterising an MRF [61].

4. MRF applications

When designing a MRF based device, it is crucial to understand what requirements have to be met i.e., what is the function the MRF device has to perform.
One of the aims of this thesis was to put the basis for the development of an innovative device based on MRFs that can be used for manufacturing applications. For this reason, the goal of this chapter is to provide a model for the relationship between the functional requirements and the corresponding combination of chemical and physical properties of the fluids and the device.
Chapter 2 was related to the physical properties of the fluid in a device and it was structured to understand the forces and the mechanism governing the MRF operational modes.
Chapter 3, instead, was related to the chemical properties of MRFs with particular reference to how to formulate MRFs with the aim of enhancing the yield stress and the resistance to sedimentation.
To gain a full knowledge on MRF technology it is necessary to point out that physical and chemical properties have to be considered as a unicum and that when considering the overall device performance, the chemical aspect cannot be considered separated from the physical aspect and vice versa.
In other words, the same device will show different performance using two different MRFs; the same MRF will show two different performance when used in two different devices.

Generally, the classic approach to designing MRF based devices starts from the MRF formulation and is called "structure-to-rheology analysis". So, for each component (carrier fluid, solid particles and additives) a proper material is selected to confer the MRF specific properties, with particular regard to yield-stress. Then, once the MRF is formulated, the fluid properties are tested and in particular the maximum yield stress of the fluid is measured (see Figure 29).
Recently an innovative approach was introduced. It is opposite to the classic one and it is named "rheology-to-structure" [118]. Accordingly, with this new design approach, the starting point is the functional requirement based on desired rheological properties. This allows to focus on the required yield stress performance while selecting materials, thus reducing experimental costs and enhancing design process efficiency (see Figure 29).

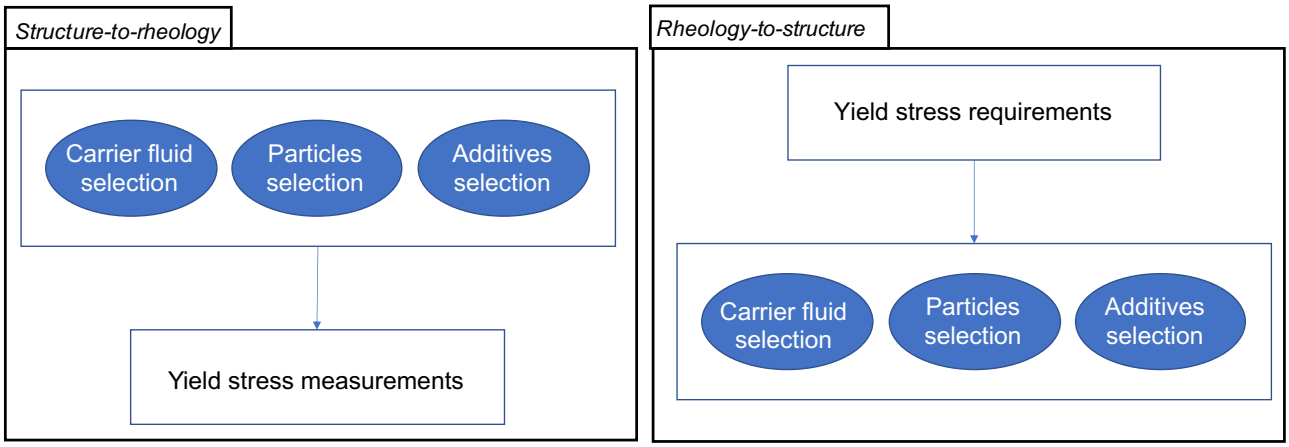

Figure 29. the two approaches to MRF formulation.

The additional step of the proposed model is the idea of taking into account other factors when formulating novel MRFs, along with the chemical variables of the fluid formulation.
Figure 30 shows the relationships between the fluid performance and its composition.

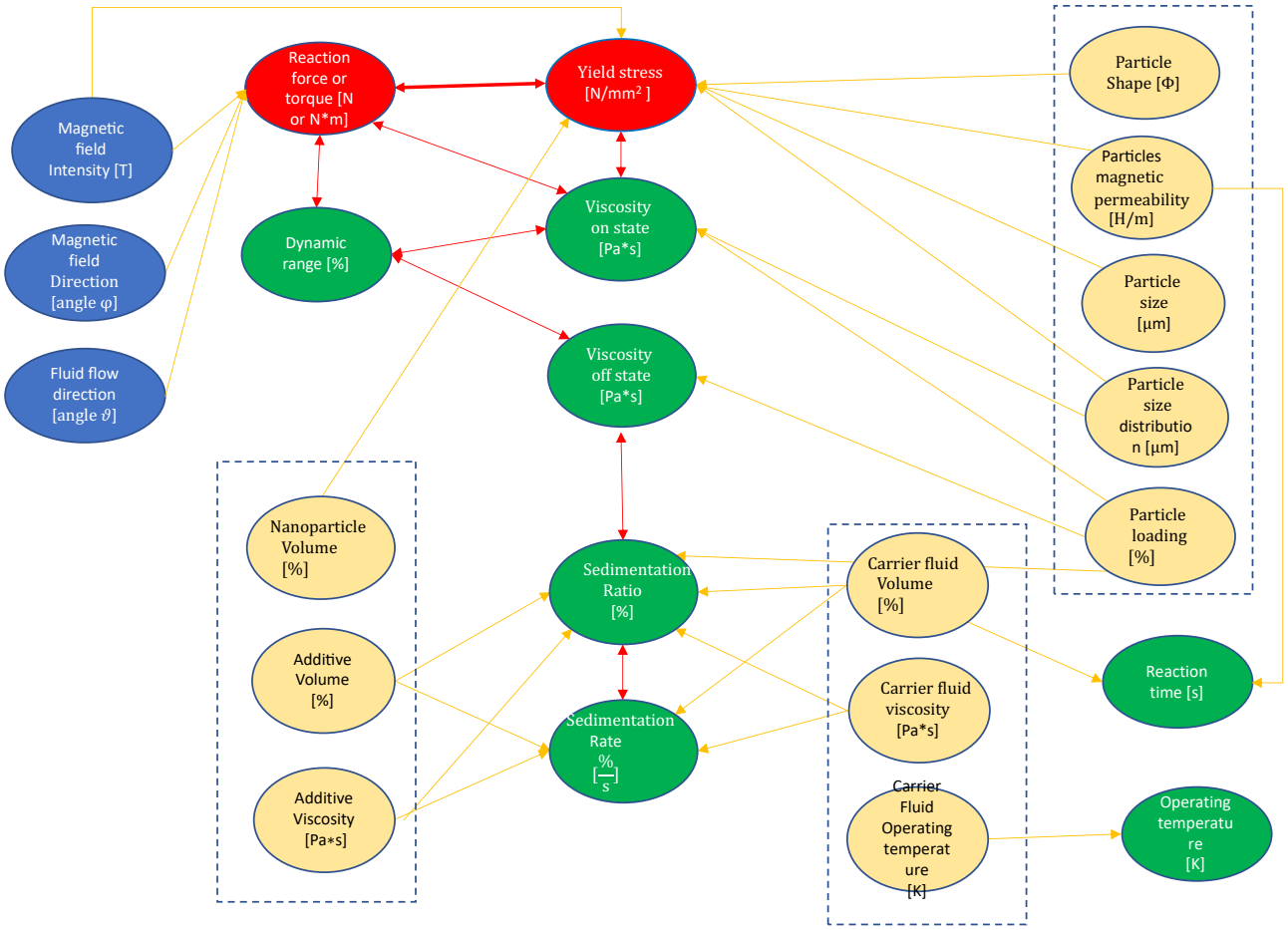

Figure 30. Model of primary factors and secondary factors.

The most important performances of an MRF, which may also be considered first level factors, are the following:

- Yield stress,
- Reaction time,
- Viscosity on-state,
- Viscosity off-state,
- Operating temperature,
- Sedimentation rate and sedimentation ratio.

First level factors have a direct impact on the performance or influence MRF characteristics; second level factors have a direct impact on first level factors.
The dynamic range is given by the difference between the viscosity on-state and the viscosity off-state.
Figure 30 highlights and summarizes what has been explained in chapter 3, which is the relationship between the first levels factors and second level factors which are represented by the parameters to be taken into account when selection the materials for the carrier fluid, the solid fraction and the additives.

It is important to note that in this scheme and model the reaction force or torque are represented: these are the most important feature or performance when considering a MRF based device. Yield stress influences this performance, in fact the relationship is represented with a strong link, but it is not the only factor: the external magnetic field (in terms of direction and intensity) has to be considered too.

Furthermore, the flow direction with respect to the direction of the magnetic field has to be considered. This means that the operational mode, and so the physical way in which the fluid is operated must be carefully studied when designing an MRF based device.
Devices based on MRF technology demonstrate highly desirable features like high controllability, fast reaction, and a simple interface between electrical power input and mechanical power output. These aspects make MRF technology attractive for many applications in different fields: civil engineering, manufacturing, biomechanics, automotive, etc.
In the previous chapters it has been shown how MRFs are can be operated and modelled (chapter 2) and how they can be formulated (chapter 3).
The aim of this chapter, instead, is to review many different MRF applications to show how the model proposed can explain the relationship between the functional requirements and the corresponding combination of chemical and physical properties of the fluids and the device (and so the MR operational mode selected) to provide a rationale to select the best fluid for the specific application.

Table 3 contains some examples of MR devices, the functional requirements they have to fulfil (depending on the application) and the characteristics of the fluid used. These are classes of applications: this means that, for every field of application, the ones presented below are the typical device in terms of operational mode/MRF composition. Note that in the "FLUID" column, the subscript "v" close to the symbol % means that the volume percentage is considered here.

FIELD	FUNCTIONAL REQUIREMENT	MRF FEATURES	FLUID	REF
MANUFACTURING; PROCESS	OPTICAL POLISHING (Valve+ Squeeze modes)	• High concentration of magnetic and abrasive particles • High resistance to oxidation • Low environmental impact • Low sedimentation	• 36%v CI, • 55%v water, • 6%v cerium oxide, • 3% stabilizers	[119]–[121] [122] [123] [124]
MANUFACTURING; TOOLING	FLEXIBLE FIXTURING (Squeeze mode)	• High yield stress	• 46%v –50%v CI • silicone oil	[125] [126]
	CHATTER SUPPRESSION (valve on shear or squeeze mode)	• High yield stress • High resistance to sedimentation	• MRF 336AG by Lord • $36\%_v$ of carbonyl iron particles • patented additives	[127] [128] [129] [130]
CIVIL ENGINEERING;	SISMIC DAMPER (Valve mode)	• High off-state viscosity • High on-state viscosity • High yield stress • Very low sedimentation • Thermal stability	MRX-140ND • 40%v CI • Hydrocarbon oil, • Patented additives	[1], [131], [132] [49]
AUTOMOTIVE;	SUSPENSION DAMPER (Valve mode)	• Low off-state viscosity • Low abrasion and friction • Thermal stability	MRX-126PD • 26%v CI, • Hydrocarbon oil, • Patented additives	[49] [83], [133] [134]
BIOMEDICAL; PROTHESIS	CLUTCH and BRAKE (Shear mode)	• High yield stress • Low off-state viscosity	• 28% CI, • Perfluorinated polyether (PFPE) oil MRF-132DG • 32%v CI, • Hydrocarbon oil, • Patented additives	[135] [136] [135], [137][138]

Table 3. MRFs applications, collected on the basis of the field of application, the functional requirements for the device, the features of the fluid, the selected fluid and references [139].

Here below we provide some deeper detail of the applications resumed in table 3.

4.1 Manufacturing application classes

Despite the interesting properties of the MRF's, still few classes of applications can be found on the available literature. Here below we provide two main classes of examples, one already available at industrial level while the other is still in the experimental phase.

4.1.1 Optical polishing

Nowadays, this manufacturing process is used for industrial applications. It exploits the friction characteristic of MRFs to obtain a given roughness of the treated surfaces lower than 1nm. The multiple axis CNC polishing machine uses a slurry of MRF running on a wheel-shaped electromagnet against which the workpiece is pushed [120], [122].
On the interface between the lens and the MRF slurry the MRF is operated in a combination of valve and squeeze modes. In fact, the volume between the electromagnet and the lens is the orifice in which the MRF flows in a controlled way (valve mode) and the fluid flowing erodes material from the lens; but, in the polishing spot the fluid is pushed along the magnetic field direction (squeeze mode) (Figure 31). This increments the yield stress. The fluid used for this application needs to be characterized by highly abrasive power, highly resistance to oxidation, low environmental impact and low sedimentation. To meet the requirements of high abrasive power, it is composed by a high percentage of solid fraction 36%v CI, 6%v cerium oxide (nonmagnetic polishing abrasive); to meet the requirement of the low environmental impact, water is used (which is also cost effective). Stabilizers (like for example organic polymers) are used to prevent oxidation (which easily occurs for water-based fluids) and sedimentation.
Until recently, the smallest MRF wheel had a diameter of 20 mm with which the minimum concave radius workable was 14 mm. This technology is being constantly improved and recently a 10 mm diameter MRF wheel was developed 10 mm so extending magnetorheological finishing technology to shorter radius concave surfaces [124].

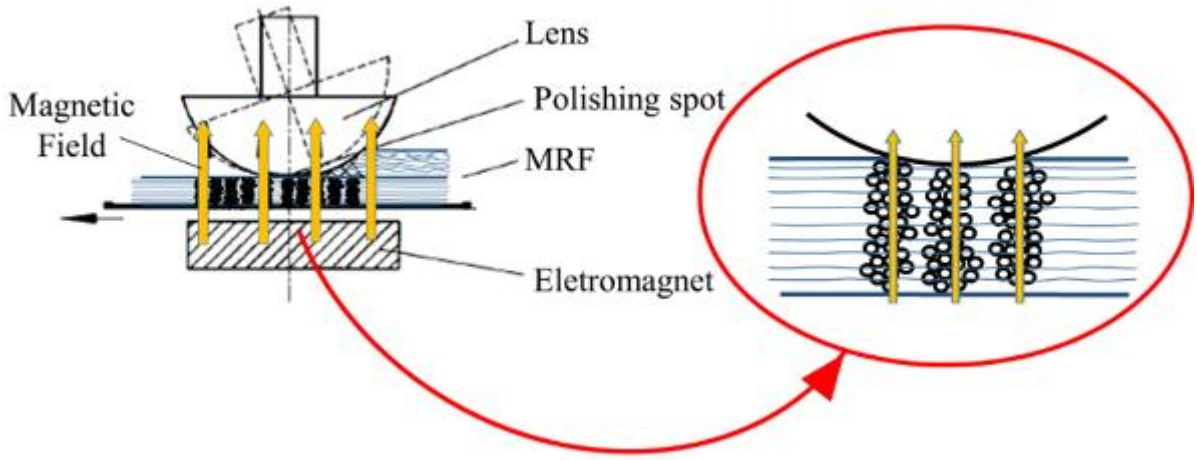

Figure 31. QED technologies optical finishing device [139].

The friction effect that MRFs can exhibit on the actuation interfaces can be endeavored to induce wear, such as in optical polishing. After the polishing process, the resulting roughness of the treated surfaces is lower than 1nm. The multiple axis CNC polishing machine uses a slurry made up of MRF

running on a wheel-shaped electromagnet. The workpiece is pushed against the MRF layer by a CNC programmed controls (Figure 32). In this way, the MRF shape and stiffness are magnetically manipulated and controlled in real time (Ghosh 2018) [140] [120][122] [121].

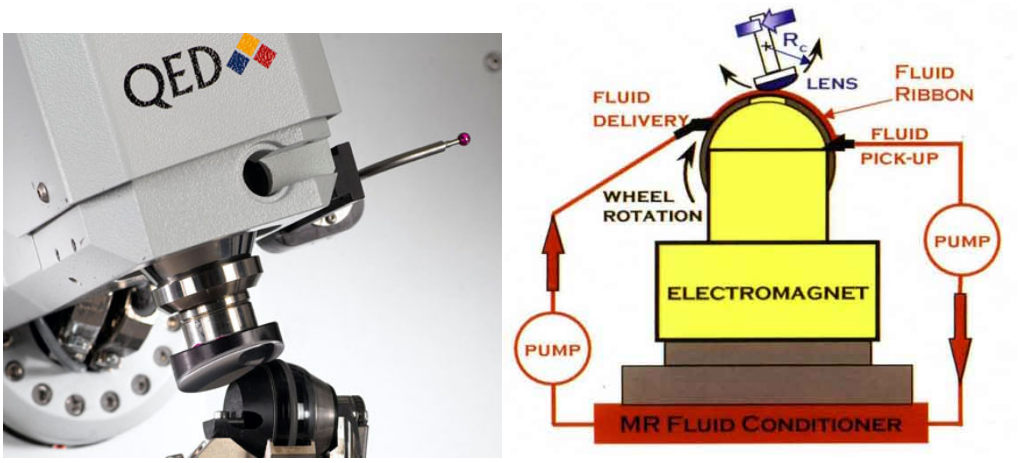

Figure 32. QED technologies optical finishing machine. [Figure from *https://goo.gl/ojw8tD* access on 07/01/2021 and *https://goo.gl/njG15Fm;* access on 24/11/2019] [139].

4.1.2 Flexible fixturing

Nowadays, manufactory industry is facing an increase in the variability of product batches in spite of their volume. This means that fixturing need to be as flexible as possible, in order to reduce as much as possible, the idle time. Figure 33 shows an experimental device for MR fixturing: the workpiece is immersed in the MRF; then the fluid state changes into solid [125], [126] [141]. The key point of this MRF application is that holding devices may adapt to different work-pieces dimension. Sliding wedges, in fact, are used to compress the fluid in the direction of the applied magnetic field ($\vec{H}$), as in Figure 33, to obtain higher values of the yield stress. It has experimentally proven that after squeezing MRF's, their yield stress may vary from 80kPa up to 800kPa. To achieve these values, MRFs need high percentage of solid particles. Typically, in these experiments, fluids have 46%v – 50%v CI. The carrier fluid is silicon oil because of its low viscosity. In this experimental application, detrimental phenomena (like sedimentation for example) are neglected and therefore no additives are added to the fluid.

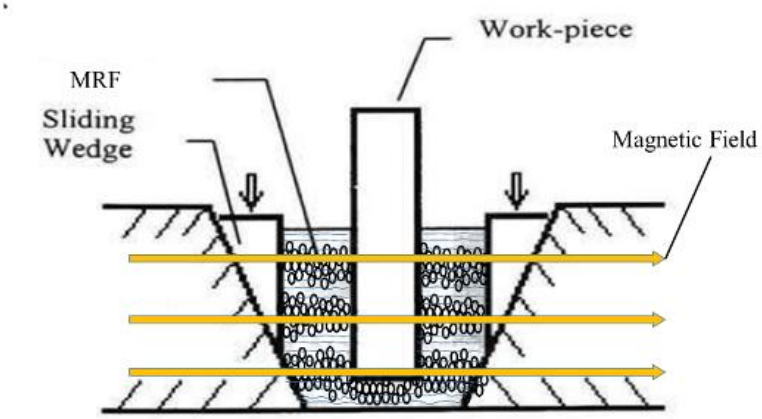

Figure 33. flexible fixturing based on MRFs [139].

4.1.3 Chatter suppression

Another MRF experimental application in manufacturing is in chatter damping. Chatter is the dynamic instability of cutting process caused by the interaction between the cutting tool and the piece under working, especially due to the inconstant section of the chip during machining operations.
The first examples of MR damping systems meant to mitigate chatter vibration by adjust the stiffness of the boring bar was presented by Sathianarayanan et al. in 2008 [127] (shown in Figures 34 e 35 and Mei at al. in 2009 [130] (shown in Figure 37). Sathianarayanan experiment is based on the typical MR damper in valve mode, which is connected to the cutting boring tool using connecting pin and a piezoelectric sensor is placed on top of the tool holder and connected to a computer through a charge coupler. The final optimized damper radius is 21mm and coil wire diameter was 0.76mm.

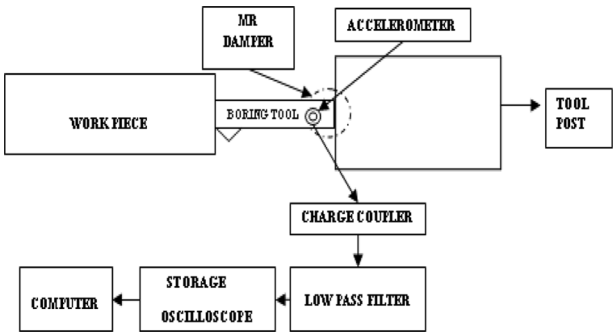

Figure 34. Experimental setup for MR damping system [127].

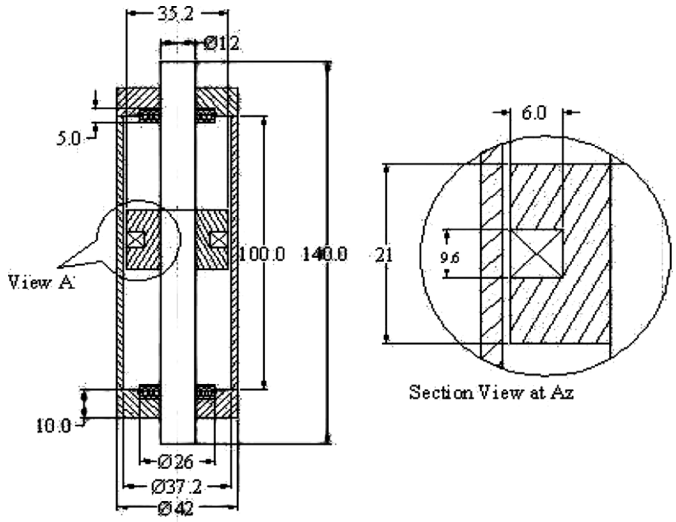

Figure 35. Specification of designed MR damper [127].

The MR damper uses MRF 336AG by Lord corporation. The fluid is constituted by silicon oil, 36%$_v$ of carbonyl iron particles and patented additives and has a high yield stress and low off-state viscosity. The overall damping of the boring process, in terms of decrease in acceleration levels of vibration at dominant frequencies in boring operation, was improved by increasing the damper current through MR damper connected to machine tool structure. When input current increased from 0 to 3A, the reduction in average acceleration levels of vibration at dominant frequencies varied from 20.27% to 80.62%. Figure 36 shows the aforementioned decrease in acceleration and also the increase in average dominant frequency in the boring operation of between 2.19% to 49.2%. Due to the nonlinearity of MR damper characteristics, in some cases the average dominant frequency shifts to lower side along with reduction in average acceleration level at dominant frequencies with increase in damper current;

while in other cases, acceleration levels along with average dominant frequency shift to higher side increases whit and increase in damper currents.

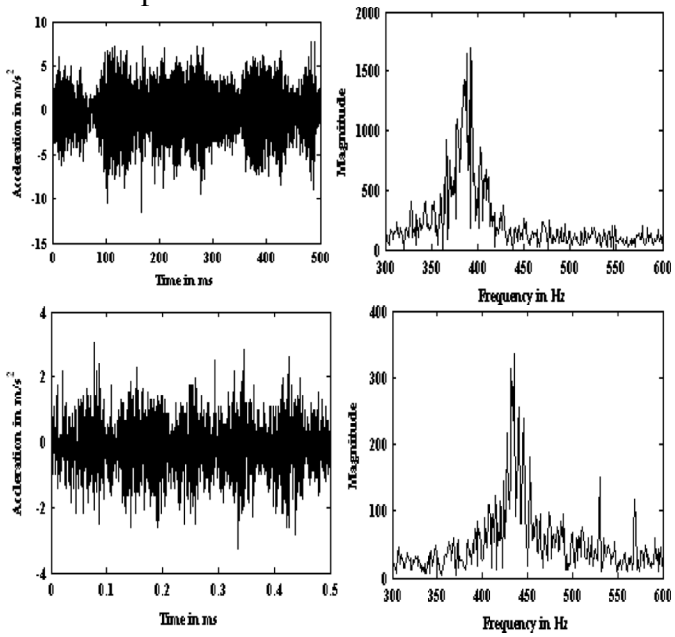

Figure 36. Acceleration and frequency range at damper current 1 A (a) and 3A (b) [127].

Mei [130] experiment, instead, contemplates a similar equipment for the experiment (Figure 37) with the basic difference of the absence of the typical MR damper connected to the boring bar, which is instead inserted in a chamber filled with MRF (as shown in Figure 38). In this way, the stiffness and natural frequency of the boring bar could be continuously varied by changing the intensity of the magnetic field. The horizontal vibration of the tool tip is measured by a piezoelectric accelerometer placed at the free end of the boring bar. When the sensor detects vibrations, the corresponding signals are sent to a power amplifier and then to a computer. Then, the control system adjusts the current applied to the coil of the magnetic circuit thus generating a controlled magnetic field acting on the MRF.

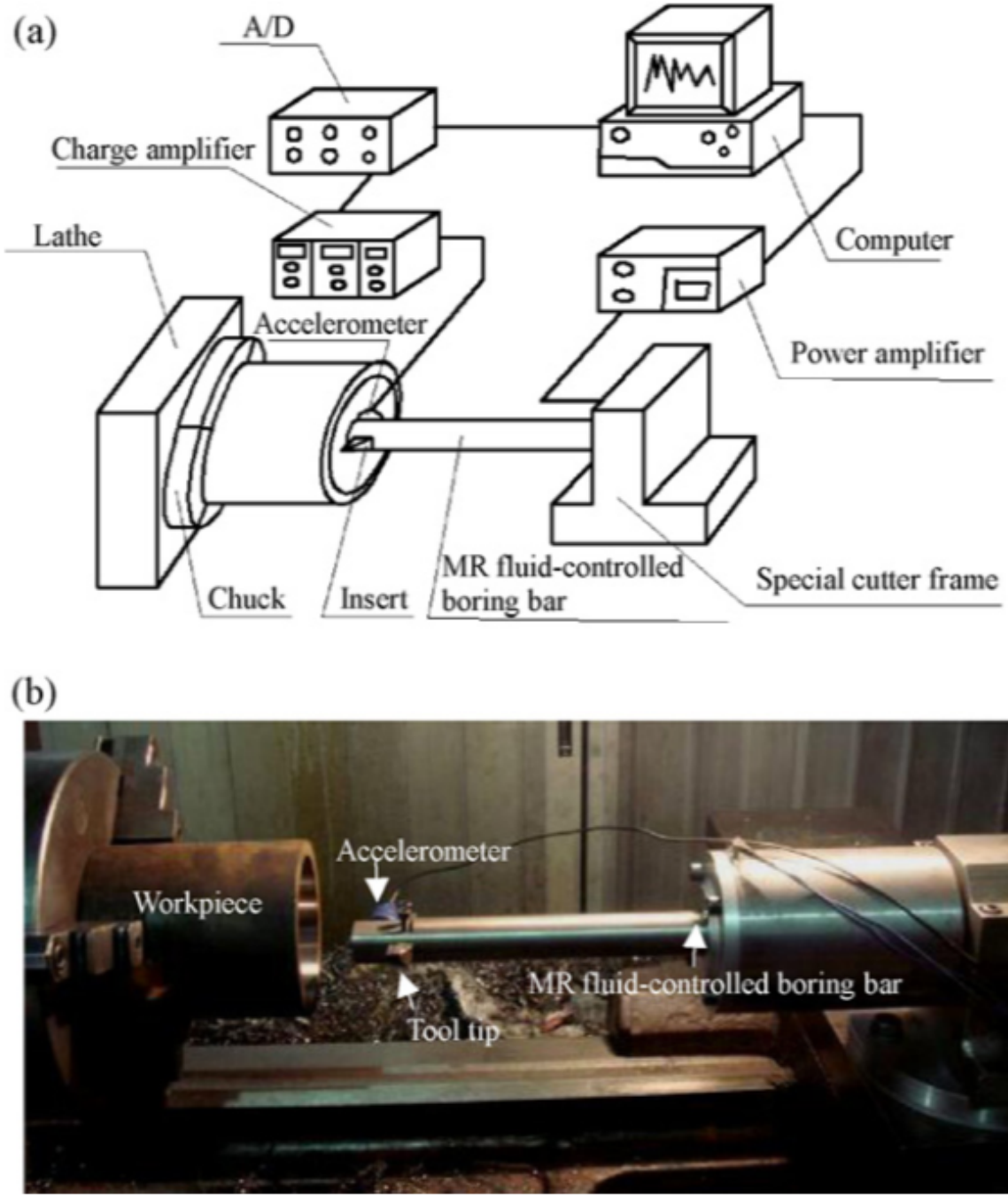

Figure 37. Experimental setup for MR damping system [130].

This experimental damping system consists of the MRF, support sleeve, non-magnetic sleeve, excitation coil and a boring bar shaft with two shoulders, marked as S1 and S2 in Figure 38. The magnetic circuit was designed using FEM analysis. The diameter of the boring bar is 30 mm, the ratio of length and diameter is 6, and the length of the fixed portion is 200 mm. The MRF is MRF-J01, produced by the Chongqing Instrument Material Research Institute in China, whose characteristics are [142]:

- Maximum yield stress 60 kPa
- Operating temperature –40–130 °C
- Shear viscosity (100 s^{-1} , 20 °C) 0.38 Pa*s
- Saturation induction 0.5 T

- Weight percentage of solid fraction 70%
- Particle size 0.1–20 μm
- Density 2650 kg*m^{-3}

So, basically the fluid is operated in shear mode.

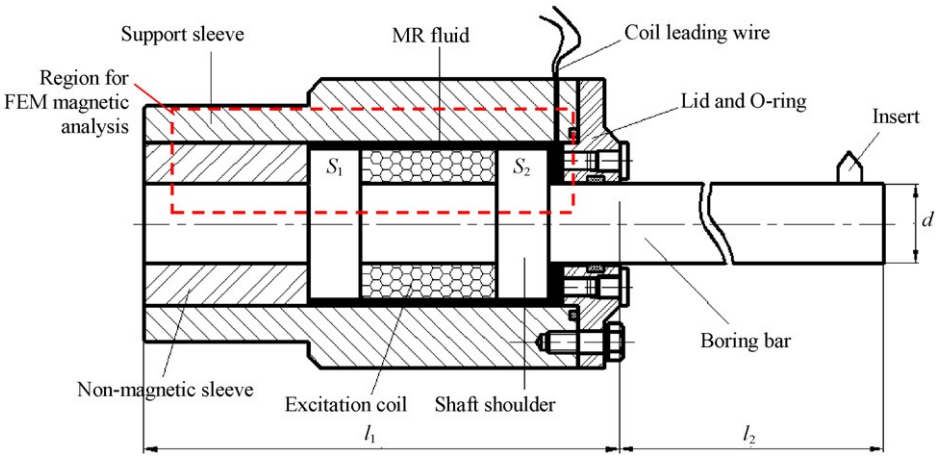

Figure 38. Structure of the MRF-controlled boring bar with chatter suppression [130].

The damping of chatter with this system resulted in surface roughness decrease from 5 to 1 μm R_a when MR control was activated.

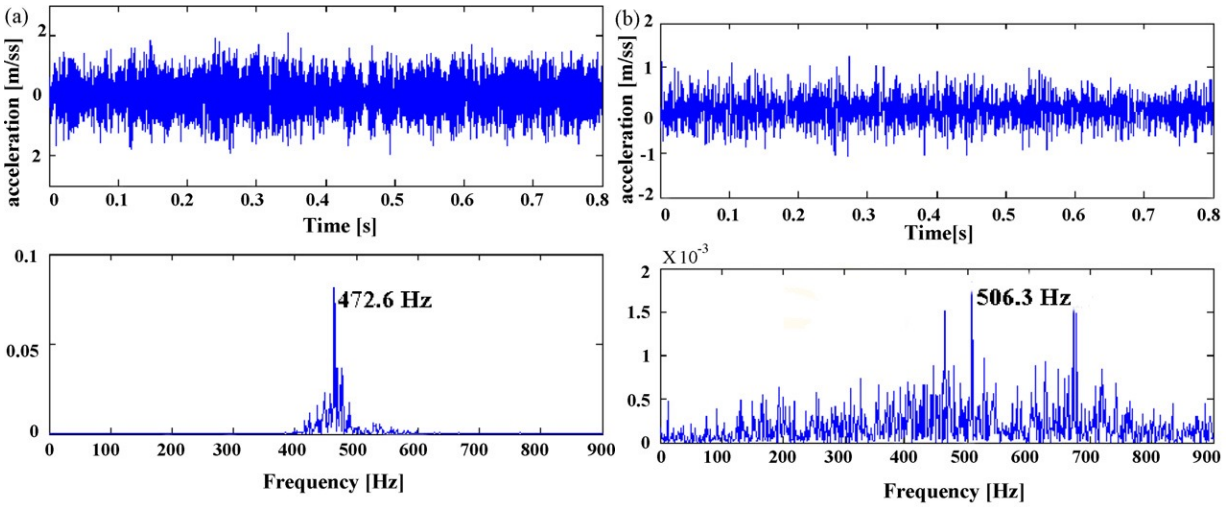

Figure 39. Vibration acceleration signal of the boring bar (spindle speed = 200 rpm). (a) Without MRF control. (b) With MRF control [130].

The beneficial effect of chatter damping is evident in Figure 39 showing acceleration signal in time and frequency domains when a) no MRF control is activated vs b) MRF damping activated. Without any control the maximum vibration acceleration amplitude is 2 m/s^2 and the main component of the chatter frequency is 473 Hz. When magnetic control is applied the acceleration decreases to 1 m/s^2 and vibration frequency is evenly distributed without a dominating peak. Furthermore, values of accelerations in the frequency domain are about 50 times lower than without MRF damping.

In 2015 Zheng et al. [128] proposed a similar device to the one just presented and shown in Figure 40. It is based on squeeze mode (since the yield stress of a magnetorheological fluid in squeeze mode is higher than that in the shear mode) and using MRF by Lord Corporation MRF-132DG.

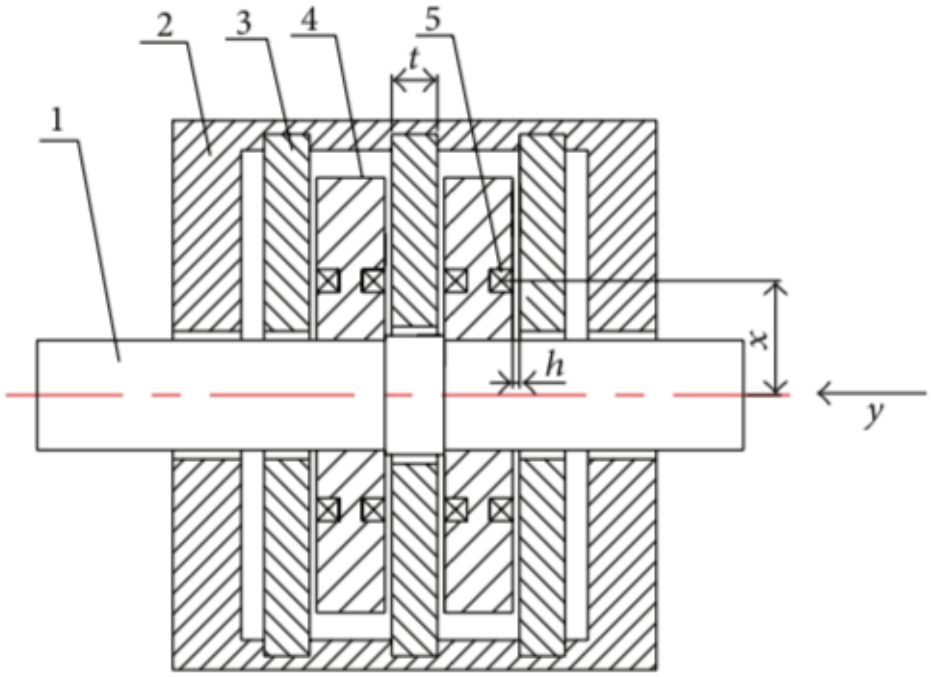

Figure 40. Structural diagram of MR damping turning tool [128].

In the damper, referring to the number present in Figure 40, the rod axle (1) replaced the original rod of the cylindrical turning tool and was rigidly connected to the cylindrical turning tool head using a Morse taper, the iron core (4) was interference fitted with the rod axle (1) and synchronously vibrated with the turning tool during the turning process, and the pole plate (3) was rigidly connected to the shell (2).
After applying current on the coil (5), magnetic field was generated in the damper. The direction of the magnetic flux lines goes from the two poles: iron core (4) and pole plate (3). Magnetic flux lines are parallel the y-direction in Figure 40. Under action of the magnetic field, the magnetorheological fluid was polarized to chains along the y-direction. When vibration occurs during operation, the iron core (4) and the turning tool undergo reciprocal motion along the y- direction in relation to pole plate (3), and thus MR chains are squeezed. The change in the applied current changed the squeeze yield strength of the MRF in such a way that the damping force can be controlled, thus damping the vibrations of the iron core (4) and turning tool.
These experimental results indicate that factors influencing the magnetic induction of this MR damping turning tool are pole gap, coil position, and plate thickness (listed in decreasing order). Finally, also in this case, data from both time- and frequency-domains show that squeeze mode MR damping turning tool can significantly reduce turning vibration.

With regards to milling machining operation, Puma-Araujo et al. proposed a new device based on MRFs to mitigate chatter for milling operations of thin-floor components [129]. The experimental device based on fluid MRF-122EG by Lord Corporation is showed in Figure 41.

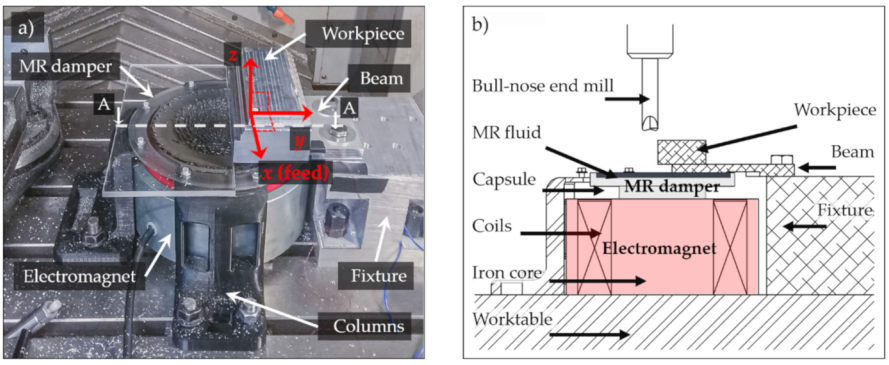

Figure 41. (a) Optical image of the experimental setup and magnetorheological (MR) damper installation; (b) Schematic of cross-section A–A, the assembling of capsule–MRF is placed above the electromagnet [129].

The MR damper device is a pool-like chamber fabricated in a non-magnetic acrylic material whose internal diameter is 200 mm and height is 19 mm. An electromagnet is placed between the worktable and the MR damper. Once the electromagnet is energized independently of the machining, it generates a magnetic flux with which it is possible to control MRF yield stress and then reaction torque. Note that the MRF is thus operated in shear mode. The beam is immersed for 1 mm in the MRF to guarantee constant contact during machining.
The results show that using MR damper device, machining is way more stable than in absence of MR damper in such a way that stable cutting conditions are enhanced, increasing the critical depth of cut from 0.5 to 1.5 mm in the range of spindle speed from 7000 to 10,000 rev/min, with an increase in the material removal rate and productivity by a factor of at least 3.

4.2 Civil Engineering Application Classes

For civil engineering applications of MRFs, dampers are the principal applications. This kind of device is mainly oriented to reduce the impact of induced vibrations on structures, such as seismic actions. Figure 42 shows such a device of a 20-ton damper: 1m length, inside diameter of 20.3 cm, stroke of ±8 cm, 5 liters of MRF, with an amount of active fluid at any given instant is approximately 90 cm3. There are three orifices between the outside diameter of the pistons and the inner part of the housing; the magnetic field is created between the outer housing and the three sections on which the electromagnetic coil is wound. The operational mode is thus the valve mode, provided vibrations have high frequencies and amplitudes in earthquakes.
Hopefully these devices are inactive for the most of their lives, so it is crucial to use MRFs with very low sedimentation. The off-state viscosity needs to be also high, to act as a passive damping system in case of failure of the magnetic and/or control system [143] [144]. For this reason, in this application the MRX-140ND was used. Here, the solid volume suspended is high (40%v) and this gives a high off-state viscosity, but also sedimentation issues. So, anti-sedimentation additives are used. Provided MRF by Lord Corporation® are patented, the additives are not known. Typically, compounds used are thixotropic agents such as greases, metallic soaps as lithium stearate and/or sodium stearate, organoclays, silica gel and carboxylic acids [90]. The carrier fluid used is hydrocarbon oil, which has a high thermal stability: its properties remain stable in the temperature range of -40/150°C. This characteristic is crucial, since these dampers usually work in extreme environmental conditions.

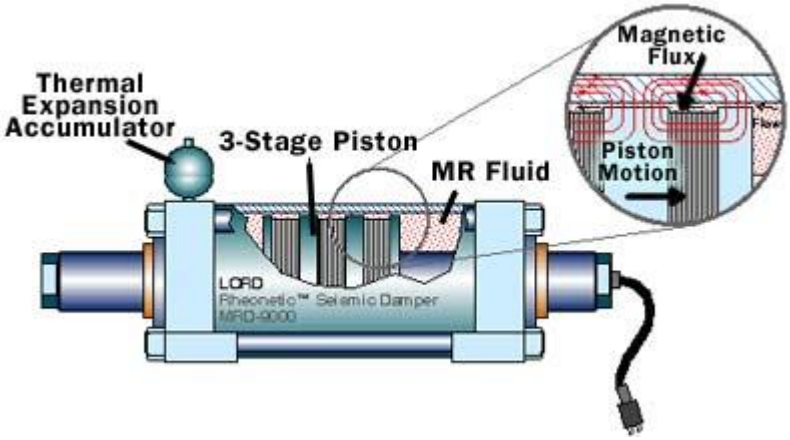

Figure 42. Schematic of large-scale MR damper by Lord Corporation [48] [139].

Another example is the bridge on Dongting Lake in China [145] [146] where the MR device is used to maintain the suspender-cables connecting the towers to the deck of the bridge to resist the vibrations induced in the structure by strong winds (see Figure 43).

Figure 43. The MR dampers connecting the cables and the deck of the bridge on Dongting Lake, China. [https://goo.gl/VUhKDO; access on 07/01/2021] [139].

4.3 Automotive Application Classes

In the automotive sector, the MRF's applications are essentially of two types: seat suspensions for large on- and off-highway vehicles and vehicle suspension system. They are mostly similar in geometry, operational mode and MRF used. The first application is here presented, since it is also the first one to appear on the market and still the most used and investigated [48] [147]. This system is commercialized by Lord Corporation: it is a small (4.1 cm in diameter, 17.9 cm length, ±2.9 cm stroke) monotube damper based on valve mode (Figure 44). The valve orifice is represented by the volume between the piston housing and an electromagnet (1A current is provided the leads through the hollow shaft) and fluid activated at any given instant is about 0.3 cm3, even if the total MRF amount is about 70 cm3. Valve operational mode are used because the damping provided high vibration frequencies and amplitude due to the road conditions are experienced. This operational mode provides a wide dynamic range of force control.

As far as the fluid formulation is concerned, the MRF contained inside the device essentially needs low off-state viscosity, low friction and then low abrasive behavior. Low off-state viscosity is necessary because it is necessary to reach a remarkable difference between viscosity in on and off-state to provide different damping behavior in the two conditions. Consequently, the concentration of solid particles is only 26%v. The anti-friction characteristic is essential to avoid abrasion on the device inner walls and also to avoid the thickening of the MRF. Again, anti-wear and anti-friction additives used for the MRF by Lord Company ® are not known in composition, but compounds with

these features are organo-molybdenum and zinc-dialkyl ditiophosphate [97]. Anti-sedimentation additives are also added, despite in these applications sedimentation behavior is less important, because the fluid is constantly mixed by the vehicle movement. In this case also, the carrier fluid used is hydrocarbon oil due to its high thermal stability: during operation, very high temperature is in fact reached.
The determination of the best characteristics of the MRF used in the MR damper is a topic constantly under investigation; in particular, the best combination of particle volume percentage and particle size is the focus of recent studies [148]

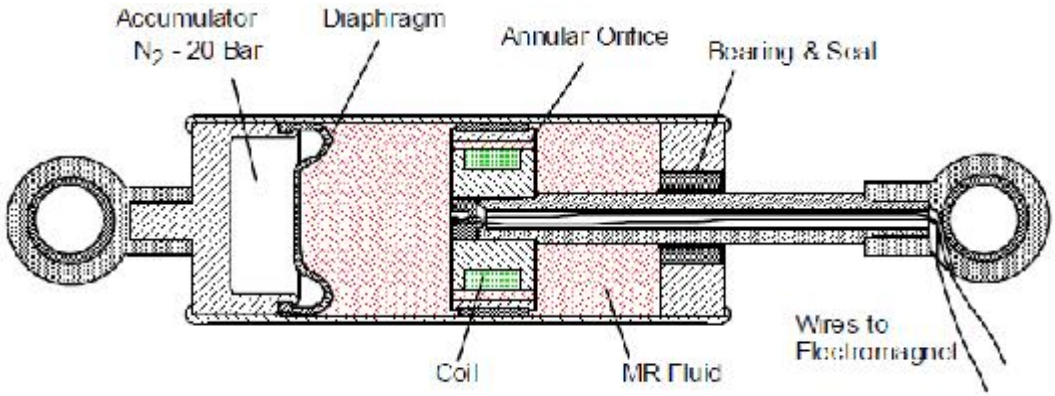

Figure 44. Commercial Linear MRF-based Damper [48].

In the automotive applications, MR dampers are used to mitigate vibrations induced either on the structure or on the driver. The seat of heavy-duty vehicle are suspended (trucks, off-highways, construction, agricultural vehicles, etc.) where the MR damper is equipped with a microprocessor and sensors [48]. The microprocessor transforms the electronic signals transmitted by position sensors in dumping action accordingly to ride conditions, operating on the viscosity of the MRF through magnetic field adjustments. The air reservoir contains compressed gas to accommodate the volume changes due to the piston movement [149].

Figure 45. Schematic representation of suspended seats MR dumpers system. [https://goo.gl/Qas5sZ; access on 21/11/20].

Interesting applications can be found also for dampings. An example the MagneRide system, firstly introduced in 2002 on GM's Cadillac Seville STS, ans now used on a wide range of high-hand car producers (Lamborghini, Audi, BMW, Chevrolette, Ferrari, Range Rover, etc.). The MagneRide (Figure 46) consists of a complex system: four MR dampers (one for each road spring) connected to a central computer that elaborates signals transmitted by a set of sensors and, acting on electromagnets contained in the dampings, adjusts the dumping force to the road conditions.

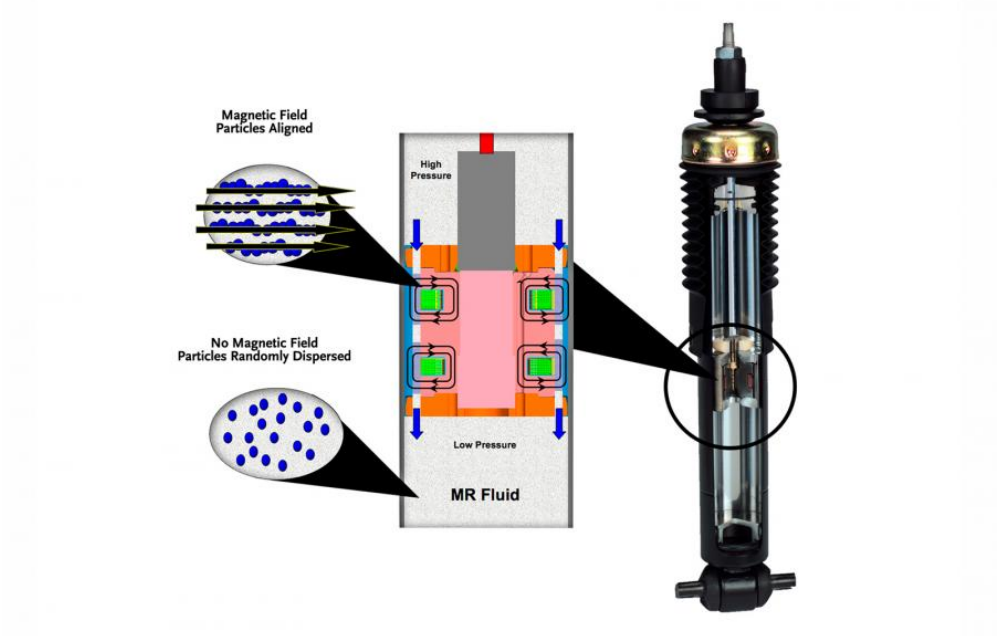

Figure 46. MagneRide suspension system based on a MR damper. [https://goo.gl/rbNEBy; access on 23/11/2020].

4.4 Biomedical Application Classes

Mostly in the biomedical application, the main device used is a hinge, while the control action is the friction, to regulate rotation velocity.

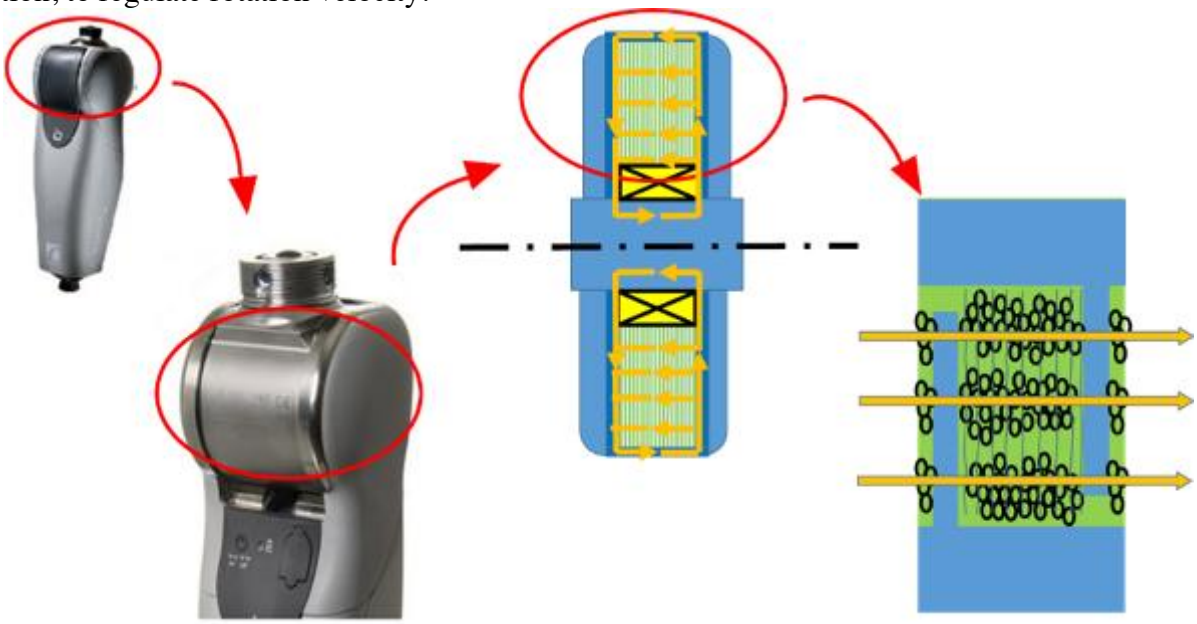

Figure 47. Rheo-Knee 3 by Ossur Inc.[https://bit.ly/2C1t9rf] [139].

Figure 48 shows a prosthesis based on a MR clutch (Herr and Wilkenfeld, 2003), that can operate also as a brake [135]. It is used for knee prosthesis for amputees. The main requirements for this device are: high field-induced braking torque (around 40Nm) and low weight (0.3-0.5kg to be comfortable to wear). Provided this device replaces the knee joint, it needs control (clutch) and eventually stop (brake) the rotation. The best mode to control surfaces moving one with respect to the other is the shear mode. For this reason, this device uses a series of thin disks close to the other ones (~20μm gap), between which the MRF is contained. When the magnetic field is generated through the electromagnets placed close to the hub of the device and the disks, the fluid is activated to operate in shear mode. As a result, there are many thin shear-mode regions active.
MRF for this device is especially designed to have high yield stress (to reduce the fluid volume used) and really low off-state viscosity in order to allow faster movements. This means that the volume percentage of the solid component is 28% (smaller than typical MRF), and thus a low off-state viscosity is achieved. The carrier fluid is perfluorinated polyether (PFPE) oil which has good thermal stability, low viscosity and good sedimentation properties (Kordonski And Golini., 1999). From the introduction in 1999 of this kind of device up to nowadays many different studies have been carried on with the aim of improving the technology, focusing especially on the device design, for example [150] and [138]. The second one, in particular used MRF-132DG by Lord Corporation, which is based on Hydrocarbon oil and a medium percentage volume of Carbonyl Iron (36%$_v$) (Becnel A. C. and Wereley N.M., 2017) to obtain a higher yield stress.

4.5 Future research

In the future MRFs will be used in many different fields and research has already started focusing on virtual reality and safety applications.

4.5.1 Virtual reality

The ability of continuously and reversibly changing their viscosity within milliseconds allows MRFs allow them to be applied for a wide range of applications requiring fast controllable damping and/or resistive force generation. Haptic interface devices are an example, representing the interaction with remote and virtual worlds by coupling the human sense through “touch” with a computer generated environment [151] [152]. Figure 48 shows one example of these devices: the articulation between two phalanxes is supported by an MR clutch. When the hand moves, the clutch moves too. The sensors, which are coupled to each clutch, register this movement variation; the corresponding signal is sent to the central unit and a corresponding feedback is sent to the player in the virtual environment.

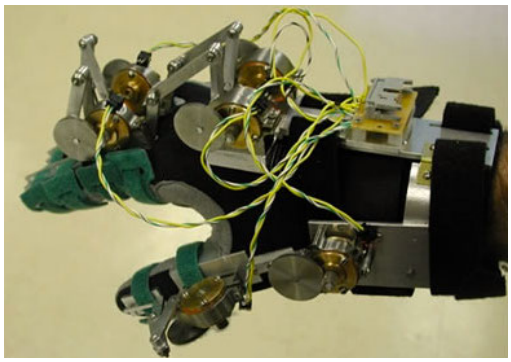

Figure 48. Architecture of an haptic interface device. [https://goo.gl/ujLE0C; access on 24/11/2020].

4.5.2 Safety applications

Regarding safety applications, the main research scope up to these days has been the bulletproof vests for military applications. Ordinary vests are made of up to thirty layers of Kevlar; MRF based ones can be made of ten layers of Kevlar. The space between two consecutive layers is filled with MRF

which is activated by coils fixed on the Kevlar layers only during the operations [153]. This means a consistent decrease in the weight of the vest and easy storage.

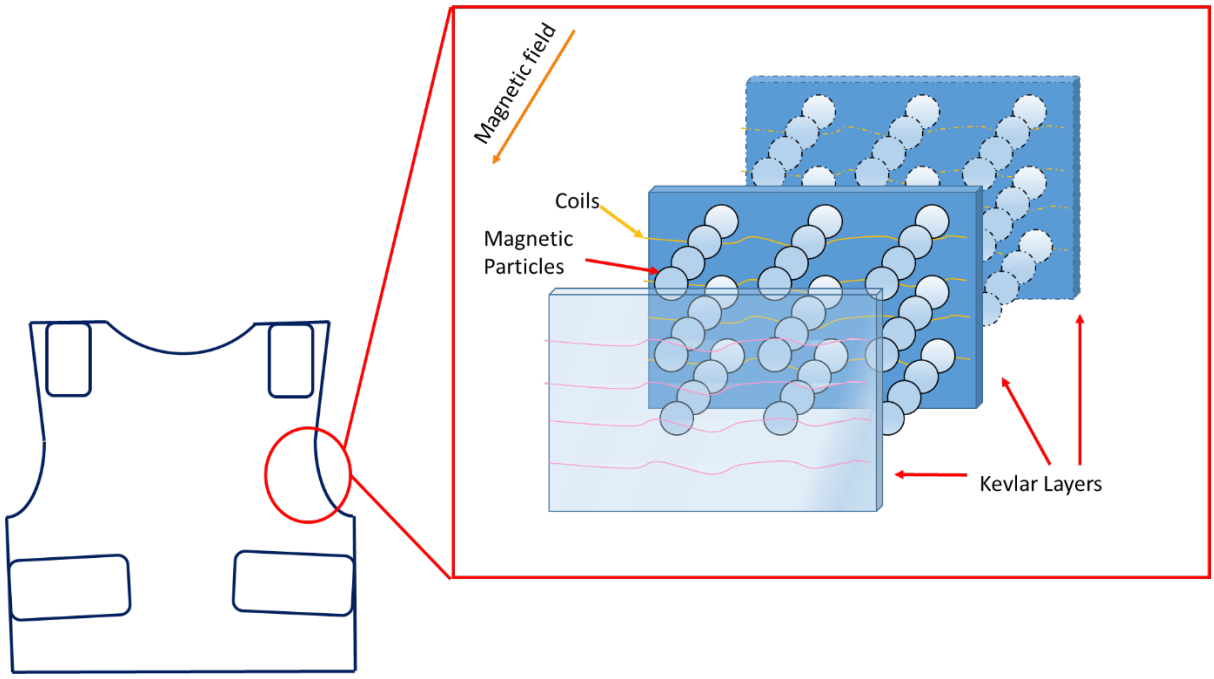

Figure 49. Representation of the activated fluid between two layers of Kevlar in bulletproof vest.

Conclusion

The aim of this chapter was to focus on the practical existing applications of MRFs in the civil application domain, to give some hints in the selection of the best combination of operational mode and MRF formulation, based on the functional requirements of the device. The operational mode is selected based on intensity and direction of the force to be controlled. The selection of MRF formulation depends on the characteristics of the combination of the carrier fluid with additives, but also on the volume percentage of solid particles. As a consequence, the main criteria of selection are:

- viscosity (on-state and off-state),
- sedimentation and redispersion behavior.

Furthermore, MRF selection is based on the working condition of the device. For example, for the MR vehicle suspension, sedimentation behavior is less crucial than off-state viscosity because of the continuous stirring condition and this is the reason for the afore-mentioned fluid formulation (see paragraph 4.3).

In conclusion, it results in a clear description of how few practical applications have still been deployed endeavoring the incredible features of MRFs. The features can be named as: rapid change of state (viscosity); flexibility of control (low magnetic fields and low power requirements) and finally limited volume required. Provided this analysis is limited to the research paper database (SCOPUS®), in the next future, also ongoing research projects and patents will be analyzed from the application point of view. In fact, provided the potentialities of ICT devices, the next extension of the use of these fluids to other useful applications, such as home automation, elderly care and other manufacturing applications (i.e. casting) seems profoundly reasonable.

5. How to design MR dampers for manufacturing applications

MRF based devices for manufacturing applications are dampers used to mitigate vibrations during machining and cutting operation.
There are three types of machining vibrations: free vibration, forced vibration, and self-excited vibration. The first kind, free vibration, rises from the collision between the tool and workpiece; forced vibration occurs when the mechanical system is subjected to time varying external disturbance and when this vibration is close to natural frequency it becomes resonance vibration; finally, the self-excited vibration comes from the interaction of factor linked to the dynamic operation of the machine, like whirl of rotor and chatter vibration. In particular, chatter vibration can be divided into primary and secondary chatter. Primary chatter is mainly due to friction and thermo-mechanical effects between the workpiece and the cutting tool, while secondary chatter comes from the dynamic interaction between previous and current cuts [154]. Of course, chatter is an undesired vibration affecting surface finish, causing cutting tool damage, and limiting the productivity of cutting process causing part rejection at the last stage of the manufacturing process.
Chatter for boring process is due to the use of the rigid boring bar characterized by long overhang length compared with other cutting tools [127]. For milling operations chatter is caused by the variable section of the chip during cutting.

In general, dampers for manufacturing are designed to achieve two main functions: to keep constant contact between the cutting tool and the working piece, while isolating the working piece from solicitations and vibrations coming from the cutting process, as already mentioned so extending the lifetime firstly of cutting tools and secondly of machines.

In general, the big advantages of MRF dampers are [127][129].

- wide frequency range manageable;
- very short time response;
- simplicity of construction;
- scalability;
- low power consumption.

MRF dampers for machining operations are still on experimental level and have not been industrialized for chatter suppression since, along with the intrinsic drawbacks of MR technology (sedimentation for example) they are negatively affected by the fact that designs are customized and suitable only for specific machine processes; further more they are characterized by excessive setup time [129].

We suggest with this thesis the idea of exploiting the peculiar feature of scalability in order to use a well-known, widespread and already industrialized device whose functional requirement is wide frequency damping, as a knowledge basis for a novel MR damper to be used in machining applications. Even if there are some examples of MR dampers based on squeeze or mixed modes, the most used and industrialized device for wide frequency damping is the MR damper in valve mode. This “universal” damper could then be used for spindle holder, tool holder, tool interchange arms, milling tools and so on just by changing the geometrical dimensions of the actuator, while maintaining the core dumping mechanism unaltered.

For this reason, this chapter focuses on the characteristics of the most widely diffused MR damper in valve mode, already industrialized for automotive and civil engineering applications. The study of

MR dampers starts from MRF damping systems (the overall system comprising sensor and central units), moves to the modelling of MR damping, summarizes the factors influencing the damper performance (reaction force) and focusses on the design solution to maximize MR damper performance.

5.1 Damping systems

As a general consideration, there are different types of damping systems allowing different levels of controllability: passive, active, or semi-active systems (see Figure 50). Passive systems are widely exploited, because of their manufacturing simplicity and high reliability, resulting in a limited cost (Figure 50A). The disadvantage is that this system cannot assure the desired dumping performance on every situation, since the damping characteristic is constant: this limitation has motivated the investigation of controlled or so-called active damping systems. An active damping system is based on controllable actuators and computer-based control devices [155] and its design is shown in Figure 50C: it is made of sensors, actuators and a central control unit. Sensors send data about the operating conditions of the cutting tool, while the central control unit elaborates sensor signals and controls actuators, which as a return module the force they can exert in order to achieve improved vibration control. Even if active damping systems can manage a wide frequency range of vibrations, disadvantages of their use are high cost, high weight, high complexity and high-power requirements compared to passive systems.

Semi-active damping systems fill the gap between their passive and active equivalents (see Figure 50B), since they offer both the reliability of the passive systems and the flexibility and high performance of active control systems. The mechanism of force control in semi-active systems is based on controlled dissipative elements as low energy is introduced into the system, differently from active systems requiring fully active actuator, and then a significant energy input.

The development of controllable dampers has attracted the attention of designers to different smart materials, like for example Electrorheological (ER) and Magnetorheological (MR) fluids [156].

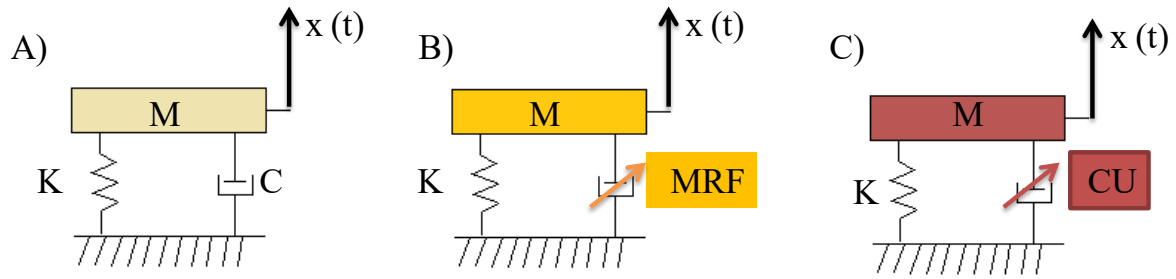

Figure 50: A) Passive damping system, B) Semi-active damping system, C) active damping system [157].

Even if both ER and MRFs show similar viscosity characteristics in the off-state (i.e. without the application of the external stimulus), in the activated state (with the application of the aforementioned external stimulus) MRFs show a significantly higher yield stress than ER fluids. For this reason, and also due to the quickness and reversibility of the very considerable change in their rheological behavior, MRFs are widely applied in vibration isolation control systems.
MR devices design has been extensively studied for a number of applications and in particular for MR-based damping systems, research has focused on how get large damping force and how to model and control MR behavior [158].

So, MRFs are used only for semi-active damping systems. In fact, the damping force can be easily controlled continuously by external magnetic fields. Other advantages are quickness of activation (low reaction time) and low power requirements: a power consumption of less than 18W has been registered [147], [159]. This is an important point, provided sustainability is always a prominent matter [160]. A typical semi-active system is shown in Figure 51. This kind of systems are based on a feedback control and contain two controllers: damper controller and system controller. In accordance with the dynamic response of the system monitored by sensors, system controller acts on the damper controller to exert a specific damping force; the damper controller controls the MR damper by adjusting the viscous properties (i.e. yield stress) of MRF through the intensity of the magnetic field produced by means of an electromagnetic coil [161] [162].

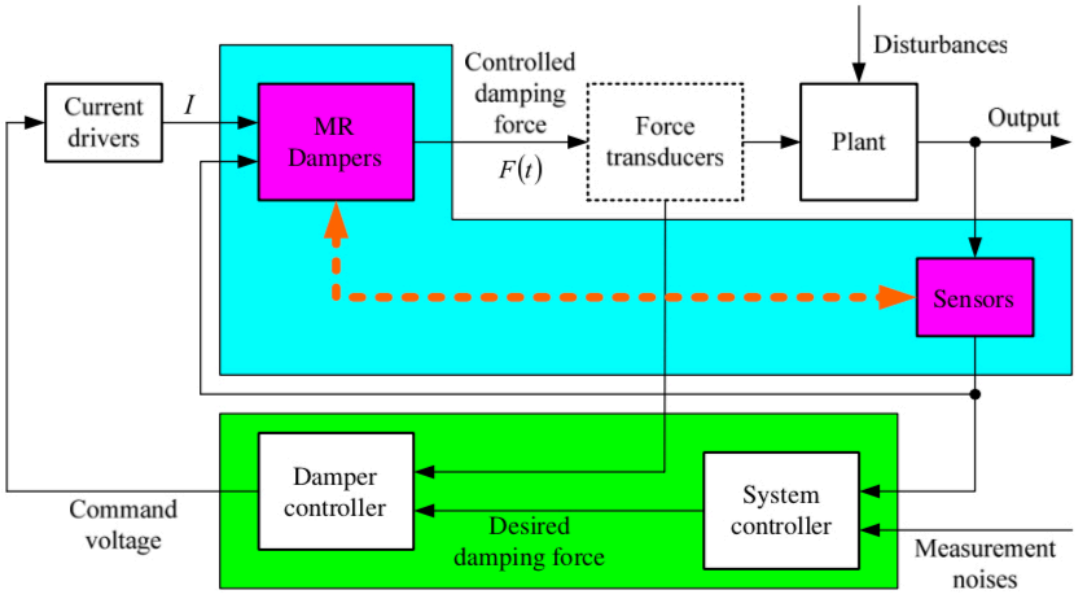

Figure 51: Schematic of semi-active control system based on MR dampers [162].

5.2 MR-damper structural design solutions

Typical designs for semi-active MR dampers are: mono-tube, twin tube and double-ended MR damper.

A traditional monotube semi-active damper is shown in Figure 52: the MR dampers normally consist of a piston moving inside a cylinder filled with MRF, magnetic coils, a bearing and seal, and an accumulator. The accumulator contains a compressed gas (usually nitrogen) [149] and its main function is to provide a level of softening by providing an extra allowance for the volume change that occurs when the piston rod enters the cylinder. The piston rod enters the cylinder, the MRF flows through the orifices in the piston from the high-pressure chamber to the low-pressure chamber in the cylinder. The volume change is compensated by the accumulator. The magnetic field generated in the activation regions by the magnetic coils changes the characteristics of the MRF depending on its intensity. Therefore, the magnitude of the input electrical current into the magnetic coils (which generates the magnetic field) determines the physical performance of the MR damper modifying the MR viscosity.

The direction of the magnetic field flux lines in respect to the direction of the MRF flow determines the operational mode on which the MR dampers is based: there are three basic operational modes (valve, shear, squeeze). Typically, MR dampers for damping systems are developed in valve mode [131] [107].

The specific damper shown in Figure 52 is the linear MRF damper based on the single-ended piston-rod structure and produced by Lord Corporation for semi-active vibration control system for heavy-

duty vehicle seat suspensions. It is based on valve mode, and the MRF valve and magnetic circuitry are contained within the piston; an input power of 5W is required to operate the damper at current of 1 A. The total MRF volume is 70 ml while the amount of fluid activated by the external magnetic field is about 0.3 ml. In Figure 53, instead, is represented the RD-1005-3 from Lord Corp, which is a short stroke monotube MR damper suitable for industrial suspension applications [163].

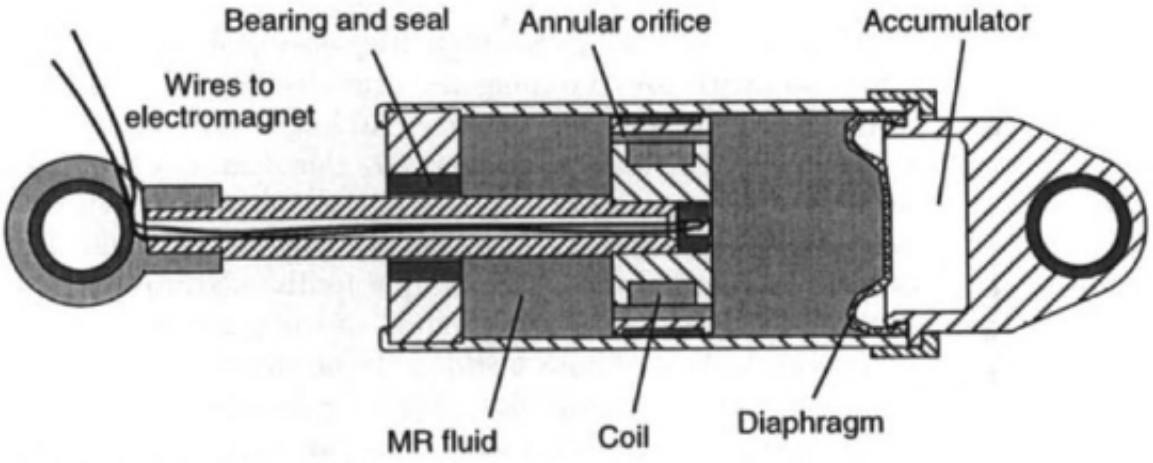

Figure 52: Cross-section of typical MRF damper [49].

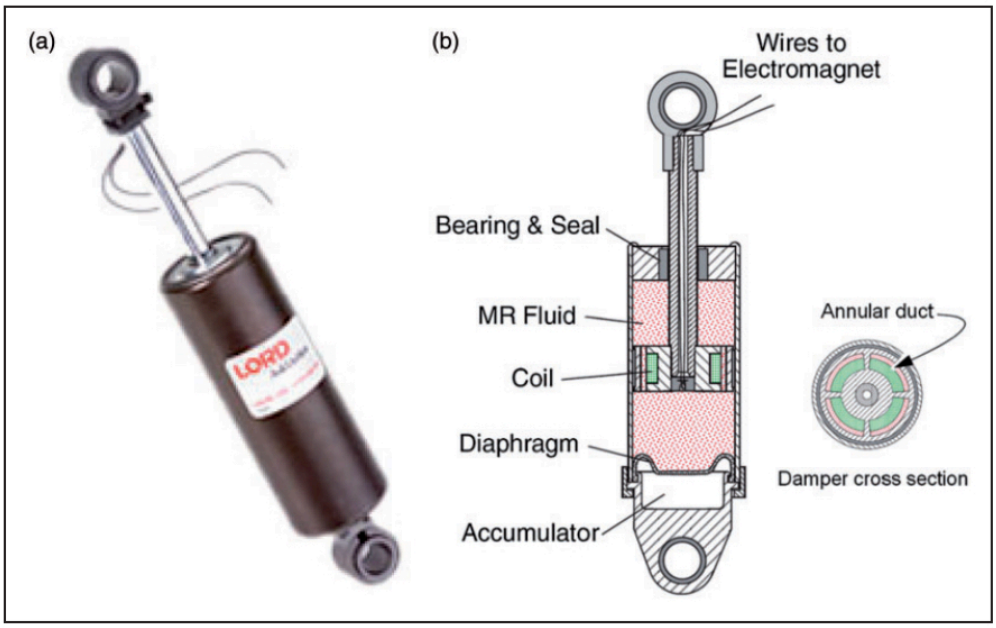

Figure 53: RD-1005-3 (short stroke) MR damper from Lord Corp. (a) and section view (b) [163].

Along with the already shown mono-tube damper (one reservoir and accumulator), the most used semi-active MR damper is the twin tube damper, represented in Figure 54. It has two fluid reservoirs, one inside of the other, and an inner and an outer housing. The inner housing works like a mono-tube damper; the outer housing is partially filled with MRF to accommodate changes in volume due to piston rod movement. A valve assembly connects the two housings to regulate the fluid flow between the two reservoirs. The MRF volume flowing from the inner housing to the outer housing is equal to the volume displaced by the piston rod as it enters the inner housing. The MRF control through the valve is placed inside the moving piston. The disadvantage of this type of design is the difficulty of heat dissipation, as MRF is directly affected by heat build-up in the coil. An increase in the temperature of MRF might cause the viscosity to drop and reduce the force capacity of the damper [164]. On the other hand, the advantage of this design over the monotube design is that the monotube

MR damper design is weaker since it incorporates a high gas pressure reservoir, susceptible to damage [149].

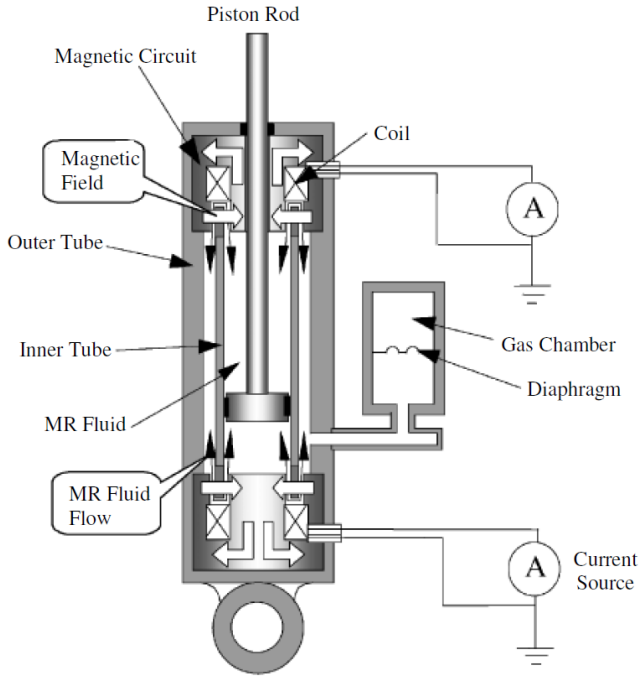

Figure 54. Twin tube MR damper with accumulator [165].

Along with monotube and twin tube design, the double-ended MR damper design shown in Figure 55 is another solution adopted [166]. Two piston rods of the same diameter enter the reservoir from both ends, so as no volume change due to the pistons relative movement occurs. For this reason, no accumulator is needed. This design has just recently been applied to suspension system by Desai et al. [159].

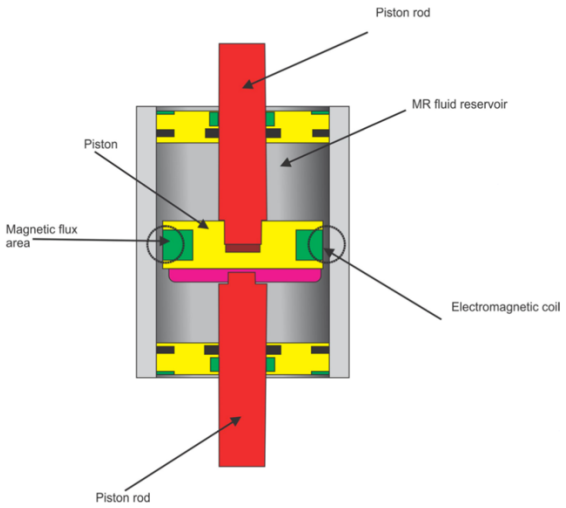

Figure 55. Double ended damper [166].

5.3MR dampers behavior modelling

The major difficulty in using MRF-based damping systems is the non-linear and hysteretic force–velocity response of MR dampers. In Figure 56 is shown the typical force plot: force–displacement plot (a) and the force-velocity plot in (b). Non-linearity is noticeable in Figure 56(a) and the hysteresis in Figure 56(b) [167].

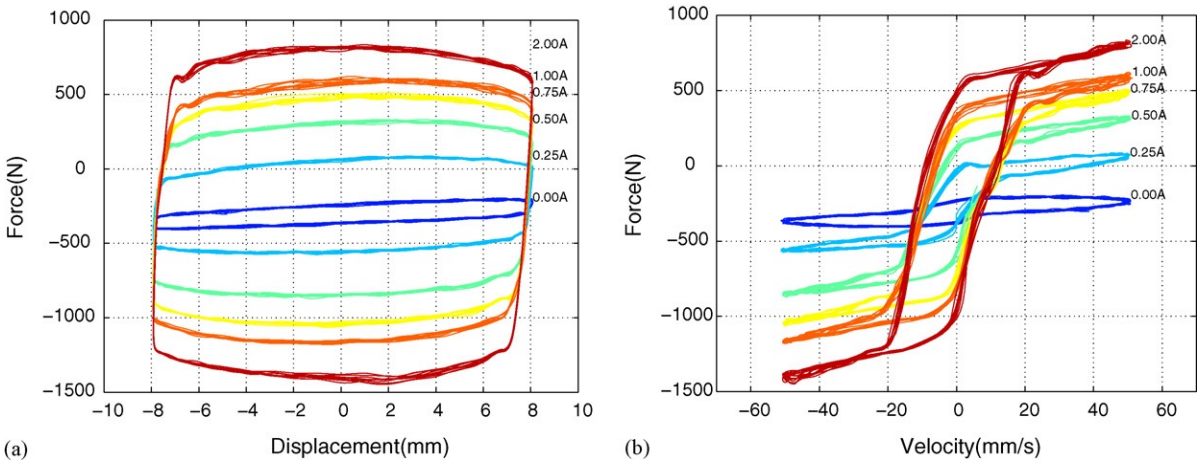

Figure 56. force plot, force–displacement plot (a) and the force-velocity plot in (b) [167].

The main difficulty in design MR damper is the selection of the best model to describe the hysteretic behavior of MR dampers because of the need to balance model accuracy and model complexity. To do so, many different models have been used. Here below are reported some of the most used.

5.3.1 Bingham model

This model is based on stress–strain visco-plastic behavior is used and a discontinuity in the damper force–velocity response. The damper force is expressed as:

$$f = f_c\, sgn(\dot{x}) + c\dot{x} + f_0, \qquad (34)$$

where f is the damping force, f_c the magnitude of hysteresis, sgn is the signum function, $\dot{x}$ the velocity, c the viscous coefficient and f_0 is an offset of the damper force. It is important to highlight that this is the most used model to describe the rheological behavior of MRFs in the activated state.

5.3.2 Bouc–Wen model

This is the most used model to describe MRF base damper behavior and contains components from a viscous damper, spring and a hysteretic component. The model can be described by the force equation 35 and the associated hysteretic variable z:

$$f = c\dot{x} + kx + \alpha z + f_0 \qquad (35)$$

$$\dot{z} = \delta\dot{x} - \beta\dot{x}|z|^n - \gamma z|\dot{x}||z|^{n-1} \qquad (36)$$

α, β, δ, γ, n are the model parameters and z is the hysteretic variable and x represents the displacement. When α=0 equation 35 represents a traditional damper.

5.3.3 Modified Bouc-Wen model

Additional parameters are introduced to increase accuracy. It is given as:

$$f = c_0(\dot{x} - \dot{y}) + k_0(x - y) + k_1 x + \alpha z + f_0 \qquad (37)$$

$$\dot{y} = (c_0 + d_1)^{-1}(c_0\dot{x} + k_0(x - y) + \alpha z) \qquad (38)$$

$$\dot{z} = \delta(\dot{x} - \dot{y}) - \beta(\dot{x} - \dot{y})|z|^n - \gamma z|\dot{x} - \dot{y}||z|^{n-1}, \qquad (39)$$

where y is an internal dynamical variable and d_1 and k_1 are additional coefficients of the added dashpot and spring in the model (Figure 57). The model complexity increased along with its accuracy.

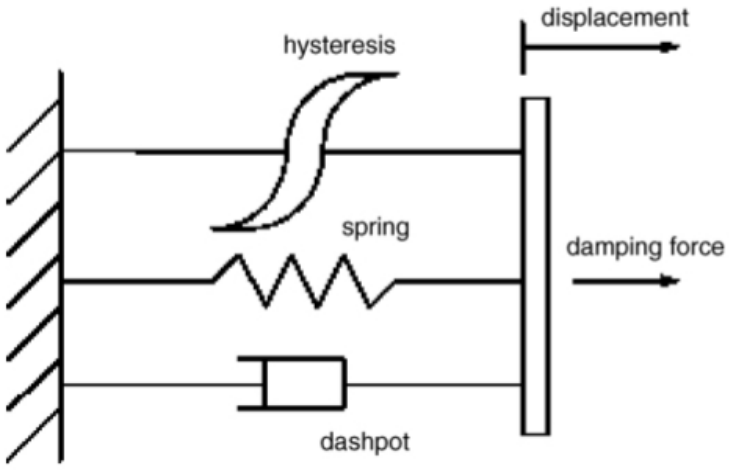

Figure 57. Elements of Modified Bouc—Wen model [167].

5.4 Damping force characteristics for MR dampers

As far as the damping force is concerned, it is important to note that its expression is based on Bingham plastic model and that it depends on the intensity of the externally applied magnetic field. For the schematic configuration of MR damper in Figure 54, assuming that MRF is incompressible, that pressure in the gap chamber is uniformly distributed and that can be considered negligible the frictional force between oil seals and fluid inertia, the damping force can be expressed as [168] [165]:

$$F = k_e x_p + c_e \dot{x_p} + P_{MR} sgn(\dot{x_p}) \qquad (40)$$

Where

$$k_e = \frac{{A_r}^2}{C_g} \qquad (41)$$

$$c_e = \frac{12\eta L}{2\pi r h^3}(A_p - A_r)^2 \qquad (42)$$

$$P_{MR} = 4\left(A_p - A_r\right)\frac{2L_m}{h_m}(\alpha H^{\beta}) \qquad (43)$$

being x_p the piston displacement, $\dot{x}_p$ the piston velocity, A_p the piston area, A_r the piston rod area, C_g the gas compliance in the gas chamber, η the viscosity of MRF, L the length of the inner cylinder, r the outer radius of the inner cylinder, h the gap size between the inner and outer cylinders, L_m the length of the magnetic pole, h_m the gap size between the magnetic poles, and H the external magnetic field.

The first term in Equation 40 represents damping force from the gas compliance, the second term is the damping force to the viscosity of the MRF, the third one is due to the yield stress of the MRF (controllable by the intensity of the magnetic field). Constants α and β are values of the MRF to be experimentally determined.

5.4.1Damping characteristics in valve mode

Typically, MR dampers are designed in valve mode. So, valve mode-based devices have been widely studied and developed for commercial applications [49] [169] [170] [171]. Damping force transmitted indicated by MR damper designs play an important role in MR damper characteristics. The design of MR damper in valve mode generates a pressure drop in the valve area. This is controlled by the viscosity of MRF under the influence of the magnetic field, which resists an output force that attacks the damper in valve mode. The pressure-drop developed in a valve mode device can be created in two ways, an independent viscous component $\Delta P\eta$ as pure rheological and a magnetic field dependent component ΔP_{mr} as magneto-rheological [172]. The pressure value drop can be expressed as:

$$\Delta P = \Delta P_{\eta} + \Delta P_{mr} = \frac{12\eta QL}{g^3 w} + \frac{c\tau L}{g} \qquad (44)$$

Where η (Pa-s) is the dynamic viscosity, τ_{mr} [N/mm2] is the yield stress variable in response to an applied magnetic field, Q [m3/s] is the volumetric flow rate of the MRF, and f (no unit) is an empirical factor that is identified experimentally. Constant f is dependent on the ratio between the pressure drop due to the magnetorheological response factor, and the pressure drop due to the natural viscosity of the fluid. The value of constant f ranges between 2 to 3 depending on the value of the $\Delta P_{mr}/\Delta P_{\eta}$ ratio of the device. If the $\Delta P_{mr}/\Delta P_{\eta}$ ratio is equal to or less than 1, the value of f is likely to be 2. However, the value of f is likely to be 3 if the $\Delta P_{mr}/\Delta P_{\eta}$ ratio is equal to or larger than 100 [2]. An MRF device in valve mode will usually follows Equation 44.

5.5 MR damper factor-function relationship

MR dampers have received great attention, because they offer the adaptability of a semi-active control system that requires a low power supply, a current of 2.54V is enough to change the rheological behavior of an MRF [173]. They potentially offer a highly reliable mechanical operation managed by a magnetic field, that change the yield stress of the MRF to then control the reaction force. Table 4 summarizes the most important factors in MR devices design and the function and utilization of each factor.

Factor	Function	Utilization
MRF properties 1-The carrier fluid 2- Particle density 3-Particle size	1-The carrier fluid acts as a dispersing medium. 2- Particle density increases the magnetic induction under the influence of the magnetic field until the saturation boundary of MRF is reached. 3- Particle size contributes to enhancement of the yield stress of the MRF in the magnetic field.	1-The carrier fluid is used to ensure the homogeneity of particles in the fluid. 2- Particles density is used to increase the saturation boundary of MRF, which influences yield stress. 3- Particles size is used to create MRF structures, which influences yield stress.
Magnetic materials	They direct the magnetic field inside the magnetic circuit.	It is used to built the MR device's structure and magnetic circuit
Magnetic circuit	It generates a magnetic field up to the saturation boundary of MRF material.	It is used to control the yield stress of the MRF in order to control reaction force.

MRF modes	They identify the type of deformation employed in the MRF device.	They are used to explain the mechanism of MR devices in order to aid in designing the magnetic circuit for the MR device.

Table 4. Factors affecting MR devices design.

5.6 Magnetic circuit design requirements

Since the action of the MRF contained inside the damper depends on the magnetic field generated by the magnetic circuit, a good design of the magnetic circuit is a crucial point. The key aspects to keep into account when designing are: magnetic flux lines path in the fluid resistance gap, the flow area geometry, the for magnetic circuit structure materials, and the effective surface area of the magnetic field [7] [174].

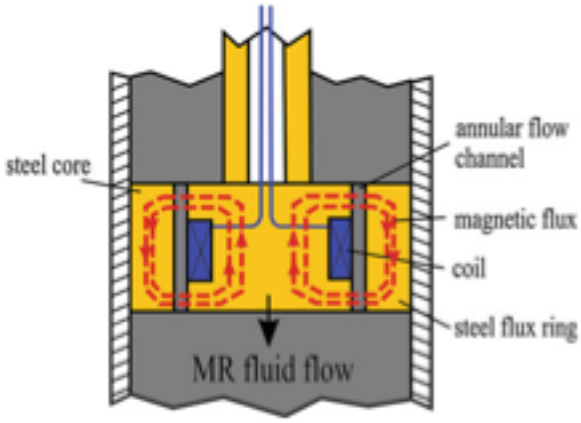

Figure 58. Magnetic circuit design for an MR device [174] [158].

The magnetic circuit usually consists of: magnetic flux lines board, magnetic core, electromagnetic coil and the MRF flow channel located between the outside of the magnetic core and the inside of the magnetic board, as shown in Figure 58 [174] [158]. When designing the magnetic circuit, accurate guidance for the magnetic flux lines into the active surface magnetic area of the MR damper should be provided, in order to control MRF viscosity and dynamic yield stress. So, the damping force of MR damper is actively controlled by the MRF change in viscosity, through the magnetic field intensity control. In absence of the magnetic field, the MR damper force exerted is due merely to the *off-state* viscosity of MRF [175] and the damper acts as a passive damper. Magnetic circuits are typically made of low carbon steel, as it has a high magnetic permeability and saturation boundary. This means that the magnetic flux lines are guided into the MR damper active area and so the magnetic flux density ϕ is controlled. The magnetic flux density ϕ through a surface represents surface integral of the normal component of the magnetic field flux density B passing through that surface.

To calculate magnetic flux density ϕ in a magnetic circuit Equation 45 is used, and it is similar to Ohm's law [176]:

$$\phi = \frac{F}{\sum \Re} \qquad (45)$$

where F is the magnetic movement force in the circuit, and $\sum \Re$ is the summation of the magnetic reluctances of each material part of the magnetic circuit. A low reluctance flux conduit is required to the electromagnetic circuit, so it is usually designed using ferromagnetic materials to guide and to focus magnetic flux density into the MRF contained in the MR damper. Figure 59 shows that the magnetic circuit design for an MR damper has two reluctances, $\Re_1$ is the reluctance of the steel and $\Re_2$ is the reluctance of the MRF.

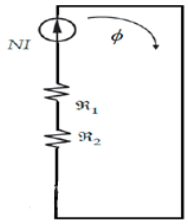

Figure 59. Reluctances in the magnetic circuit [174].

Equation 46 is used to calculate the reluctance in each material utilized in a magnetic circuit as:

$$\Re = \frac{l}{\mu A} \quad (46)$$

where l is the length of magnetic path, A is the cross-sectional area of the flux path and μ is the permeability of the material. The permeability μ can be determined from the BH curve for each material and calculated by Equation 47:

$$\mu = \frac{B}{H} \quad (47)$$

The BH curve can be used to determine the saturation magnetization point for each material and then used for MR damper design.

5.7 MRF material performance

MRF-based dampers change their performance on the basis of the MRF used. Generally speaking, the most influencing parameters are: volume fraction of solid particles (also called "particle loading"), particle size and viscosity of the carrier fluid. A high ratio of solid particles to carrier liquid in the MRF is an indication of high magnetic properties [177]. Jolly et al. in 1996 [3] concluded that the magnetic properties of MRFs vary significantly due to particle density loading in the MRF. The theoretical model results demonstrate that magnetic induction increases with field strength until the saturation boundary of the fluid is reached. This is due to the particles forming chain-like structures (MR structures) parallel to the magnetic field lines. The more the particles, the more the MR chains are formed; this increases the on-state viscosity (when the magnetic field is applied) as well as the off-state viscosity (in absence of magnetic field).

With regards to particle size, it has been demonstrated that fluids with two different distributions of particles size (one being characterized by an average diameter significantly bigger than the other) offer a higher yield stress than those fluids with a single average diameter distribution for particle size [100]. The ratio is that, when the MRF is activated, there is a greater magnetostatic interaction between larger magnetic particles while smaller particles fill the voids between big particles, so reinforcing the MR chains at the same time. The best result is obtained when the solid fraction is constituted by 75% of big particles, and 25% of small ones [70] [80].

Some studies also report that adding nanoparticles ad an additive to a MRF can improve the yield stress because nanoparticles in the on-state reinforce the MR chains [178] [179].

In order to better formulate MRFs, it is important to take into account also the evolution of the materials over time with particular regard to yield stress. One of the most recent studies by Utami et al. [180] demonstrated once again the detrimental effect of In Use Thickening (IUT): during damper operations, particles are forced in contact one with the other and also with the damper walls, which causes friction and breakage of magnetic particles. This leads to an increase in the viscosity of the MRF either in the on-state or in the off-state. So, durability in working conditions is very relevant problem for the damper design and the fluid should be formulated with particular attention to the stabilizers adopted (see chapter 3).

5.8 Other MR damper performances

Other performance to be considered in damper design for vehicle suspension systems are: response time, range of operating temperature.
The response-time is an important parameter particularly of controllable dampers performance. Fast response time is required for real-time control applications. A high level of sensitivity to solicitations is required for the overall suspension performance in terms of acceleration and deceleration transmissibility to the damper response-time and corresponds to the employed control strategy. Many different control strategies have been developed over time: the two-state Skyhook control [181], the linear quadratic control [182], the linear parameter varying LPV/H∞ control [183], LQ-clipped [184], the model-predictive control [185], semi-active H∞ control [186], neural network control [187], but their investigation falls outside the scope of this chapter.

In general, the acceleration and deceleration transmissibility display higher values with increasing response-time and is related to a weaker performing damper. A suitable limit for the reaction time should be identified for the specific control technique employed in a specific damper design. A convenient response-time should be no more than ~20ms. MRFs are activated in a time span of less than 1 ms [8] [17] that makes this class of materials particularly suitable to be used in vehicle suspension systems.
The range of operating temperature for MRF- based dampers depends basically on the carrier fluid thermal stability, which means that the MRF properties remain stable a defined temperature range. For example, hydrocarbon-oil based MRF remain stable over a temperature range of -40/130°C.
At the same time, another design parameter is the active volume of MRF, which is the portion of MRF volume influenced by the magnetic field. Since the damping force the damping force depends on the active volume and on the value of the magnetic flux density, it is necessary to have a high magnetic flux density influencing a large active volume.

5.9 Optimization of MR damper design

The optimization problem for an MR damper takes into account volume constraints and involves the following factors:

I) the damping force,
II) the dynamic range (the different forces in the on- and off- states),
III) the response time.

It has already been shown that the damping force (I) and the dynamic range (II) depend on the fluid characteristics (yield stress, carrier fluid viscosity, particle loading etc.), but also on the design and on the characteristics of the magnetic circuit.

Focusing on response time (III), its reduction depends on MRF time response, inductance of MR damper coil, eddy currents induced in the magnetic circuit. Since MRF time response is very short (few milliseconds), the other two components give a sensible contribution to long time response for the MR damper. The contribution of coil inductance to reaction time was studied by Yang et al. [1]. The solution was using a current controller keeping an input voltage approximately five times higher than one calculated with Ohm's law until the desired current in the circuit is reached. So the time response of the damper went from 300 ms (without current controller) to 60 ms (with the current controller).
Recently Strecker et al. [17] faced the problem of eddy currents. A response time of less than 1.5 ms was achieved when fast current controller was used, by using a material with high relative permeability and low electrical conductivity, such as ferrite. The use of ferrite has the advantage of reducing also remanent induction in piston body in the off-state, but presented also some important

drawback, especially in comparison with steel: a) poor mechanical properties, because ferrite is a very fragile material and the tensile strength limit (30 N/mm2) is lower than steel; b) low magnetic saturation so as, given a fixed geometry, the maximum induction in the resistance gap (the afore-mentioned fluid resistance space) is lower than in the case of magnetic circuit made of steel.

With concerns to the maximization of the damping force and the dynamic range (ii), the first study with the aim of maximizing the afore-mentioned two performances was proposed by Spencer et al. [132] presenting a multi-coil MR damper to increase the total damping force for a seismic protection system (Figure 60).

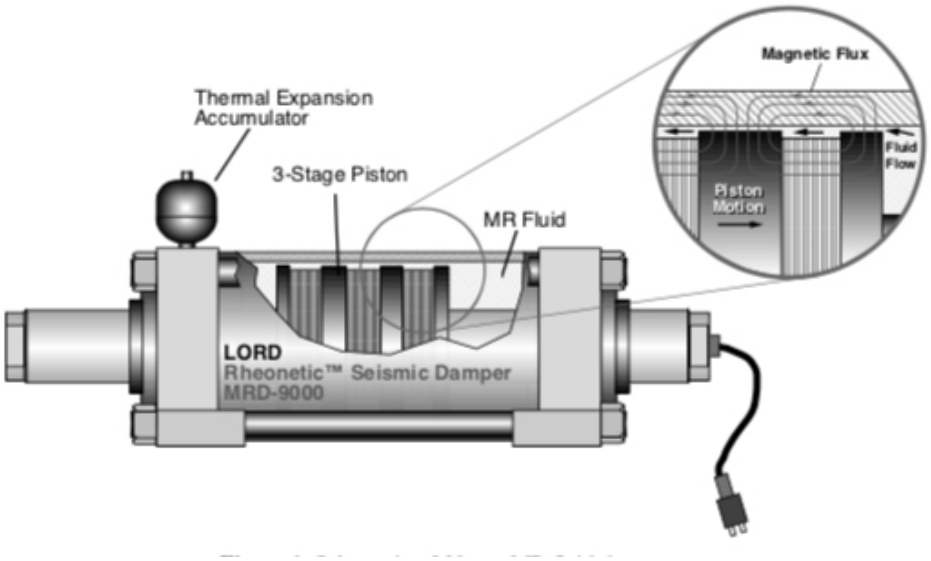

Figure 60. Schematic of 20-ton MRF damper [133].

With the same objective Potnuru et al [188] proposed a tapered annular flow channel to obtain different damping forces in compression and rebound, as shown in Figure 61. Usually, MR dampers have regular geometry and linear flow channels, and the magnetic field is constant along the length of the gap. In this case, the resistance gap has a varying cross-section to obtain different pressure drops, and so forces, in compression and rebound. When the piston moves, and the fluid enters the wider section from the narrow (from zone1 to zone 5) the orifice acts as a nozzle and the pressure drop is higher. On the contrary, in the opposite direction the orifice acts as a diffuser, resulting in small pressure drops.

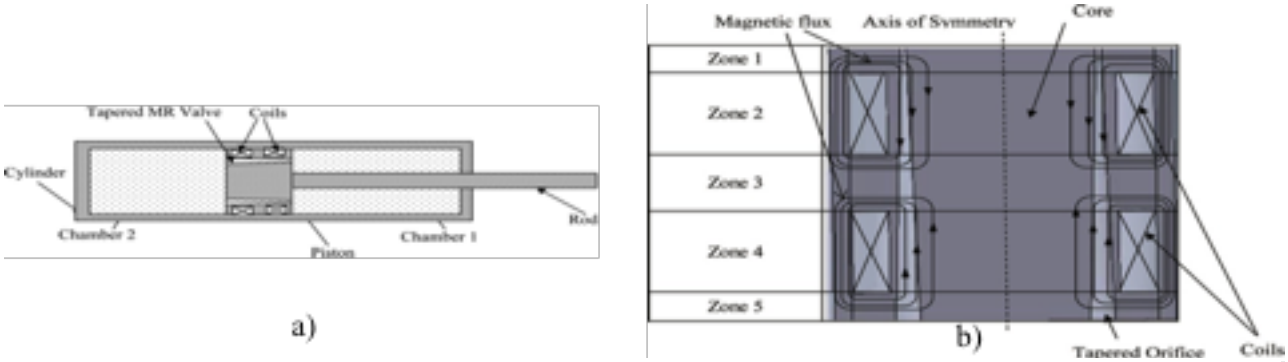

Figure 61. a) Schematic of MR damper with tapered MR valve; b) Magnetic field along the tapered MR valve [185].

The evolution of this latter design, in combination with the multi-coil system, is shown in Figure 62 and was proposed by Zheng et al. [189]. Four different MR valves are presented with four individual voltage sources. In comparison with a traditional multicoil based MR damper, the performance of the damping force at V = 0.75 m/s and I = 1.5A is F= 6000N vs F=3000N of the traditional damper (see Figure 63).

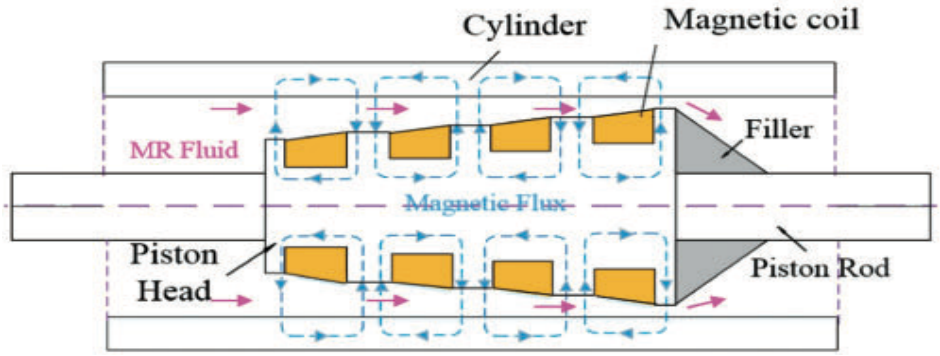

Figure 62. Multi-coil MR damper with a variable resistance gap [186].

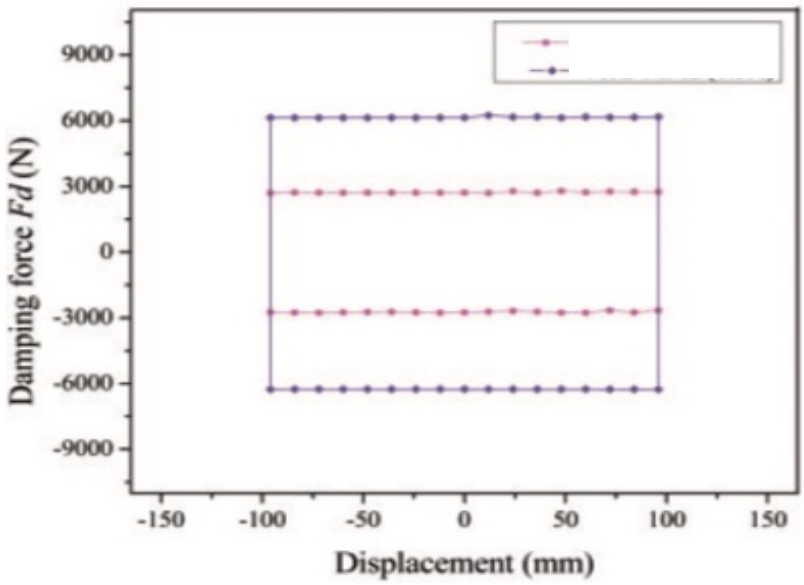

Figure 63. Damping force vs. displacement curve for current 1.5 A, V=0.75 m/s for traditional damper and tapered annular flow damper [186].

With the same objective of enhancing damping force and reducing response time (but also enhancing heat dissipation efficiency and structural compactness), a pumping MR damper was proposed by Zhang et al. [190], as shown in Figure 64. The fluid in the damper is forced to flow only in one direction using unidirectional piston and foot valves, with the advantages of increasing the structure flexibility of the magnetic system (coil configuration and the effective resistance geometry can be easily reconfigured) and improving heat dissipation efficiency (the heated fluid conveys the generated heat directly to the outer cylinder). The reaction forces are 600–3000 N in extension and 225–1200 N in compression.

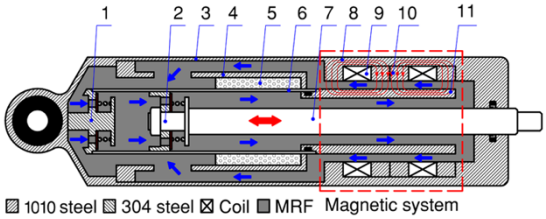

Figure 64. Schematic representation of pumping MR damper [190].

5.10 Future trends in MR damper design

To conclude the overview on the recent evolution on MR damper for suspension systems it is important to mention self-sensing and self-powered energy-saving smart MR dampers, especially nowadays when energy saving alternatives to traditional devices are so important. With traditional suspension systems there is a big share of wasted energy, deriving from road vibration due to highway roughness, car speed and damping capacity of passive systems. A traditional four dampers system on a vehicle on a rough highway at a speed of 13.4 m/s dissipates 200W while traveling. Self- sensing and self-powered systems have no harmful effects on the environment and improved the credibility of whole MR damper systems as effective alternative to the traditional passive damping systems [191].

The first step toward the smart innovation in MR damper suspension system was set by Wang and Wang [158] with the introduction of self-sensing magnetorheological dampers, in order to tackle the problems of system cost, system structure complexity, installation space and system reliability. The idea was to integrate the relative displacement sensor into the MR damper, so dynamic response sensors and relative connectors were eliminated, thus reducing costs and enhancing the system reliability. The magnetic circuit of this innovative MR damper is here mainly constituted by two coils: an exciting coil-wound on the piston and an induction coil wound on the cylinder made of nonmagnetic material. The exciting coil acts at the same time both on the MRF and on the integrated displacement sensor. The piston, piston rod and cylinder cover are made of soft steel with high magnetic permeability, while the cylinder, exciting coil cover are made of nonmagnetic steel. The exciting coil is stimulated with a signal obtained by the superposition of a harmonic voltage signal on a direct current. The direct current acts on the MRF yield stress to control the damping force. The harmonic voltage signal, instead, induces a harmonic magnetic field along the primary flux path shown in Figure 65 and so induces the same harmonic voltage signal with the same frequency in the induction coil. The movement of the piston changes the number of the active turns of the induction coil in the primary flux path, varying the induced voltage on the induction coil. In this way the piston movement and the induced voltage are directly linked and through the interpretation of the induced voltage signal it is possible to define the relative displacement of piston and cylinder in the MR damper.

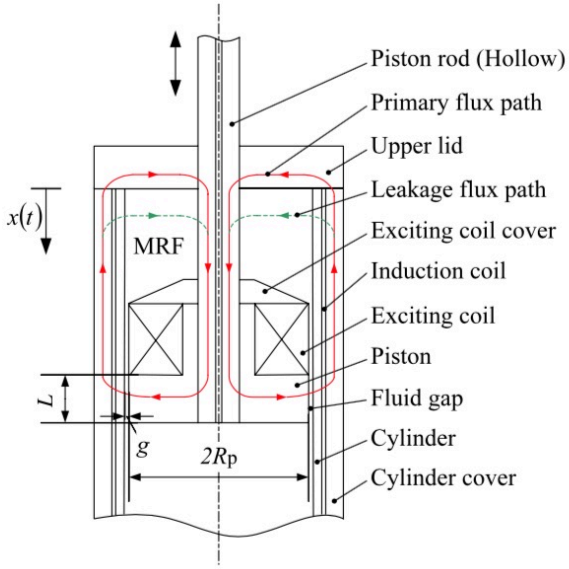

Figure 65. Schematic representation of self-sensing MR damper [158].

Finally, focusing on self-powered systems, the idea of using linear vibrations of MR damper systems to provide regenerative energy was firstly introduced by Choi and Wereley [192]. This is still an interesting topic because of the following advantages: energy saving, independence of extra batteries, less maintenance. In fact, one of the latest studies was conducted by Chen et al. in 2018 [193]adapting the self-powered MR damper to stringent constrains of motorcycle dampers. The general idea at the basis of such design is to convert part of the vibration energy in electrical energy to power itself and change the rheological characteristics of the MRF contained in the damper. The schematic for this damping system is shown in Figure 66. The suspension system is made of an MR damper, an electromagnetic power generator, a motion conversion unit (to possibly convert the linear movement of the MR damper into a desirable motion for the power generator) and energy-harvesting and control circuits. There are two alternative ways to apply electrical energy to the MR damper coil: a semi-active control or the direct-feedback technique. With the first method the electrical energy is processed and accumulated in energy-harvesting devices; then, with an appropriate control algorithm, it is applied to the electromagnetic coil to provide a suitable magnetic field to act on the MRF. With the second method, instead, the induced voltage of the power generator is directly applied to the MR damper coil.

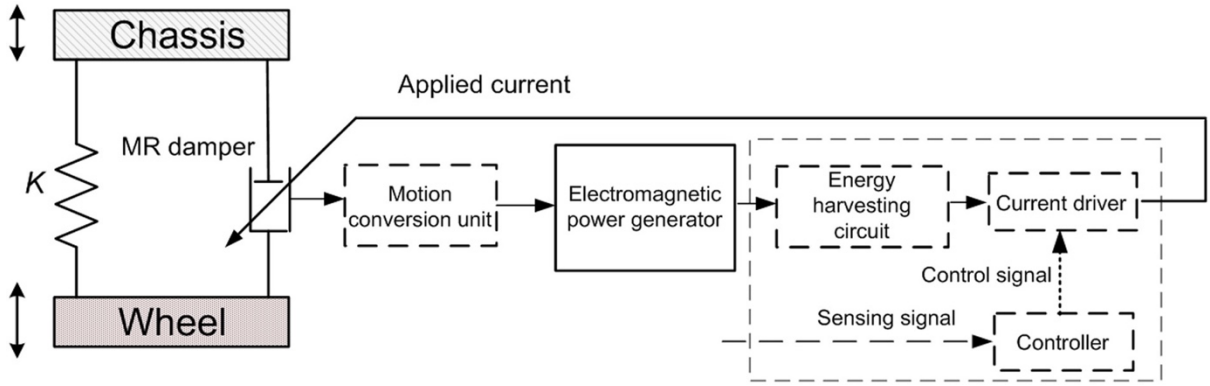

Figure 66. Schematic diagram of the self-powered MR damper suspension [193].

Conclusion

The aim of this chapter was to review the existing MRF dampers, starting from the experimental MRF dampers designed for manufacturing applications and expanding the scope to other fields. In fact, due to the peculiar characteristic of scalability for this kind of devices, the considerations valid for MRF dampers used in automotive or civil engineering can be also used for machining operations. When designing a new damper many factors need to be taken into account: MRF materials and properties, magnetic materials, magnetic circuitry, damping behavior modelling. These factors are used to improve design techniques leading to better performance of MRF dampers with reduced cost and improved sustainability.

The first factors are MRF materials and properties. The force that MR devices can exert is affected by the MRF specifications, such as iron particle loading by volume and iron particle size. When the iron particle loading by volume is increased, magnetic flux density is increased. Larger iron particles size increases the particles dimensions and contributes to a greater yield stress of the MRF in a magnetic field.

The second factor is magnetic materials and the designing of magnetic circuit. An accurate selection of diamagnetic, paramagnetic, or ferromagnetic materials allows to direct and control the magnetic field through the MR damper, and to focus the magnetic field on the MRF in an effective and specific surface area of the damper.

Finally, using or defining an appropriate model to describe and control force–velocity response of MR dampers is crucial.

Each one of these factors (and many others) are constantly under research and evolution.

6. Novel MRF for manufacturing damper applications in valve mode

Magnetorheological fluids are suspensions of micron-sized (from 10^{-7} to 10^{-5} m) magnetizable particles in a nonmagnetic carrier fluid. MRFs exploitability lies in their capability to swiftly and reversibly change their viscosity in response to an externally applied magnetic field and, accordingly, their mechanical properties. This is due to the particles forming chain-like structures (MR structures) parallel to the magnetic field lines. The most used material for the MRF's solid fraction is SOFT carbonyl iron powder (CIP), because of the higher iron content (with respect to HARD CIP) and the consequently higher magnetic properties. Several researches have been performed to improve the mechanical performance of MRFs. The simplest solution proposed so far is to increase the volume fraction of micron-sized particles in the fluid, but this implies a higher value of the viscosity in absence of external magnetic field. This latter effect is undesirable, because devices based on MR effect operate for a major part of their life in absence of magnetic field and are designed for low values of viscosity. It has been shown that the best compromise to keep relatively low *off-state* viscosity (absence of magnetic field) and high *on-state* yield stress (presence of magnetic field) is using MRFs formulated with a bi-disperse distribution of micron-sized particles in the solid phase [100]. This means that there are two distributions of micron-sized particles, characterized by two different average diameters, one significantly bigger than the other. The best result is obtained when the solid fraction is constituted by 75% of big particles, and 25% of small ones; but also a 50% and 50% composition represents a fair compromise [70].

As it has already been shown in chapter 2, the yield stress depends on the interaction between the materials used for the solid fraction of MRFs and the externally applied magnetic field, with particular reference to the intensity of the magnetic field. The advantage of bidisperse fluids lies in the capability of smaller particles to fill the voids of MR chains in the *on-state* regularizing them.

In general, the application of MRFs to devices is now limited by the drawback of their stability in terms of sedimentation behavior: in the *off-state,* particles tend to agglomerate due to residual magnetization and then sediment [8]. Ferrofluids (FFs), on the other hand, are colloidal dispersions of magnetic nanoparticles (10 nm) and exhibit the same basic functioning mechanism of MRFs. The main difference is that FFs are characterized by long term stability [194], but also, unfortunately, by lower yield stresses than MRFs [195]. Since this second flaw is prevalent over the stability, their exploitation is even more limited to date with respect to MRFs. Table 5 offers a comparison between the properties of MRFs and FFs.

In particular, a comparison can be operated on the basis of the energy factor λ. This factor can be defined for an individual particle in terms of ratio between Brownian thermal energy and magnetic polarization energy as follows:

$$\lambda = \frac{\mu_0 * P_{mag}^2 * V}{12 * k * T} \quad (48)$$

where P_{mag} is the polarization, V is the particle volume, k is Bolzmann's constant and T is the temperature.

Representative feature	MRF	FF
Energy factor λ	>1	<1
Maximum yield stress	100kPa	10kPa
Particle size	μm	nm
Particle material	Carbonyl iron	Iron oxide
Fraction by volume	Up to 50%	Up to 10%
Stability	Controllable shear stress	Controllable liquid flow

Table 5. MRF vs FF properties [2].

Many studies have been devoted formulating MRFs using micron-sized magnetizable particles disperse in an FF acting as a carrier fluid. This class of materials is called "Inverse Ferrofluids" (IF). In the *off-state*, the sedimentation phenomenon is prevented because nanoparticles disposition breaks micron-sized particles aggregates (due to residual magnetization), provided nanoparticles are characterized by a high value of the surface-to-volume ratio, which balances the density mismatch between carrier fluid and micron-sized particles [77]. In the *on-state*, instead, nanoparticles fill the voids between micron-sized particles regularizing MR structures. This fact, together with higher magnetic permeability of nanoparticles, causes a considerable increase in the yield stress [26].
Concerning the adoption of nanoparticles, a crucial issue to be solved is their shape. Nanospheres are commonly used, but it is also known that nanowires can particularly enhance yield stress at lower magnetic field, since they align along the magnetic field lines enhancing the mechanical resistance of the as-formed MR structures [196]. Up to now, a major part of researches conducted on yield stress, sedimentation, and magnetic behaviors of IFs involve one size distribution of micron-sized particles [104] [197]. Only few analyses focused on the effect of adding magnetic nanoparticles to a bi-disperse MRF, obtaining a so-called three-disperse MRF. The aim of this work is to formulate a novel MRF with improved resistance to sedimentation to be used in manufacturing applications for damping chatter in devices designed in valve mode. For this purpose, magnetite nanoparticles of two shapes were used: spheres and hexagonal platelets, the latter being used for the first time in MRF formulations.

A second aim of this chapter is to model and investigate the modification induced on the behavior of magnetization by nanoparticles addition. To do so, the Ising model was selected because of its effectiveness to theoretically describe the phenomenon of ferromagnetism [198]. It was used to fit experimental magnetization curves.

6.1 Ising model introduction

Consider N magnetic particles subject to the action of a uniform magnetic field H in a fixed direction (say z with no loss of generality). Each particle is characterized by a classical spin S with two possible orientations in the z direction, s_i=+1 for spin up or s_i=-1 for down, being s_i the z-component of the i-th spin. The total energy of the system is:

$$E = -J \sum_{<ij>} s_i s_j - \mu H \sum_{1=1,N} s_i \quad (49)$$

where we denote <ij> for the sum over nearest neighboring pairs of magnetic particles, J is the exchange energy, μ is the atomic magnetic moment.
The term $-J \sum_{<ij>} s_i s_j$ expresses exchange interaction due to the Pauli exclusion principle and indicates a decrease in overall energy if neighboring spins are aligned. For instance, two electrons with parallel spins cannot come close in space in the same orbital. This is possible, instead, if they are characterized by anti-parallel spins. The exchange energy J measures the different level of energy due to magnetic interaction magnetic moments generated the spins. An exactly solvable modification of this model can be useful to describe the systems with long-range. Introducing the "mean field approximation", the energy of i-th particle can be written as follows:

$$e_i = -\frac{J}{2} \sum_{k=1,z} s_k s_i - \mu H s_i \quad (50)$$

considering the summation over the z nearest neighbors of particle i. The factor 1/2 is used to avoid counting twice each pair of neighboring particles when considering the total energy

$$E = \sum_{1=1,N} e_i \quad (51)$$

We can introduce the effective magnetic field H_{eff} such that

$$e_i = -\mu H_{eff} s_i \qquad (52)$$

This field is made of two components as:

$$H_{eff} = H + \frac{J}{2\mu}\sum_{k=1,z} s_k \qquad (53)$$

where H is the external magnetic field, and $\frac{J}{2\mu}\sum_{K=1,z} s_k$ is the internal field generated by neighboring particles.
Focusing on a single particle in a magnetic field H_m in thermal equilibrium with a heat bath at temperature T, the following expression can be used to express the average value of the spin, according to the Boltzmann distribution:

$$\bar{s} = \frac{e^{+\beta\mu H_m} - e^{-\beta\mu H_m}}{e^{+\beta\mu H_m} + e^{-\beta\mu H_m}} \quad (54)$$

where $\beta = 1/kT$, k being the Boltzmann constant. This expression comes from the energy of the "spin up" state (s=+1) being $-\mu H$, while the energy of the "spin down" state (s=-1) being $+\mu H$. Thus, we have that

$$\bar{s} = \tanh(\beta\mu H_m). \qquad (55)$$

Assuming that all particles have identical spins i.e., $\bar{s} = s_i$ the mean field approximation corresponds to substituting this average in the expression of the effective field experienced by a single particle

$$H_{eff} = H + \frac{zJ\bar{s}}{2\mu} \qquad (56)$$

with z the number of neighboring magnetic particles.
Combining equations 55 and 56 it can be obtained the following expression:

$$\bar{s} = \tanh\left(\beta\mu H + \beta\frac{zJ\bar{s}}{2}\right) \qquad (57)$$

representing a self-consistent equation for the average value of the spin of a particle at fixed values of external field, temperature and magnetic parameters characterizing the interaction.

6.2 Experimental Section

6.2.1 Aims of the experiment

The first aim of the experiment performed was to analyze the effect on sedimentation (in terms of ratio and rate) of the addition of nanospheres and hexagonal platelets to a bi-disperse MRF. At the same time, the aim was to study the interaction between nanoparticles and CIPs (SOFT as well as HARD).
A second aim experiment was to study the effect of nanoparticles addition on magnetization curves. Experimental magnetization curves were generated using a magnetometer and the Ising model was used to fit them and predict the changes.

6.2.2 Materials

Four different Carbonyl-Iron Powders (CIPs, supplied by BASF SE - Germany) in two different types (HARD and SOFT) and dimensions were used (see Table 6) to formulate a reference MRF. This MRF is then modified by addition of nanoparticles. HARD and SOFT particles differ from each other for their skin structure, mechanical properties, Fe and other elements (C, N, O). In particular, HARD carbonyl iron powders are produced from the primary thermal decomposition of iron pentacarbonyl ($[Fe(CO)_5]$), without further chemical processing and are characterized by onion-skin structure, high mechanical hardness and relatively high content of other elements (C_{max} 1.0 %, N_{max} 0.9 %, O_{max} 0.5 %). SOFT carbonyl iron powders, instead, are produced by annealing of HARD grade carbonyl iron powder under hydrogen. In this process, producing mechanically soft particles, the onion skin structure is lost, and the content of C, N and O is reduced.
Two sizes ("large" and "small" in Table 6) were chosen both for HARD and SOFT CIPs:

Carbonyl-Iron powders	HARD	SOFT
LARGE	"CIP EM" 4.5-6.0 μm (density 7.8 g/cm^3)	"CIP CM" 7.0–9.5 μm (density 7.8 g/cm^3)
SMALL	"CIP HQ" 2.0 μm (density 7.8 g/cm^3)	"CIP SM" 3.5 μm (density 7.8 g/cm^3)

Table 6. Types and dimensions of CIPs from BASF SE. Particle sizes refer to the diameter of at least the 50% of the particles in the sample [178].

Paraffin Oil from Carlo Erba was used as carrier fluid (viscosity 110 ÷ 230 mPa·s; density 0.827 ÷ 0.890 g/cm^3); Oleic acid and bis-(2-ethylhexyl) sebacate 95% (both purchased from Alfa Aesar) were used as additives. As concerns nanoparticles, two different types were selected: magnetite nanospheres from Sigma-Aldrich (50 ÷ 100 nm) and in-house prepared magnetite hexagonal nano-platelets (see Figure 67) [199].

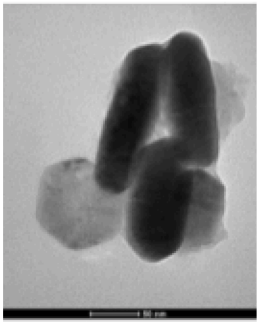

Figure 67. Representative low-magnification TEM images of a hexagonal nano-platelet of magnetite [199].

6.2.3 Preparation of the suspensions

For our experiments, 12 novel MRFs listed in Table 7 were prepared by pouring oleic acid and the two additives (Oleic Acid and Sebacate) in a glass container. Then nanoparticles were added in order to obtain FFs. The as- prepared mixture was stirred using Vortex instrument to ensure a homogeneous dispersion. Then, CIP were added in the same glass container (first large particles and then small ones). Again, the mixture was stirred using Vortex. Then, ultrasonic bath was used for 1 h to prevent nanoparticles agglomeration. The first letter H or S indicates the kind of carbonyl iron used (HARD or SOFT). The first number represents the percentage of large particles of carbonyl iron used; the second one, the percentage of small particles. The last letter stays for the nanoparticles: N, if none are present, A if nanoparticles are spherical, S if they are hexagonal platelets.

HARD	SOFT
H-75-25-N	S-75-25-N
H-50-50-N	S-50-50-N
H-75-25-A	S-75-25-A
H-50-50-A	S-50-50-A
H-75-25-S	S-75-25-S
H-50-50-S	S-50-50-S

Table 7. List of experimental fluids [178].

6.3 Testing procedure

6.3.1 Sedimentation

The sedimentation behavior of the as-prepared three-disperse MRFs and MRF-122EG (a commercial MRF by Lord Corporation used as benchmark), was studied by monitoring the evolution with time of the sediment-supernatant interface. For this purpose, a cylindrical glass tube (10 cm height; 10 ml volume) was filled with 8.0 ml of an MRF and the evolution was recorded by taking photographs at predefined intervals of time: the first seven days one picture every five minutes for 240 minutes. Then one picture for day 8 and one after 36 days. Figure 68 shows the MRFs at the beginning (time = 0) and at the end of the study after 36 days.

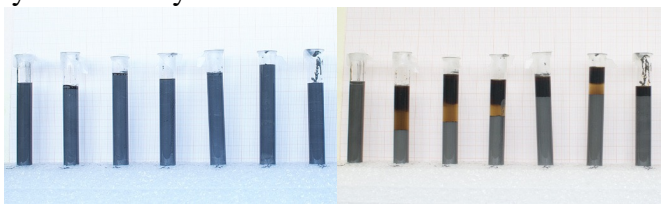

Figure 68. Left, samples at beginning of experiment; right, after 36 days [178].

The initial height of the suspensions and the height of the sediment-supernatant interface were measured using the software Image-J®.

6.3.2 Magnetization

The magnetic properties of the prepared MRFs and the commercial fluid were investigated using a magnetometer VSM (vibrating sample magnetometer) from MicroSense - Model 10. No particular operation was performed before testing the materials, so the liquid samples were simply poured in the testing rig container. Then, at room temperature, the fluids were tested varying the magnetic field and measuring the magnetization in response. The magnetic field was changed from 0T to 2T and then from 2T to -2T and then again from -2T to 0T to highlight the magnetization loop present. The magnetization curves were then plotted.

6.4 Results and Discussion

6.4.1 Sedimentation

The height of the sediment-supernatant interface normalized by the initial height of the suspensions is plotted as a function of time (Figures 69 and 70).

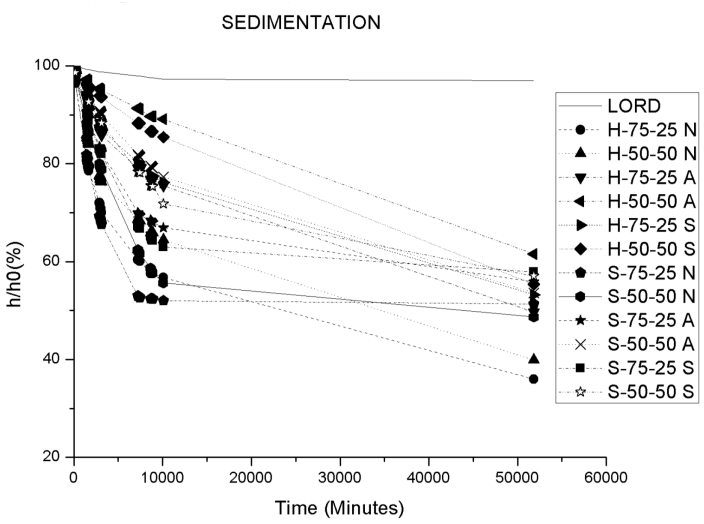

Figure 69. Relative height (h/h0) of the sediment-supernatant interface as a function of time for all samples, from minute 0 to minute 51840 (36 days) [178].

From Figure 69 it results that the commercial fluid (by Lord) remains stable over time, while the experimental MRF is subjected to sedimentation. Experimental MRFs curves show a steep decrease with time, so sedimentation rate is high, independently from size distribution, presence and shape of nanoparticles or type of CIP used. After a long time (t>10000min), for the SOFT-particles based fluids sedimentation rate slows down and a sort of stationary state is reached. For HARD-based fluids, instead, even after 36 days no plateau is reached. This indicates that HARD-based fluids are less stable than SOFT-based ones in the long term. Focusing on the particle size distribution, HARD-based fluids with 75% of large particles (independently from the presence and shape of nanoparticles) sediment more than fluids with 50% of large particles. For SOFT-based fluids, this behavior is confirmed until the stationary state is reached, around t=10000min (7 days). After this threshold, the behavior is the opposite: MRFs with the 75% of large particles show a lower sedimentation ratio than fluids containing 50% of large particles.
As far as nanoparticle contribution to sedimentation is concerned, in general fluids without nanoparticles have the worst performance (see H-75-25N and then H-50-50N), while fluids containing spherical nanoparticles show the best performance (see H-75-25A and then H-50-50A). Hexagonal nano-platelets generally mitigate the sedimentation process, but with a reduced effect in comparison to spherical nanoparticles.

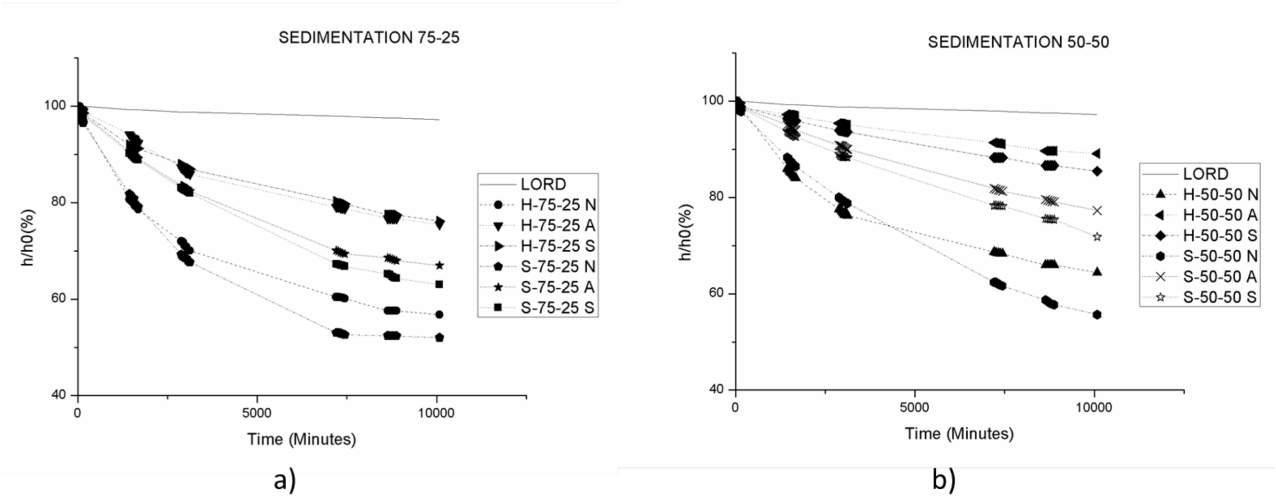

Figure 70. Relative height (h/h0) of the sediment-supernatant interface as a function of time for samples containing a) 75% of big particles and 25% of small particles, and b) 50% of big particles and 50% of small particles from minute 0 to minute 10080 (7 days) [178].

Figure 70 allows to focus on the "short" term (t_{max}= 10080 min). Figure 70a shows the behavior of fluids with 75% of large particles: generally, the absence of nanoparticles results in the worst MRF performance in terms of sedimentation, where HARD based MRFs sediment less than SOFT-based ones. For HARD-based fluids the sole presence of nanoparticles (independently from their shape) stabilizes the sedimentation phenomenon. Instead, for SOFT-based fluids, a significant beneficial effect is provided by spherical nanoparticles. The same can be observed for fluids with 50% of large particles (Figure 70b).

6.4.2 Magnetization

The magnetization is expressed as a function of external magnetic induction given by μH.
Figures 72 and 73 show the magnetization curves for fluid based on 75-25 composition (AY, NY, SY hard and soft), while Figures 74 and 75 show the magnetization curves for fluid based on 50-50 composition (AY, NY, SY hard and soft).
The magnetization curve of the Lord fluid as benchmark shows that, differently from the novel MRFs tested, the commercial fluid does show hysteresis phenomenon. See Figure 71.
Experimental magnetization curves, on the other hand, show that there are no significant differences between experimental fluids independently of their composition expressed in terms of quality (hard and soft) and quantity (75-25 or 50-50) of the solid fraction or the presence or the shape (spherical or hexagonal) of magnetic nanoparticles.

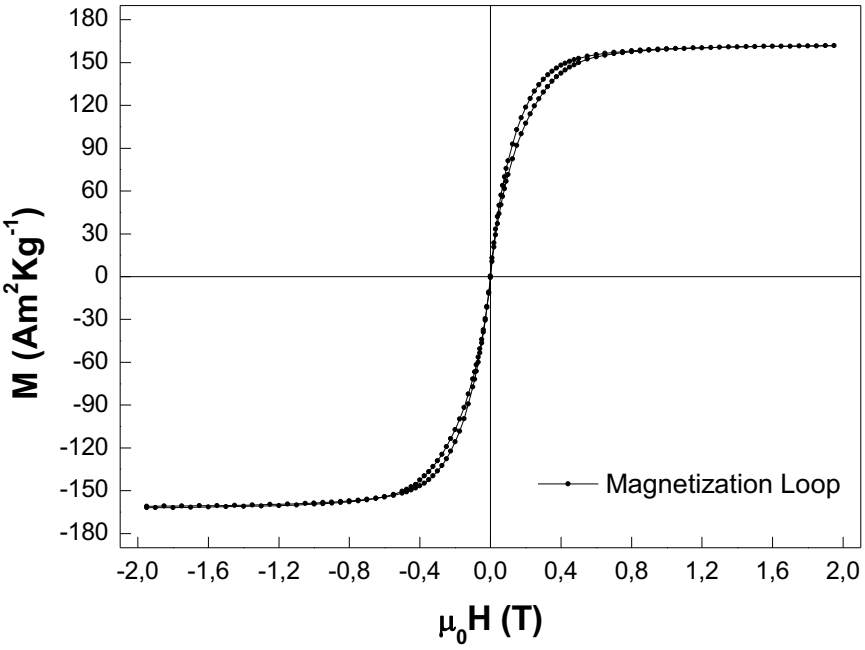

Figure 71. magnetization curve for the Lord commercial fluid.

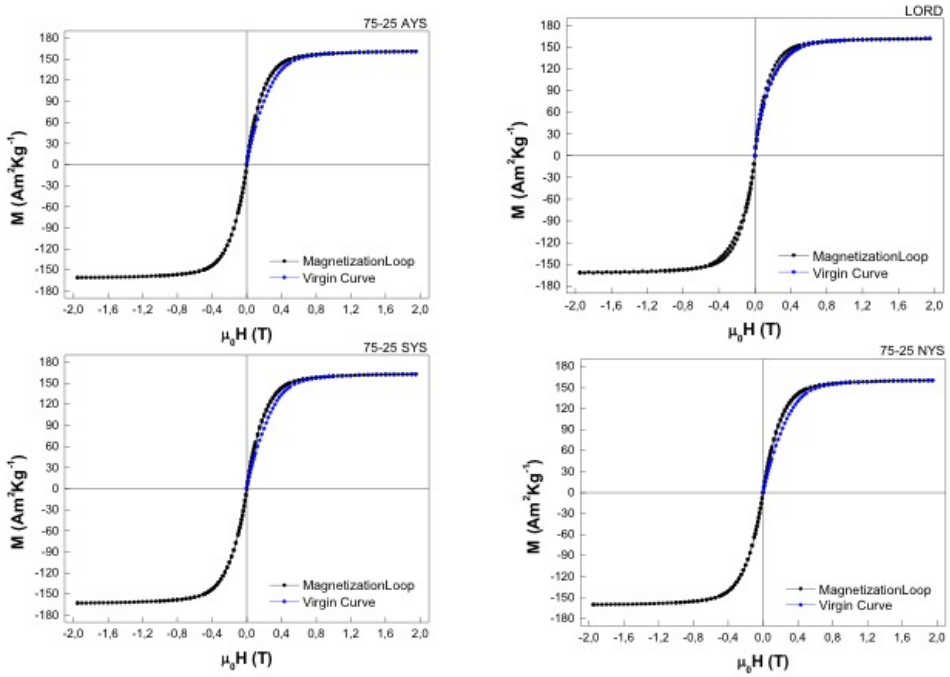

Figure 72. Clockwise magnetization curves for 75-25 AYS, Lord commercial fluid, 75-25 NYS, 75-25 SYS fluids.

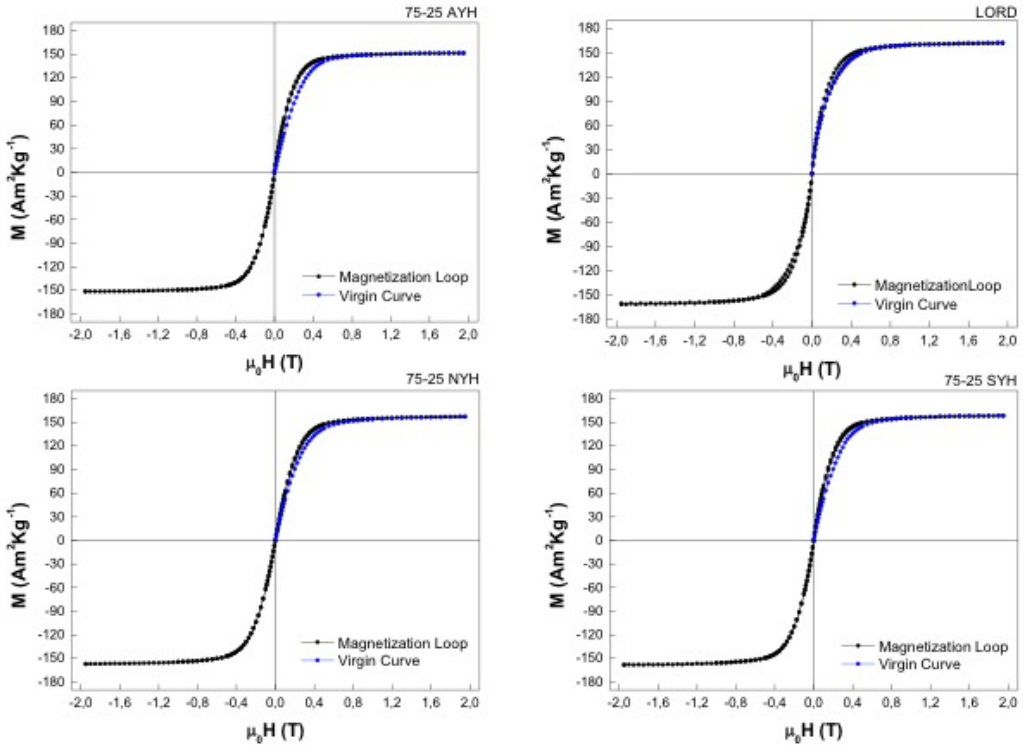

Figure 73. Clockwise magnetization curves for 75-25 AYH, Lord commercial fluid, 75-25 SYH, 75-25 NYH fluids.

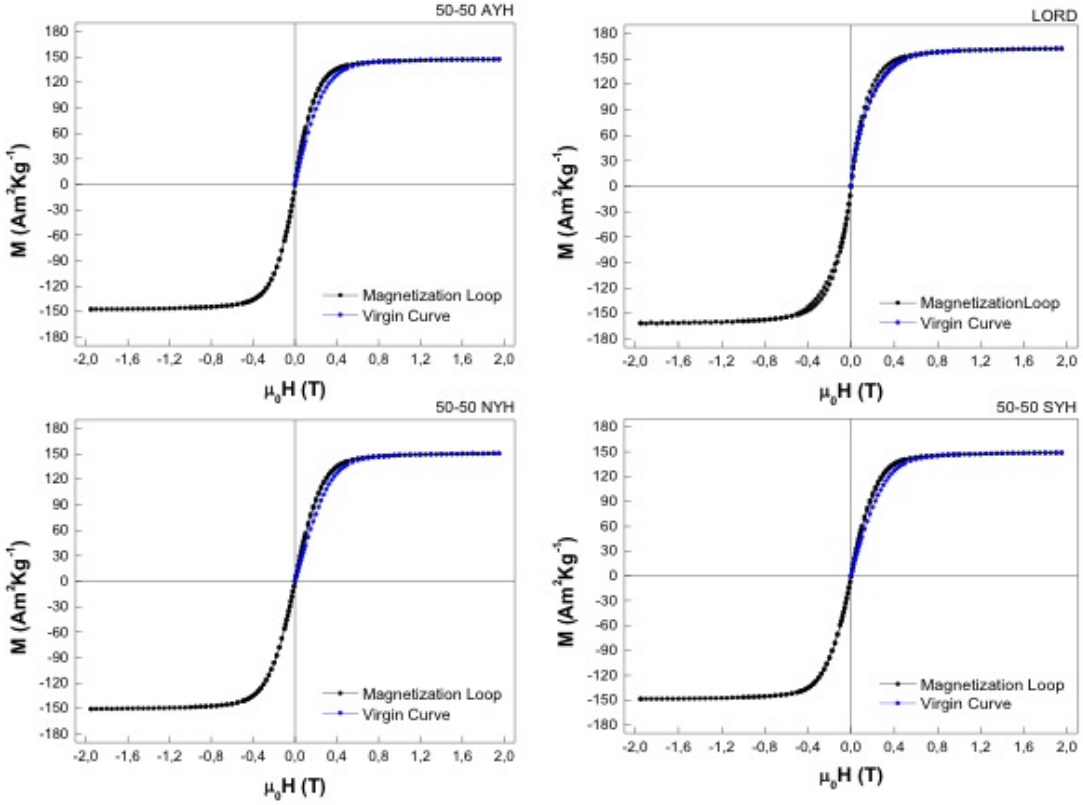

Figure 74. Clockwise magnetization curves for 50-50 AYH, Lord commercial fluid, 50-50 SYH, 50-50 NYH fluids.

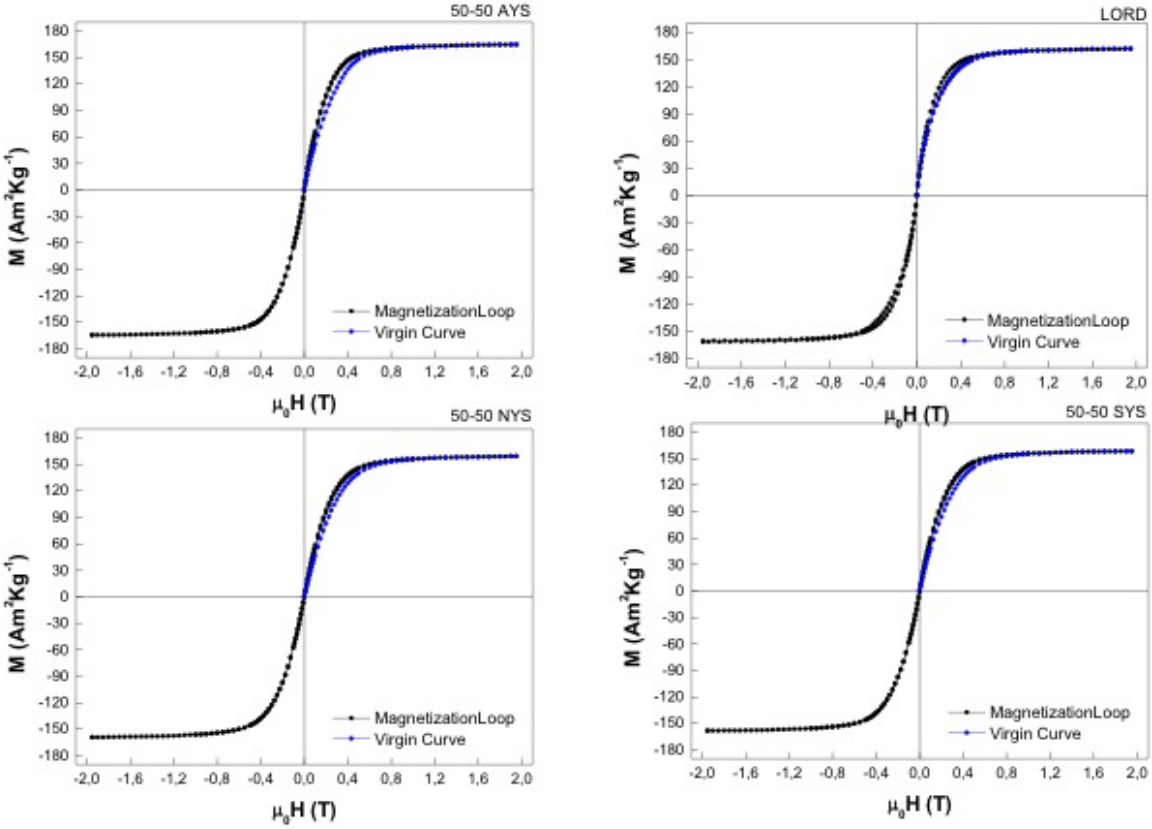

Figure 75. Clockwise magnetization curves for 50-50 AYS, Lord commercial fluid, 50-50 SYS, 50-50 NYS fluids.

By using Mathematica software, the Ising model used to fit the experimental curves is expressed as:

$m - \tanh[(\beta * coeff1 * H) + (coeff2 * m)] == 0.$

Each fluid was plotted 3 times:

- virgin curve (with magnetic field varying from 0 to 2T);
- descending curve (from 2T to -2T);
- ascending curve (from -2T to 2T).

Even for the fitted curves there is not significant evidence that the magnetic behavior is influenced at all by the composition of solid fraction (hard/soft or 75-25/50-50) or the presence of nanoparticles with different shapes. To show this, the descending curves for 75-25AY HARD and SOFT fluids were selected and are shown in Figure 76. In Figure 77 there is the representation of the standard error for both the curves.

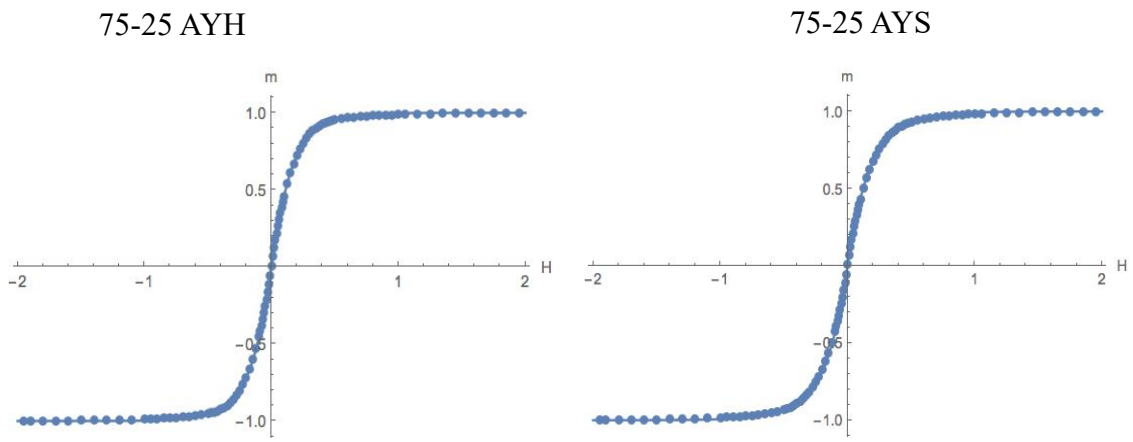

Figure 76. Magnetization curves for fluids 75-25 AYH and 75-25 AYS.

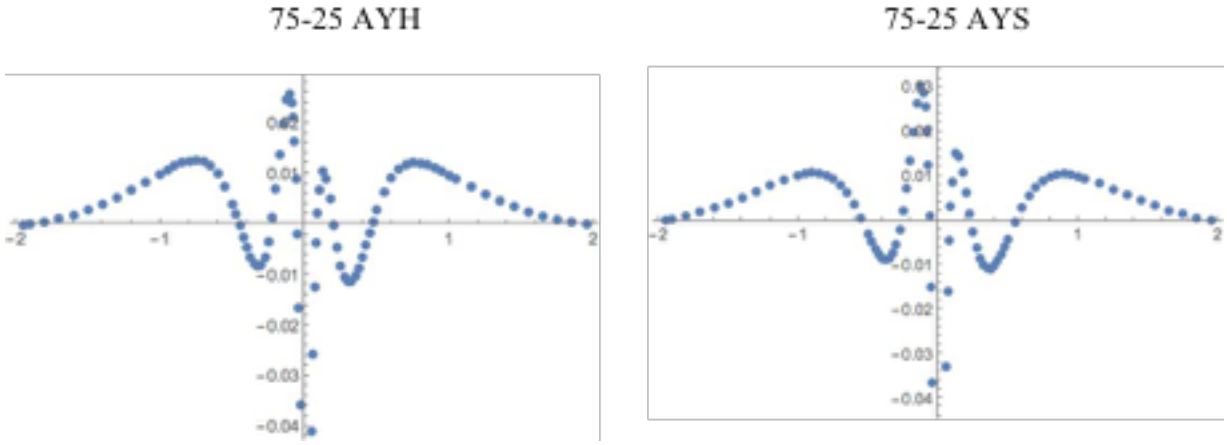

Figure 77. Standard error curves for fluids 75-25 AYH and 75-25 AYS.

Conclusion

The behavior of three-disperse MRFs obtained by addition of nanoparticles to a bi- disperse MRF was studied. In general, with regards to sedimentation, it has been shown that the absence of nanoparticles has a detrimental effect on the sedimentation behavior, while the presence of nanoparticles (particularly the spherical ones) mitigates the effect of sedimentation, independently from the type of CIP used. There is no significant evidence that hexagonal shape of nano-platelets enhances the sedimentation behavior. Furthermore, it is evident that SOFT-particles based MRFs generally show a more stable sedimentation behavior than HARD-particle based fluids, because their sedimentation rate slows down in the long term (after 1 week). At the same time, it is clear that HARD-particle based MRFs show smaller sedimentation ratio (around 10% difference between HARD-based fluids and SOFT based fluids). Finally, fluids characterized by 75% of large particles, show a higher sedimentation ratio than fluids containing 50% of large particles, even in presence of nanoparticles. This might be due to the higher weight of the solid fraction. In conclusion, it is evident from the experimental MRFs synthesized are not stable over time: further investigation is needed to clarify whether this behavior depends either on the additives used or on the preparation procedure.

With regards to the magnetization behavior, the modelling with the Ising model did not show any significant difference in magnetic behavior due to the different formulation of the novel three-dispersed experimental MRFs.
This might be due to the "mean field approximation" used, because the particle interaction is distributed and so the model can easily fit all the particle domain behavior, especially considering the spatial distribution of MR chains under the influence of externally applied magnetic field.
Further investigation would be needed to explain if samples preparation might have influenced the magnetic behavior study. In fact, MRFs have been tested after a long time. Sedimentation may have occurred in the meanwhile and nanoparticles might have agglomerated to form magnetic domain comparable to the ones provided by "big" μsized particles. New magnetic measurements have to be provided in that case after a new cycle of redispersion and sonification to show this conclusion due to the breaking of nanoparticles agglomerates.

Conclusion

According to the aims of this thesis put in the introduction we can state these were studied accurately.

As concerns the design an innovative MRF with improved response to the sedimentation drawback to be employed in the damping device for manufacturing applications, several solutions of a novel three-dispersed magnetorheological fluid were formulated, varying for the solid fraction a combination of the two different average diameters of the micron-sized particles and the nanoparticles. These combinations were tested from the point of view of sedimentation and from the point of view of magnetic behavior. Results on the sedimentation process were interesting, since it was observed the phenomenon induced by the presence of spherical nanoparticles that mitigates sedimentation process, expressed in terms of sedimentation ratio and velocity. No significant difference in magnetic behavior was, instead, distinguished even with the modelling based on Ising model. Further investigation may bring to a better performing fluids useful for commercial manufacturing operations, provided the sedimentation is one of the most critical performance parameters for such an application.

As concerns the knowledge base for the development of an innovative device based on MRFs that can be used for manufacturing applications, with particular reference to its capability of damping external forces characterized by different frequencies for manufacturing applications was met by a deep classification of all the scientific literature available on the subject. The study was conducted starting from the analysis of the design approach of MRF based devices, then moved on to the investigation of existing corpus of knowledge on how to properly combine the MRF device design and MRF formulation to meet specific design requirements, up to finally focus on a widespread classification of all existing MRF based dampers with the aim of including all the possible applications in manufacturing operations.

The damping function is assured as a function of the contained dimensions and damping performance. The framework out of the corpus of knowledge studied recognized the following key drivers for a correct design process:

- structural design solution,
- models used to describe damping behavior,
- damping characteristics in valve mode,
- damping performance,
- factors influencing damping performance,
- magnetic circuit design requirements.

The classification of behavioral models for MRF dampers extrapolated from this accurate study of the state of the art allows to explain the conditions to realize an effective damping mechanism. This corpus of knowledge can be used to explain and forecast how the damping effect of these devices is exerted. Damping systems based on MRFs exert a damping force in reaction to the excitation frequency given by a specific forcing solicitation (frequency and intensity), that differs only for the range values depending on the application domain.
Once this knowledge on the MRF damping functioning is gained, it can be extended also to other applications, such as manufacturing ones. Dampers can be easily used in the equipment for spindle, spindle holder, tool holder, tool interchange arms, milling tools and so on just by changing the geometrical dimensions of the actuator, while maintaining the core dumping mechanism unaltered.
Design a novel MRF-based damper for manufacturing applications is thus a consequence of the corpus of knowledge here summarized.

This thesis has traced the path for different future works.

Firstly, using the corpus ok knowledge here collected, an experimental MRF based damping device might be designed and tested for specific manufacturing applications, like the afore mentioned equipment for spindle, spindle holder, tool holder, tool interchange arms, milling tools, with the aim of managing and damping different frequencies and nature of vibrations.

Secondly, starting from the three-dispersed experimental MRFs here presented, a novel MRF should be formulated and tested, with particular regards to improved response to sedimentation, by using different additives and/or different techniques for the preparation process.

Then this "second generation" novel three-dispersed MRF with improved resistance to sedimentation might be used in the experimental MRF based damping device, since -as it has been demonstrated with this thesis- the combination of device and MRF has to be considered a *unicum*, specifically designed to fulfil specific functional requirements.

References

[1] G. Yang, B. F. Spencer Jr., J. D. Carlson, e M. K. Sain, «Large-scale MR fluid dampers: modeling and dynamic performance considerations», *Eng. Struct.*, vol. 24, n. 3, pagg. 309–323, mar. 2002, doi: 10.1016/S0141-0296(01)00097-9.

[2] a G. Olabi e a. Grunwald, «Design and application of magneto-rheological fluid», *Mater. Des.*, vol. 28, n. 10, pagg. 2658–2664, gen. 2007, doi: 10.1016/j.matdes.2006.10.009.

[3] M. R. Jolly, J. D. Carlson, e B. C. Muñoz, «A model of the behaviour of magnetorheological materials», *Smart Mater. Struct.*, vol. 5, n. 5, pag. 607, 1996, doi: 10.1088/0964-1726/5/5/009.

[4] K. D. Weiss e T. G. Duclos, «Controllable fluids: the temperature dependence of post-yield properties», *Int. J. Mod. Phys. B*, vol. 08, n. 20n21, pagg. 3015–3032, set. 1994, doi: 10.1142/S0217979294001275.

[5] J. Rabinow, «The magnetic fluid clutch», *Trans. Am. Inst. Electr. Eng.*, vol. 2, n. 67, pagg. 1308–1315, 1948.

[6] Winslow WM, «Induced fibrillation of suspensions», *J Appl Phys*, pagg. 1137–1140, 1949.

[7] J. M. Ginder e L. C. Davis, «Shear stresses in magnetorheological fluids: Role of magnetic saturation», *Appl. Phys. Lett.*, vol. 65, n. 26, pagg. 3410–3412, dic. 1994, doi: 10.1063/1.112408.

[8] F. D. Goncalves, «A Review of the State of the Art in Magnetorheological Fluid Technologies - Part I: MR fluid and MR fluid models», *Shock Vib. Dig.*, vol. 38, n. 3, pagg. 203–219, 2006, doi: 10.1177/0583102406065099.

[9] M. Dassisti e G. Brunetti, «Introduction to Magnetorheological Fluids», in *Reference Module in Materials Science and Materials Engineering*, 2021.

[10] M. Hagenbüchle e J. Liu, «Chain formation and chain dynamics in a dilute magnetorheological fluid.», *Appl. Opt.*, vol. 36, n. 30, pagg. 7664–71, ott. 1997.

[11] J. M. Ginder, «Behavior of Magnetorheological Fluids», *MRS Bull.*, vol. 23, n. 08, pagg. 26–29, ago. 1998, doi: 10.1557/S0883769400030785.

[12] J. m. Ginder, L. c. Davis, e L. d. Elie, «Rheology of magnetorheological fluids: models and measurements», *Int. J. Mod. Phys. B*, vol. 10, n. 23n24, pagg. 3293–3303, ott. 1996, doi: 10.1142/S0217979296001744.

[13] G. B. Y. Grasselli, «Structure induced in suspensions by a magnetic field», *http://dx.doi.org/10.1051/jp2:1994127*, vol. 4, n. 2, 1994, doi: 10.1051/jp2:1994127.

[14] E. Lemaire, C. Paparoditis, e G. Bossis, «Yield stress in magnetic suspensions», in *Trends in Colloid and Interface Science V*, M. Corti e F. Mallamace, A c. di Steinkopff, 1991, pagg. 425–427.

[15] P. Forte, M. Patern□, e E. Rustighi, «A Magnetorheological Fluid Damper for Rotor Applications», *Int. J. Rotating Mach.*, vol. 10, n. 3, pagg. 175–182, mag. 2004, doi: 10.1080/10236210490426253.

[16] X. Z. Zhang, X. L. Gong, P. Q. Zhang, e Q. M. Wang, «Study on the mechanism of the squeeze-strengthen effect in magnetorheological fluids», *J. Appl. Phys.*, vol. 96, n. 4, pag. 2359, 2004, doi: 10.1063/1.1773379.

[17] Z. Strecker, J. Roupec, I. Mazurek, O. Machacek, M. Kubik, e M. Klapka, «Design of magnetorheological damper with short time response», *J. Intell. Mater. Syst. Struct.*, vol. 26, n. 14, pagg. 1951–1958, set. 2015, doi: 10.1177/1045389X15591381.

[18] S. Genc, «Rheological properties of magnetorheological fluids», vol. 11, pagg. 140–146, 2002.

[19] E. Lemaire e G. Bossis, «Yield stress and wall effects in magnetic colloidal suspensions», *J. Phys. Appl. Phys.*, vol. 24, n. 8, pag. 1473, 1991, doi: 10.1088/0022-3727/24/8/037.

[20] W. Li e X. Zhang, «The effect of friction on magnetorheological fluids», *Fac. Eng. - Pap. Arch.*, pagg. 45–50, gen. 2008.

[21] A. J. F. Bombard e J. de Vicente, «Thin-Film Rheology and Tribology of Magnetorheological Fluids in Isoviscous-EHL Contacts», *Tribol. Lett.*, vol. 47, n. 1, pagg. 149–162, mag. 2012, doi: 10.1007/s11249-012-9971-2.

[22] W. C. Leung, W. A. Bullough, P. L. Wong, e C. Feng, «The effect of particle concentration in a magneto rheological suspension on the performance of a boundary lubricated contact», *Proc. Inst. Mech. Eng. Part J J. Eng. Tribol.*, vol. 218, n. 4, pagg. 251–264, apr. 2004, doi: 10.1243/1350650041762622.
[23] W. L. Song, C. H. Lee, S. B. Choi, e M. W. Cho, «The Effect of Particle Concentration and Magnetic Field on Tribological Behavior of Magneto-Rheological Fluid», *Adv. Mater. Res.*, vol. 314–316, pagg. 58–61, ago. 2011, doi: 10.4028/www.scientific.net/AMR.314-316.58.
[24] F. Gordaninejad, B. M. Kavlicoglu, e X. Wang, «Friction factor of magneto-rheological fluid flow in grooved channels», *Int. J. Mod. Phys. B*, vol. 19, n. 07n09, pagg. 1297–1303, apr. 2005, doi: 10.1142/S0217979205030219.
[25] P. L. Wong, W. A. Bullough, C. Feng, e S. Lingard, «Tribological performance of a magneto-rheological suspension», vol. 247, pagg. 33–40, 2001.
[26] N. M. Wereley *et al.*, «Bidisperse Magnetorheological Fluids using Fe Particles at Nanometer and Micron Scale», *J. Intell. Mater. Syst. Struct.*, vol. 17, n. 5, pagg. 393–401, gen. 2006, doi: 10.1177/1045389X06056953.
[27] S. A. Khan, A. Suresh, e N. SeethaRamaiah, «Principles, Characteristics and Applications of Magneto Rheological Fluid Damper in Flow and Shear Mode», *Procedia Mater. Sci.*, vol. 6, pagg. 1547–1556, 2014, doi: 10.1016/j.mspro.2014.07.136.
[28] R. Stanway, J. L. Sproston, e A. K. El-Wahed, «Applications of electro-rheological fluids in vibration control: a survey», *Smart Mater. Struct.*, vol. 5, n. 4, pag. 464, 1996, doi: 10.1088/0964-1726/5/4/011.
[29] Y. T. Choi, J. U. Cho, S. B. Choi, e N. M. Wereley, «Constitutive models of electrorheological and magnetorheological fluids using viscometers», *Smart Mater. Struct.*, vol. 14, n. 5, pagg. 1025–1036, ott. 2005, doi: 10.1088/0964-1726/14/5/041.
[30] N. D. Sims, N. J. Holmes, e R. Stanway, «A unified modelling and model updating procedure for electrorheological and magnetorheological vibration dampers», *Smart Mater. Struct.*, vol. 13, n. 1, pag. 100, 2004, doi: 10.1088/0964-1726/13/1/012.
[31] S. Guo, S. Yang, e C. Pan, «Dynamic Modeling of Magnetorheological Damper Behaviors», *J. Intell. Mater. Syst. Struct.*, vol. 17, n. 1, pagg. 3–14, gen. 2006, doi: 10.1177/1045389X06055860.
[32] A. Farjoud, N. Yahdati, e Y. F. Fah, «Mathematical Model of Drum-type MR Brakes using Herschel-Bulkley Shear Model», *J. Intell. Mater. Syst. Struct.*, mag. 2007, doi: 10.1177/1045389X07077851.
[33] X. Wang e F. Gordaninejad, «Flow Analysis of Field-Controllable, Electro- and Magneto-Rheological Fluids Using Herschel-Bulkley Model», *J. Intell. Mater. Syst. Struct.*, vol. 10, n. 8, pagg. 601–608, gen. 1999, doi: 10.1106/P4FL-L1EL-YFLJ-BTRE.
[34] P. Yadmellat e M. R. Kermani, «Study of limit cycle in antagonistically coupled Magneto-Rheological actuators», in *2014 IEEE International Conference on Robotics and Automation (ICRA)*, mag. 2014, pagg. 1084–1089, doi: 10.1109/ICRA.2014.6906989.
[35] J. de Vicente, J. P. Segovia-Gutiérrez, E. Andablo-Reyes, F. Vereda, e R. Hidalgo-Alvarez, «Dynamic rheology of sphere- and rod-based magnetorheological fluids», *J. Chem. Phys.*, vol. 131, n. 19, pag. 194902, nov. 2009, doi: 10.1063/1.3259358.
[36] J. de Vicente, D. J. Klingenberg, e R. Hidalgo-Alvarez, «Magnetorheological fluids: a review», *Soft Matter*, vol. 7, n. 8, pagg. 3701–3710, apr. 2011, doi: 10.1039/C0SM01221A.
[37] M. Parthasarathy e D. J. Klingenberg, «Large amplitude oscillatory shear of ER suspensions», *J. Non-Newton. Fluid Mech.*, vol. 81, n. 1–2, pagg. 83–104, feb. 1999, doi: 10.1016/S0377-0257(98)00096-2.
[38] J. de Vicente, M. T. López-López, J. D. G. Durán, e G. Bossis, «A slender-body micromechanical model for viscoelasticity of magnetic colloids: Comparison with preliminary experimental data», *J. Colloid Interface Sci.*, vol. 282, n. 1, pagg. 193–201, feb. 2005, doi: 10.1016/j.jcis.2004.08.128.
[39] J F Brady e and G. Bossis, «Stokesian Dynamics», *Annu. Rev. Fluid Mech.*, vol. 20, n. 1,

pagg. 111–157, 1988, doi: 10.1146/annurev.fl.20.010188.000551.
[40] G. Bossis, O. Volkova, S. Lacis, e A. Meunier, «Magnetorheology : Fluids , Structures and Rheology», pagg. 202–230, 2002.
[41] N. Nguyen, «This document is downloaded from DR-NTU , Nanyang Technological University Library , Singapore . Micro magnetofluidics – interactions between magnetism and fluid flow on the microscale», 2012.
[42] S. P. Jang e S. U. S. Choi, «Role of Brownian motion in the enhanced thermal conductivity of nanofluids», *Appl. Phys. Lett.*, vol. 84, n. 21, pagg. 4316–4318, mag. 2004, doi: 10.1063/1.1756684.
[43] R. Patel, «Mechanism of chain formation in nanofluid based MR fluids», *J. Magn. Magn. Mater.*, vol. 323, n. 10, pagg. 1360–1363, mag. 2011, doi: 10.1016/j.jmmm.2010.11.046.
[44] D. J. Klingenberg, C. H. Olk, M. A. Golden, e J. C. Ulicny, «Effects of nonmagnetic interparticle forces on magnetorheological fluids», *J. Phys. Condens. Matter*, vol. 22, n. 32, pag. 324101, ago. 2010, doi: 10.1088/0953-8984/22/32/324101.
[45] M. C. Heine, J. de Vicente, e D. J. Klingenberg, «Thermal transport in sheared electro- and magnetorheological fluids», *Phys. Fluids 1994-Present*, vol. 18, n. 2, pag. 023301, feb. 2006, doi: 10.1063/1.2171442.
[46] H. C. Hamaker, «The London—van der Waals attraction between spherical particles», *Physica*, vol. 4, n. 10, pagg. 1058–1072, ott. 1937, doi: 10.1016/S0031-8914(37)80203-7.
[47] J. N. Israelachvili, *Intermolecular and Surface Forces, Third Edition*, 3 edition. San Diego, Calif.: Academic Press, 2011.
[48] M. R. Jolly, J. W. Bender, e J. D. Carlson, «Properties and applications of commercial magnetorheological fluids», 1998, vol. 3327, pagg. 262–275, doi: 10.1117/12.310690.
[49] J. D. Carlson e M. R. Jolly, «MR fluid, foam and elastomer devices», *Mechatronics*, vol. 10, n. 4–5, pagg. 555–569, giu. 2000, doi: 10.1016/S0957-4158(99)00064-1.
[50] B. Deffenbaugh, H. Herr, G. Pratt, e M. Wittig, «Electronically controlled prosthetic knee», US20010029400 A1, ott. 11, 2001.
[51] N. Rosenfeld e N. Wereley, «Volume-Constrained Optimization of Magnetorheological Valves», in *44th AIAA/ASME/ASCE/AHS/ASC Structures, Structural Dynamics, and Materials Conference*, American Institute of Aeronautics and Astronautics.
[52] M. R. Jolly, J. W. Bender, e J. D. Carlson, «Properties and applications of commercial magnetorheological fluids», 1998, vol. 3327, pagg. 262–275, doi: 10.1117/12.310690.
[53] J. An e D.-S. Kwon, «Modeling of a Magnetorheological Actuator Including Magnetic Hysteresis», *J. Intell. Mater. Syst. Struct.*, vol. 14, n. 9, pagg. 541–550, gen. 2003, doi: 10.1177/104538903036506.
[54] F. Ikhouane e S. J. Dyke, «Modeling and identification of a shear mode magnetorheological damper», *Smart Mater. Struct.*, vol. 16, n. 3, pag. 605, 2007, doi: 10.1088/0964-1726/16/3/007.
[55] C. C. C. T. T. Tse e C. C. Chang, «Shear-Mode Rotary Magnetorheological Damper for Small-Scale Structural Control Experiments», *J. Struct. Eng.-Asce - J STRUCT ENG-ASCE*, vol. 130, n. 6, 2004, doi: 10.1061/(ASCE)0733-9445(2004)130:6(904).
[56] P. Chen, X.-X. Bai, L.-J. Qian, e S.-B. Choi, «A magneto-rheological fluid mount featuring squeeze mode: analysis and testing», *Smart Mater. Struct.*, vol. 25, n. 5, pag. 055002, 2016, doi: 10.1088/0964-1726/25/5/055002.
[57] J. Wang, «Vibration Control of Rotor by Squeeze Film Damper with Magnetorheological Fluid», *J. Intell. Mater. Syst. Struct.*, vol. 17, n. 4, pagg. 353–357, apr. 2006, doi: 10.1177/1045389X06055623.
[58] Z. Parlak e T. Engin, «Mechatronics Optimal design of MR damper via finite element analyses of fluid dynamic and magnetic field», *Mechatronics*, 2012, doi: 10.1016/j.mechatronics.2012.05.007.
[59] Y. P. Seo, S. Han, J. Choi, A. Takahara, H. J. Choi, e Y. Seo, «Searching for a Stable High-Performance Magnetorheological Suspension», *Adv. Mater.*, vol. 30, n. 42, pag. 1704769, 2018, doi: https://doi.org/10.1002/adma.201704769.

[60] I. Bica, Y. D. Liu, e H. J. Choi, «Physical characteristics of magnetorheological suspensions and their applications», *J. Ind. Eng. Chem.*, vol. 19, n. 2, pagg. 394–406, mar. 2013, doi: 10.1016/j.jiec.2012.10.008.
[61] P. Mastrorilli, A. Rizzuti, M. Dassisti, e G. Brunetti, «Key-Elements of Magnetorheological Fluids», 2020.
[62] M. Ashtiani, S. H. Hashemabadi, e A. Ghaffari, «A review on the magnetorheological fluid preparation and stabilization», *J. Magn. Magn. Mater.*, vol. 374, pagg. 716–730, gen. 2015, doi: 10.1016/j.jmmm.2014.09.020.
[63] J. Liu, «Magnetorheological Fluids: From Basic Physics to Application», *JSME Int. J. Ser. B*, vol. 45, pagg. 55–60, 2002, doi: 10.1299/jsmeb.45.55.
[64] A. J. Margida, K. D. Weiss, e J. D. Carlson, «Magnetorheological materials based on iron alloy particles», *Int. J. Mod. Phys. B*, vol. 10, n. 23n24, pagg. 3335–3341, ott. 1996, doi: 10.1142/S0217979296001781.
[65] M. E. Mendoza, F. Donado, R. Silva, M. A. Pérez, e J. L. Carrillo, «Magnetite microcrystals for magneto-rheological fluids», *J. Phys. Chem. Solids*, vol. 66, n. 6, pagg. 927–931, giu. 2005, doi: 10.1016/j.jpcs.2004.06.019.
[66] J. de Vicente, G. Bossis, S. Lacis, e M. Guyot, «Permeability measurements in cobalt ferrite and carbonyl iron powders and suspensions», *J. Magn. Magn. Mater.*, vol. 251, n. 1, pagg. 100–108, ott. 2002, doi: 10.1016/S0304-8853(02)00484-5.
[67] M. Molazemi, H. Shokrollahi, e B. Hashemi, «The investigation of the compression and tension behavior of the cobalt ferrite magnetorheological fluids synthesized by co-precipitation», *J. Magn. Magn. Mater.*, vol. 346, pagg. 107–112, nov. 2013, doi: 10.1016/j.jmmm.2013.06.053.
[68] A. V. Anupama, V. Kumaran, e B. Sahoo, «Magnetorheological fluids containing rod-shaped lithium–zinc ferrite particles: the steady-state shear response», *Soft Matter*, vol. 14, n. 26, pagg. 5407–5419, lug. 2018, doi: 10.1039/C8SM00807H.
[69] J. C. Ulicny, M. P. Balogh, N. M. Potter, e R. A. Waldo, «Magnetorheological fluid durability test—Iron analysis», *Mater. Sci. Eng. A*, vol. 443, n. 1–2, pagg. 16–24, gen. 2007, doi: 10.1016/j.msea.2006.06.050.
[70] R. T. Foister, «Magnetorheological fluids», US5667715 A, set. 16, 1997.
[71] M. T. López-López, P. Kuzhir, e G. Bossis, «Magnetorheology of fiber suspensions. I. Experimental», *J. Rheol. 1978-Present*, vol. 53, n. 1, pagg. 115–126, gen. 2009, doi: 10.1122/1.3005402.
[72] J. A. Starkovich e E. M. Shtarkman, «High yield stress magnetorheological material for spacecraft applications - Dimensions», US6610404B2, 2003.
[73] Z. Gu, X. Xiang, G. Fan, e F. Li, «Facile Synthesis and Characterization of Cobalt Ferrite Nanocrystals via a Simple Reduction−Oxidation Route», *J. Phys. Chem. C*, pagg. 18459–18466, nov. 2008, doi: 10.1021/jp806682q.
[74] M. S. Cho, S. T. Lim, I. B. Jang, H. J. Choi, e M. S. Jhon, «Encapsulation of spherical iron-particle with PMMA and its magnetorheological particles», *IEEE Trans. Magn.*, vol. 40, n. 4, pagg. 3036–3038, lug. 2004, doi: 10.1109/TMAG.2004.830413.
[75] F. F. Fang, M. S. Yang, e H. J. Choi, «Novel Magnetic Composite Particles of Carbonyl Iron Embedded in Polystyrene and Their Magnetorheological Characteristics», *IEEE Trans. Magn.*, vol. 44, n. 11, pagg. 4533–4536, nov. 2008, doi: 10.1109/TMAG.2008.2001665.
[76] W. P. Wu, B. Y. Zhao, Q. Wu, L. S. Chen, e K. A. Hu, «The strengthening effect of guar gum on the yield stress of magnetorheological fluid», *Smart Mater. Struct.*, vol. 15, n. 4, pagg. N94–N98, giu. 2006, doi: 10.1088/0964-1726/15/4/N04.
[77] Y. D. Liu, H. J. Choi, e S.-B. Choi, «Controllable fabrication of silica encapsulated soft magnetic microspheres with enhanced oxidation-resistance and their rheology under magnetic field», *Colloids Surf. Physicochem. Eng. Asp.*, vol. 403, pagg. 133–138, giu. 2012, doi: 10.1016/j.colsurfa.2012.04.002.
[78] M. Mrlík, M. Ilčíková, V. Pavlínek, J. Mosnáček, P. Peer, e P. Filip, «Improved

thermooxidation and sedimentation stability of covalently-coated carbonyl iron particles with cholesteryl groups and their influence on magnetorheology», *J. Colloid Interface Sci.*, vol. 396, pagg. 146–151, apr. 2013, doi: 10.1016/j.jcis.2013.01.027.
[79] F. F. Fang, Y. D. Liu, e H. J. Choi, «Carbon nanotube coated magnetic carbonyl iron microspheres prepared by solvent casting method and their magneto-responsive characteristics», *Colloids Surf. Physicochem. Eng. Asp.*, vol. 412, pagg. 47–56, ott. 2012, doi: 10.1016/j.colsurfa.2012.07.013.
[80] H. Chiriac, G. Stoian, e M. Lostun, «Magnetorheological fluids based on amorphous magnetic microparticles», *J. Phys. Conf. Ser.*, vol. 149, pag. 012045, feb. 2009, doi: 10.1088/1742-6596/149/1/012045.
[81] W. Jiang, Y. Zhang, S. Xuan, C. Guo, e X. Gong, «Dimorphic magnetorheological fluid with improved rheological properties», *J. Magn. Magn. Mater.*, vol. 323, n. 24, pagg. 3246–3250, dic. 2011, doi: 10.1016/j.jmmm.2011.07.024.
[82] M. Kciuk, S. Kciuk, e R. Turczyn, «Magnetorheological characterisation of carbonyl iron based suspension», *J. Achiev. Mater. Manuf. Eng.*, vol. Vol. 33, n. nr 2, pagg. 135–141, 2009.
[83] J. D. Carlson e K. D. Weiss, «Magnetorheological materials based on alloy particles», US5382373A, gen. 17, 1995.
[84] C. Guerrero-Sanchez, T. Lara-Ceniceros, E. Jimenez-Regalado, M. Raşa, e U. S. Schubert, «Magnetorheological Fluids Based on Ionic Liquids», *Adv. Mater.*, vol. 19, n. 13, pagg. 1740–1747, 2007, doi: https://doi.org/10.1002/adma.200700302.
[85] L. Rodríguez-Arco, A. Gómez-Ramírez, J. D. G. Durán, e M. T. López-López, «New Perspectives for Magnetic Fluid-Based Devices Using Novel Ionic Liquids as Carriers», *Smart Actuation Sens. Syst. - Recent Adv. Future Chall.*, ott. 2012, doi: 10.5772/51398.
[86] J. E. Kim e H. J. Choi, «Magnetic Carbonyl Iron Particle Dispersed in Viscoelastic Fluid and Its Magnetorheological Property», *IEEE Trans. Magn.*, vol. 47, n. 10, pagg. 3173–3176, ott. 2011, doi: 10.1109/TMAG.2011.2156396.
[87] R. Gu, X. Gong, W. Jiang, L. Hao, S. Xuan, e Z. Zhang, «Synthesis and rheological investigation of a magnetic fluid using olivary silica-coated iron particles as a precursor», *J. Magn. Magn. Mater.*, vol. 320, n. 21, pagg. 2788–2791, nov. 2008, doi: 10.1016/j.jmmm.2008.06.016.
[88] J. L. Viota, J. de Vicente, J. D. G. Durán, e A. V. Delgado, «Stabilization of magnetorheological suspensions by polyacrylic acid polymers», *J. Colloid Interface Sci.*, vol. 284, n. 2, pagg. 527–541, apr. 2005, doi: 10.1016/j.jcis.2004.10.024.
[89] M. Kciuk, R. Turczyn, F. Materials, e P. Technologies, «Properties and application of magnetorheological fluids», *Manuf. Eng.*, vol. 18, n. 1, pagg. 127–130, 2006.
[90] E. M. Shtarkman, «Fluid responsive to a magnetic field», US4992190A, feb. 12, 1991.
[91] S. T. Lim, M. S. Cho, I. B. Jang, e H. J. Choi, «Magnetorheological characterization of carbonyl iron based suspension stabilized by fumed silica», *J. Magn. Magn. Mater.*, vol. 282, pagg. 170–173, nov. 2004, doi: 10.1016/j.jmmm.2004.04.040.
[92] S. E. Premalatha, R. Chokkalingam, e M. Mahendran, «Magneto Mechanical Properties of Iron Based MR Fluids», *Am. J. Polym. Sci.*, vol. 2, n. 4, pagg. 50–55, 2012.
[93] B. G. Shetty e P. s. s Prasad, «Rheological Properties of a Honge Oil-based Magnetorheological Fluid used as Carrier Liquid», *Def. Sci. J.*, pagg. 583–589, 2011.
[94] P. J. Rankin, A. T. Horvath, e D. J. Klingenberg, «Magnetorheology in viscoplastic media», *Rheol. Acta*, vol. 38, n. 5, pagg. 471–477, doi: 10.1007/s003970050198.
[95] P. Kuzhir, G. Bossis, V. Bashtovoi, e O. Volkova, «Flow of magnetorheological fluid through porous media», *Eur. J. Mech. - BFluids*, vol. 22, n. 4, pagg. 331–343, lug. 2003, doi: 10.1016/S0997-7546(03)00040-2.
[96] X. h. Liu, Z. m. Fu, X. y. Yao, e F. Li, «Performance of Magnetorheological Fluids Flowing Through Metal Foams», *Meas. Sci. Rev.*, vol. 11, pagg. 144–148, gen. 2011, doi: 10.2478/v10048-011-0028-8.
[97] A. Hajalilou, S. a. Mazlan, H. Lavvafi, e K. Shameli, *Field Responsive Fluids as Smart*

Materials | Abdollah Hajalilou | Springer. 2016.
[98] A. Dang, L. Ooi, J. Fales, e P. Stroeve, «Yield Stress Measurements of Magnetorheological Fluids in Tubes», pagg. 2269–2274, 2000.
[99] C. Burda, X. Chen, R. Narayanan, e M. A. El-Sayed, «Chemistry and properties of nanocrystals of different shapes», *Chem. Rev.*, vol. 105, n. 4, pagg. 1025–1102, apr. 2005, doi: 10.1021/cr030063a.
[100] M. Chand, A. Shankar, Noorjahan, K. Jain, e R. P. Pant, «Improved properties of bidispersed magnetorheological fluids», *RSC Adv.*, vol. 4, n. 96, pagg. 53960–53966, ott. 2014, doi: 10.1039/C4RA07431A.
[101] B. J. Park, K. H. Song, e H. J. Choi, «Magnetic carbonyl iron nanoparticle based magnetorheological suspension and its characteristics», *Mater. Lett.*, vol. 63, n. 15, pagg. 1350–1352, 2009, doi: 10.1016/j.matlet.2009.03.013.
[102] K. H. Song, B. J. Park, e H. J. Choi, «Effect of Magnetic Nanoparticle Additive on Characteristics of Magnetorheological Fluid», *IEEE Trans. Magn.*, vol. 45, n. 10, pagg. 4045–4048, ott. 2009, doi: 10.1109/TMAG.2009.2025390.
[103] G. R. Iglesias, J. D. G. Durán, e A. V. Delgado, «Journal of Colloid and Interface Science Dynamic characterization of extremely bidisperse magnetorheological fluids», *J. Colloid Interface Sci.*, vol. 377, n. 1, pagg. 153–159, 2012, doi: 10.1016/j.jcis.2012.03.077.
[104] S. a. N. Leong, P. Mohd Samin, A. Idris, S. Amri Mazlan, e A. H. A. Rahman, «Synthesis, characterization and magnetorheological properties of carbonyl iron suspension with superparamagnetic nanoparticles as an additive», *Smart Mater. Struct.*, vol. 25, pag. 025025, feb. 2016, doi: 10.1088/0964-1726/25/2/025025.
[105] M. T. López-López, P. Kuzhir, J. Caballero-Hernández, L. Rodríguez-Arco, J. D. G. Duran, e G. Bossis, «Yield stress in magnetorheological suspensions near the limit of maximum-packing fraction», *J. Rheol. 1978-Present*, vol. 56, n. 5, pag. 1209, set. 2012, doi: 10.1122/1.4731659.
[106] R. T. Foister, R. Hills, e M. I. Us, «(12) United States Patent Experimental Adsorption lsotherm for Surfacant», vol. 2, n. 12, 2004.
[107] J. D. Carlson, «What Makes a Good MR Fluid?», *J. Intell. Mater. Syst. Struct.*, vol. 13, n. 7–8, pagg. 431–435, gen. 2002, doi: 10.1106/104538902028221.
[108] Z. Feng, «Study of Sedimentation Stability of Magnetorheological Fluid», *Adv. Mater.*, vol. 4, n. 1, pag. 1, 2015, doi: 10.11648/j.am.20150401.11.
[109] H. Pu e F. Jiang, «Towards high sedimentation stability : magnetorheological fluids based on CNT / Fe 3 O 4 nanocomposites», vol. 16, pagg. 1486–1489, 2005, doi: 10.1088/0957-4484/16/9/012.
[110] X.-M. Dong, Y. U. Miao, C.-R. Liao, e W.-M. Chen, «A new variable stiffness absorber based on magneto-rheological elastomer», *Trans. Nonferrous Met. Soc. China*, vol. 19, pagg. s611–s615, 2009.
[111] P. P. Phulé, «Synthesis of Novel Magnetorheological Fluids», *MRS Bull.*, vol. 23, n. 08, pagg. 23–25, ago. 1998, doi: 10.1557/S0883769400030773.
[112] V. R. Iyengar e R. T. Foister, «Durable magnetorheological fluid compositions», US6599439 B2, lug. 29, 2003.
[113] R. T. Foister, V. R. Iyengar, e S. M. Yurgelevic, «Low-cost MR fluids with powdered iron», US6787058 B2, set. 07, 2004.
[114] C. Miao, R. Shen, M. Wang, S. N. Shafrir, H. Yang, e S. D. Jacobs, «Rheology of Aqueous Magnetorheological Fluid Using Dual Oxide-Coated Carbonyl Iron Particles», *J. Am. Ceram. Soc.*, vol. 94, n. 8, pagg. 2386–2392, ago. 2011, doi: 10.1111/j.1551-2916.2011.04423.x.
[115] S. R. Sunkara, T. W. Root, J. C. Ulicny, e D. J. Klingenberg, «Iron oxidation and its impact on MR behavior», *J. Phys. Conf. Ser.*, vol. 149, n. 1, pag. 012081, 2009, doi: 10.1088/1742-6596/149/1/012081.
[116] J. L. Pons, *Emerging Actuator Technologies: A Micromechatronic Approach*. John Wiley & Sons, 2005.
[117] J. Gołdasz e B. Sapiński, *Insight into Magnetorheological Shock Absorbers*. Springer, 2014.

[118] A. Z. Nelson e R. H. Ewoldt, «Design of yield-stress fluids: a rheology-to-structure inverse problem», *Soft Matter*, vol. 13, n. 41, pagg. 7578–7594, ott. 2017, doi: 10.1039/C7SM00758B.
[119] W. I. Kordonski, «CHAPTER 11. Magnetorheological Fluid-Based High Precision Finishing Technology», in *RSC Smart Materials*, N. M. Wereley, A c. di Cambridge: Royal Society of Chemistry, 2013, pagg. 261–277.
[120] W. I. Kordonski e D. Golini, «Fundamentals of Magnetorheological Fluid Utilization in High Precision Finishing», *J. Intell. Mater. Syst. Struct.*, vol. 10, n. 9, pagg. 683–689, gen. 1999, doi: 10.1106/011M-CJ25-64QC-F3A6.
[121] W. Kordonski e D. Golini, «Progress Update in Magnetorheological Finishing», *Int. J. Mod. Phys. B*, vol. 13, n. 14n16, pagg. 2205–2212, giu. 1999, doi: 10.1142/S0217979299002320.
[122] D. Golini, W. I. Kordonski, P. Dumas, e S. J. Hogan, «Magnetorheological finishing (MRF) in commercial precision optics manufacturing», in *Optical Manufacturing and Testing III*, nov. 1999, vol. 3782, pagg. 80–91, doi: 10.1117/12.369174.
[123] ghosh, «Fabrication of Optical Components by Ultraprecision Finishing Processes», *springerprofessional.de*, 2018. https://www.springerprofessional.de/en/fabrication-of-optical-components-by-ultraprecision-finishing-pr/15136632 (consultato dic. 31, 2020).
[124] C. Maloney e W. Messner, «Extending magnetorheological finishing to address short radius concave surfaces and mid-spatial frequency errors», 2019, doi: 10.1117/12.2536920.
[125] X. Tang, X. Zhang, e R. Tao, «Flexible fixture device with magneto-rheological fluids», in *Electro-Rheological Fluids and Magneto-Rheological Suspensions*, 0 voll., WORLD SCIENTIFIC, 2000, pagg. 700–708.
[126] X. Tang, X. Zhang, R. Tao, e Y. Rong, «Structure-enhanced yield stress of magnetorheological fluids», *J. Appl. Phys.*, vol. 87, n. 5, pagg. 2634–2638, mar. 2000, doi: 10.1063/1.372229.
[127] D. Sathianarayanan, L. Karunamoorthy, J. Srinivasan, G. S. Kandasami, e K. Palanikumar, «Chatter Suppression in Boring Operation Using Magnetorheological Fluid Damper», *Mater. Manuf. Process.*, vol. 23, n. 4, pagg. 329–335, apr. 2008, doi: 10.1080/10426910701860897.
[128] Y. Zhang, N. M. Wereley, W. Hu, M. Hong, e W. Zhang, «Magnetic Circuit Analyses and Turning Chatter Suppression Based on a Squeeze-Mode Magnetorheological Damping Turning Tool», *Shock and Vibration*, lug. 26, 2015. https://www.hindawi.com/journals/sv/2015/304698/ (consultato gen. 04, 2021).
[129] S. D. Puma-Araujo, D. Olvera-Trejo, O. Martínez-Romero, G. Urbikain, A. Elías-Zúñiga, e L. N. López de Lacalle, «Semi-Active Magnetorheological Damper Device for Chatter Mitigation during Milling of Thin-Floor Components», *Appl. Sci.*, vol. 10, n. 15, Art. n. 15, gen. 2020, doi: 10.3390/app10155313.
[130] D. Mei, T. Kong, A. J. Shih, e Z. Chen, «Magnetorheological fluid-controlled boring bar for chatter suppression», *J. Mater. Process. Technol.*, vol. 209, n. 4, pagg. 1861–1870, feb. 2009, doi: 10.1016/j.jmatprotec.2008.04.037.
[131] A. Grunwald e A. G. Olabi, «Design of magneto-rheological (MR) valve», *Sens. Actuators Phys.*, vol. 148, n. 1, pagg. 211–223, nov. 2008, doi: 10.1016/j.sna.2008.07.028.
[132] B. F. Spencer e M. K. Sain, «Controlling buildings: a new frontier in feedback», *IEEE Control Syst. Mag.*, vol. 17, n. 6, pagg. 19–35, 1997, doi: 10.1109/37.642972.
[133] S. Sassi, A. Sassi, K. Cherif, e F. Tarlochan, «Magnetorheological damper with external excitation for more efficient control of vehicles' dynamics», *J INTEL MAT SYST STR.*, 2018.
[134] Harun*, Azhari, R. Yunos, A. K. Mat Yamin, e M. Z. Sariman, «Characterization of a Magnetorheological Fluid Damper Applied to Semi-Active Engine Mounting System / M. Hafiz Harun...[et al.]», *J. Mech. Eng. JMechE*, vol. SI 5, n. 3, Art. n. 3, 2018.
[135] K. H. Gudmundsson, F. Jonsdottir, e F. Thorsteinsson, «A geometrical optimization of a magneto-rheological rotary brake in a prosthetic knee», *Smart Mater. Struct.*, vol. 19, n. 3, pag. 035023, feb. 2010, doi: 10.1088/0964-1726/19/3/035023.
[136] H. Herr e A. Wilkenfeld, «User-adaptive control of a magnetorheological prosthetic knee»,

Ind. Robot Int. J., vol. 30, n. 1, pagg. 42–55, gen. 2003, doi: 10.1108/01439910310457706.
[137] F. Jonsdottir, E. T. Thorarinsson, H. Palsson, e K. H. Gudmundsson, «Influence of Parameter Variations on the Braking Torque of a Magnetorheological Prosthetic Knee», *J. Intell. Mater. Syst. Struct.*, vol. 20, n. 6, pagg. 659–667, apr. 2009, doi: 10.1177/1045389X08094303.
[138] R. S. T. Saini, S. Chandramohan, S. Sujatha, e H. Kumar, «Design of bypass rotary vane magnetorheological damper for prosthetic knee application», *J. Intell. Mater. Syst. Struct.*, pag. 1045389X20942577, lug. 2020, doi: 10.1177/1045389X20942577.
[139] M. Dassisti e G. Brunetti, «Magnetorheological fluids applications», in *Reference Module in Materials Science and Materials Engineering*, 2021.
[140] W. Song, S. Choi, D. Lee, e C. Lee, «Micro-precision surface finishing using magneto-rheological fluid», *Sci. China Technol. Sci.*, vol. 55, n. 1, pagg. 56–61, nov. 2011, doi: 10.1007/s11431-011-4653-0.
[141] X. Jiang, G. Zhao, e W. Lu, «Vibration suppression of complex thin-walled workpiece based on magnetorheological fixture», *Int. J. Adv. Manuf. Technol.*, vol. 106, n. 3, pagg. 1043–1055, gen. 2020, doi: 10.1007/s00170-019-04612-2.
[142] D. Wang, B. Zi, Y. Zeng, F. Xie, e Y. Hou, «An investigation of thermal characteristics of a liquid-cooled magnetorheological fluid-based clutch», *Smart Mater. Struct.*, vol. 24, mag. 2015, doi: 10.1088/0964-1726/24/5/055020.
[143] W. W. Chooi e S. O. Oyadiji, «Design, modelling and testing of magnetorheological (MR) dampers using analytical flow solutions», *Comput. Struct.*, vol. 86, n. 3–5, pagg. 473–482, feb. 2008, doi: 10.1016/j.compstruc.2007.02.002.
[144] C. Daniel, G. Hemalatha, L. Sarala, D. Tensing, e S. Sundar Manoharan, «Seismic Mitigation of Building Frames using Magnetorheological Damper (TECHNICAL NOTE)», *Int. J. Eng.*, vol. 32, n. 11, pagg. 1543–1547, nov. 2019, doi: 10.5829/ije.2019.32.11b.05.
[145] Z. Q. Chen, X. Y. Wang, J. M. Ko, Y. Q. Ni, B. F. Spencer Jr., e G. Yang, «MR damping system on Dongting Lake cable-stayed bridge», ago. 2003, vol. 5057, pagg. 229–235, doi: 10.1117/12.498072.
[146] Y. F. Duan, Y. Q. Ni, e J. M. Ko, «Cable Vibration Control using Magnetorheological Dampers», *J. Intell. Mater. Syst. Struct.*, vol. 17, n. 4, pagg. 321–325, gen. 2006, doi: 10.1177/1045389X06054997.
[147] R. M. Desai, M. E. H. Jamadar, H. Kumar, S. Joladarashi, S. C. Rajasekaran, e G. Amarnath, «Evaluation of a commercial MR damper for application in semi-active suspension», *SN Appl. Sci.*, vol. 1, n. 9, pag. 993, ago. 2019, doi: 10.1007/s42452-019-1026-y.
[148] S. Acharya, T. R. S. Saini, e H. Kumar, «Determination of optimal magnetorheological fluid particle loading and size for shear mode monotube damper», 2019, Consultato: gen. 07, 2021. [Online]. Disponibile su: https://idr.nitk.ac.in/jspui/handle/123456789/10523.
[149] X. Zhu, X. Jing, e L. Cheng, «Magnetorheological fluid dampers: A review on structure design and analysis», *J. Intell. Mater. Syst. Struct.*, pag. 1045389X12436735, mar. 2012, doi: 10.1177/1045389X12436735.
[150] S. Seid, S. Chandramohan, e S. Sujatha, «Design and Evaluation of a Magnetorheological Damper Based Prosthetic Knee», *Int. J. Eng.*, vol. 32, n. 1, pagg. 146–152, gen. 2019.
[151] W. H. Li, B. Liu, P. B. Kosasih, e X. Z. Zhang, «A 2-DOF MR actuator joystick for virtual reality applications», *Sens. Actuators Phys.*, vol. 137, n. 2, pagg. 308–320, 2007.
[152] N. Sgambelluri, R. Rizzo, E. P. Scilingo, M. Raugi, e A. Bicchi, «Free Hand Haptic Interfaces Based on Magnetorheological Fluids», in *2006 14th Symposium on Haptic Interfaces for Virtual Environment and Teleoperator Systems*, mar. 2006, pagg. 367–371, doi: 10.1109/HAPTIC.2006.1627124.
[153] A. Wiśniewski, «The possibility of use of the magneto-rheological fluids in armours», *Probl. Tech. Uzbroj.*, vol. R. 40, z. 117, 2011, Consultato: set. 20, 2016. [Online]. Disponibile su: http://yadda.icm.edu.pl/baztech/element/bwmeta1.element.baztech-article-PWAA-0028-0018.
[154] B. B. Muhammad, M. Wan, J. Feng, e W.-H. Zhang, «Dynamic damping of machining

vibration: a review», *Int. J. Adv. Manuf. Technol.*, vol. 89, n. 9, pagg. 2935–2952, apr. 2017, doi: 10.1007/s00170-016-9862-z.
[155] R. S. Sharp e S. A. Hassan, «The Relative Performance Capabilities of Passive, Active and Semi-Active Car Suspension Systems», *Proc. Inst. Mech. Eng. Part Transp. Eng.*, vol. 200, n. 3, pagg. 219–228, lug. 1986, doi: 10.1243/PIME_PROC_1986_200_183_02.
[156] E. Guglielmino, T. Sireteanu, C. W. Stammers, G. Ghita, e M. Giuclea, *Semi-active Suspension Control: Improved Vehicle Ride and Road Friendliness*. London: Springer-Verlag, 2008.
[157] M. Dassisti, G. Brunetti, e A. G. Olabi, «Magnetorheological dampers for vehicle suspension systems», in *Reference Module in Materials Science and Materials Engineering*, 2021.
[158] D. H. Wang e T. Wang, «Principle, design and modeling of an integrated relative displacement self-sensing magnetorheological damper based on electromagnetic induction», *Smart Mater. Struct.*, vol. 18, n. 9, pag. 095025, lug. 2009, doi: 10.1088/0964-1726/18/9/095025.
[159] R. M. Desai, M. E. H. Jamadar, H. Kumar, S. Joladarashi, e S. C. Raja Sekaran, «Design and experimental characterization of a twin-tube MR damper for a passenger van», *J. Braz. Soc. Mech. Sci. Eng.*, vol. 41, n. 8, pag. 332, lug. 2019, doi: 10.1007/s40430-019-1833-5.
[160] Y. Eslami, M. Dassisti, M. Lezoche, e H. Panetto, «A survey on sustainability in manufacturing organisations: dimensions and future insights», *Int. J. Prod. Res.*, vol. 57, n. 15–16, pagg. 5194–5214, ago. 2019, doi: 10.1080/00207543.2018.1544723.
[161] F. Casciati, J. Rodellar, e U. Yildirim, «Active and semi-active control of structures – theory and applications: A review of recent advances», *J. Intell. Mater. Syst. Struct.*, vol. 23, n. 11, pagg. 1181–1195, lug. 2012, doi: 10.1177/1045389X12445029.
[162] D.-H. Wang e W.-H. Liao, «Semiactive Controllers for Magnetorheological Fluid Dampers», *J. Intell. Mater. Syst. Struct.*, vol. 16, pagg. 983–993, dic. 2005, doi: 10.1177/1045389X05055281.
[163] A. Spaggiari, D. Castagnetti, N. Golinelli, E. Dragoni, e G. Scirè Mammano, «Smart materials: Properties, design and mechatronic applications», *Proc. Inst. Mech. Eng. Part J. Mater. Des. Appl.*, vol. 233, n. 4, pagg. 734–762, apr. 2016, doi: 10.1177/1464420716673671.
[164] M. Dogruoz, E. Wang, F. Gordaninejad, e A. Stipanovic, «Augmenting Heat Transfer from Fail-Safe Magneto-Rheological Fluid Dampers Using Fins», *J. Intell. Mater. Syst. Struct. - J INTEL MAT SYST STRUCT*, vol. 14, pagg. 79–86, feb. 2003, doi: 10.1177/1045389X03014002002.
[165] H.-S. Lee e S.-B. Choi, «Control and Response Characteristics of a Magneto-Rheological Fluid Damper for Passenger Vehicles», *J. Intell. Mater. Syst. Struct.*, vol. 11, n. 1, pagg. 80–87, gen. 2000, doi: 10.1106/412A-2GMA-BTUL-MALT.
[166] J. Poynor, «Innovative Designs for Magneto-Rheological Dampers», Virginia Polytechnic Institute and State University, 2001.
[167] N. M. Kwok, Q. P. Ha, T. H. Nguyen, J. Li, e B. Samali, «A novel hysteretic model for magnetorheological fluid dampers and parameter identification using particle swarm optimization», *Sens. Actuators Phys.*, vol. 132, n. 2, pagg. 441–451, nov. 2006, doi: 10.1016/j.sna.2006.03.015.
[168] S.-B. Choi, M.-H. Nam, e B.-K. Lee, «Vibration Control of a MR Seat Damper for Commercial Vehicles», *J. Intell. Mater. Syst. Struct.*, vol. 11, n. 12, pagg. 936–944, dic. 2000, doi: 10.1106/AERG-3QKV-31V8-F250.
[169] Q.-H. Nguyen e S.-B. Choi, «Optimal design of MR shock absorber and application to vehicle suspension», *Smart Mater. Struct.*, vol. 18, n. 3, pag. 035012, feb. 2009, doi: 10.1088/0964-1726/18/3/035012.
[170] J. Go\ldasz e S. Dzier\.zek, «Parametric study on the performance of automotive MR shock absorbers», *IOP Conf. Ser. Mater. Sci. Eng.*, vol. 148, pag. 012004, set. 2016, doi: 10.1088/1757-899X/148/1/012004.
[171] X. Dong, J. Yu, W. Wang, e Z. Zhang, «Robust design of magneto-rheological (MR) shock absorber considering temperature effects», *Int. J. Adv. Manuf. Technol.*, vol. 90, n. 5, pagg. 1735–1747, mag. 2017, doi: 10.1007/s00170-016-9480-9.
[172] M. R. Jolly, J. W. Bender, e J. D. Carlson, «Properties and applications of commercial magnetorheological fluids», 1998, vol. 3327, pagg. 262–275, doi: 10.1117/12.310690.

[173] S.-W. Cho, H.-J. Jung, e I.-W. Lee, «Smart passive system based on magnetorheological damper», *Smart Mater. Struct.*, vol. 14, n. 4, pagg. 707–714, giu. 2005, doi: 10.1088/0964-1726/14/4/029.
[174] A. A. Alghamdi, R. Lostado, e A.-G. Olabi, «Magneto-Rheological Fluid Technology», in *Modern Mechanical Engineering*, J. P. Davim, A c. di Springer Berlin Heidelberg, 2014, pagg. 43–62.
[175] H. Böse, J. Ehrlich, e A.-M. Trendler, «Performance of magnetorheological fluids in a novel damper with excellent fail-safe behavior», *J. Phys. Conf. Ser.*, vol. 149, pag. 012039, feb. 2009, doi: 10.1088/1742-6596/149/1/012039.
[176] J. D. Kraus, *Electromagnetics*, 4th edition. New York: McGraw-Hill, 1991.
[177] S. A. Mazlan, N. B. Ekreem, e A. G. Olabi, «An investigation of the behaviour of magnetorheological fluids in compression mode», *J. Mater. Process. Technol.*, vol. 201, n. 1–3, pagg. 780–785, mag. 2008, doi: 10.1016/j.jmatprotec.2007.11.257.
[178] M. Dassisti, G. Brunetti, A. Rizzuti, e P. Mastrorilli, «Three-Disperse Magnetorheological Fluids Based on Ferrofluids Induced Modification of Sedimentation by Addition of Nanoparticles», *Key Engineering Materials*, 2020. https://www.scientific.net/KEM.865.73 (consultato dic. 21, 2020).
[179] G. Wang, Y. Ma, Y. Tong, e X. Dong, «Development of manganese ferrite/graphene oxide nanocomposites for magnetorheological fluid with enhanced sedimentation stability», *J. Ind. Eng. Chem.*, vol. 48, pagg. 142–150, apr. 2017, doi: 10.1016/j.jiec.2016.12.032.
[180] D. Utami *et al.*, «Material Characterization of a Magnetorheological Fluid Subjected to Long-Term Operation in Damper», *Materials*, vol. 11, n. 11, Art. n. 11, nov. 2018, doi: 10.3390/ma11112195.
[181] C. Poussot-Vassal, O. Sename, L. Dugard, R. Ramirez-Mendoza, e L. Flores, «OPTIMAL SKYHOOK CONTROL FOR SEMI-ACTIVE SUSPENSIONS», *IFAC Proc. Vol.*, vol. 39, n. 16, pagg. 608–613, gen. 2006, doi: 10.3182/20060912-3-DE-2911.00106.
[182] D. Hrovat, «Survey of Advanced Suspension Developments and Related Optimal Control Applications11This paper was not presented at any IFAC meeting. This paper was recommended for publication in revised form by Editor Karl Johan Åström.,22Simple, mostly LQ-based optimal control concepts gave useful insight about performance potentials, bandwidth requirements, and optimal structure of advanced vehicle suspensions. The present paper reviews these optimal control applications and related practical developments.», *Automatica*, vol. 33, n. 10, pagg. 1781–1817, ott. 1997, doi: 10.1016/S0005-1098(97)00101-5.
[183] A. Zin, O. Sename, P. Gaspar, L. Dugard, e J. Bokor, «Robust LPV– ∞ control for active suspensions with performance adaptation in view of global chassis control», *Veh. Syst. Dyn.*, vol. 46, n. 10, pagg. 889–912, ott. 2008, doi: 10.1080/00423110701684587.
[184] M. Canale, M. Milanese, C. Novara, e Z. Ahmad, «Semi-active suspension control using "fast" model predictive control», in *Proceedings of the 2005, American Control Conference, 2005.*, giu. 2005, pagg. 274–281 vol. 1, doi: 10.1109/ACC.2005.1469945.
[185] N. Giorgetti, A. Bemporad, H. E. Tseng, e D. Hrovat, «Hybrid Model Predictive Control Application Towards Optimal Semi-Active Suspension», in *Proceedings of the IEEE International Symposium on Industrial Electronics, 2005. ISIE 2005.*, giu. 2005, vol. 1, pagg. 391–398, doi: 10.1109/ISIE.2005.1528942.
[186] H. Du, K. Yim Sze, e J. Lam, «Semi-active H∞ control of vehicle suspension with magneto-rheological dampers», *J. Sound Vib.*, vol. 283, n. 3, pagg. 981–996, mag. 2005, doi: 10.1016/j.jsv.2004.05.030.
[187] D. L. Guo, H. Y. Hu, e J. Q. Yi, «Neural Network Control for a Semi-Active Vehicle Suspension with a Magnetorheological Damper», *J. Vib. Control*, vol. 10, n. 3, pagg. 461–471, mar. 2004, doi: 10.1177/1077546304038968.
[188] M. R. Potnuru, X. Wang, S. Mantripragada, e F. Gordaninejad, «A compressible magneto–rheological fluid damper–liquid spring system», *Int. J. Veh. Des.*, vol. 63, n. 2–3, 2013, Consultato: dic. 23, 2020. [Online]. Disponibile su: https://trid.trb.org/view/1261394.

[189] J. Zheng, Y. Li, e J. Wang, «Design and multi-physics optimization of a novel magnetorheological damper with a variable resistance gap», *Proc. Inst. Mech. Eng. Part C J. Mech. Eng. Sci.*, vol. 231, n. 17, pagg. 3152–3168, set. 2017, doi: 10.1177/0954406216643109.
[190] X. Zhang, Z. Li, K. Guo, F. Zheng, e Z. Wang, «A novel pumping magnetorheological damper: Design, optimization, and evaluation», *J. Intell. Mater. Syst. Struct.*, vol. 28, n. 17, pagg. 2339–2348, ott. 2017, doi: 10.1177/1045389X17689937.
[191] M. Rahman, Z. C. Ong, S. Julai, M. M. Ferdaus, e R. Ahamed, «A review of advances in magnetorheological dampers: their design optimization and applications», *J. Zhejiang Univ.-Sci. A*, vol. 18, n. 12, pagg. 991–1010, dic. 2017, doi: 10.1631/jzus.A1600721.
[192] Y.-T. Choi e N. M. Wereley, «Self-Powered Magnetorheological Dampers», *J. Vib. Acoust.*, vol. 131, n. 044501, lug. 2009, doi: 10.1115/1.3142882.
[193] C. Chen, Y. S. I. Chan, L. Zou, e W. Liao, «Self-powered magnetorheological dampers for motorcycle suspensions», 2018, doi: 10.1177/0954407017723761.
[194] L. J. Felicia e J. Philip, «Probing of Field-Induced Structures and Tunable Rheological Properties of Surfactant Capped Magnetically Polarizable Nanofluids», *Langmuir*, vol. 29, n. 1, pagg. 110–120, gen. 2013, doi: 10.1021/la304118b.
[195] Y. Yang, L. Li, e G. Chen, «Static yield stress of ferrofluid-based magnetorheological fluids», *Rheol. Acta*, vol. 48, n. 4, pagg. 457–466, feb. 2009, doi: 10.1007/s00397-009-0346-z.
[196] R. C. Bell, D. T. Zimmerman, e N. M. Wereley, «CHAPTER 2. Magnetorheology of Fe Nanofibers Dispersed in a Carrier Fluid», in *RSC Smart Materials*, N. M. Wereley, A c. di Cambridge: Royal Society of Chemistry, 2013, pagg. 31–55.
[197] I. Arief, R. Sahoo, e P. K. Mukhopadhyay, «Dynamic and rate-dependent yielding behavior of Co0.9Ni0.1 nanocluster based magnetorheological fluids», *J. Magn. Magn. Mater.*, vol. 397, pagg. 57–63, gen. 2016, doi: 10.1016/j.jmmm.2015.08.080.
[198] R. J. Baxter, *Exactly Solved Models in Statistical Mechanics*. Courier Corporation, 2007.
[199] A. Rizzuti *et al.*, «Shape-control by microwave-assisted hydrothermal method for the synthesis of magnetite nanoparticles using organic additives», *J. Nanoparticle Res.*, vol. 17, n. 10, pag. 408, ott. 2015, doi: 10.1007/s11051-015-3213-0.